4740

~~CONFIDENTIAL~~

CONTRACT REQUIREMENTS	CONTRACT ITEM	MODEL	CONTRACT NO.	DATE
Exhibit E, Para 5.1	13	LEM	NAS 9-1100	1/14/63

Type II

GROUP-4
Downgraded at 3 year intervals;
declassified after 12 years

Primary No. 693

REPORT

NO. LED-500-1

DATE: 11 August 1964

TRAJECTORY CHARACTERISTICS DURING THE LEM MISSION (U)

CODE 26512

A. Nathan
PREPARED BY:
A. Nathan
V. Asbedian
H. Sperling
T. Hamilton

R. Fleisig
E.F. Baird
APPROVED BY:
R. Fleisig/E.F.Baird

K. Speiser
CHECKED BY:
K. Speiser

A. B. Whitaker
APPROVED BY:
A. B. Whitaker

REVISIONS

DATE	REV. BY	REVISIONS & ADDED PAGES	REMARKS

~~HEADQUARTERS ONLY~~

~~Available to NASA Offices and NASA Centers Only.~~

~~CONFIDENTIAL~~

TABLE OF CONTENTS

GLOSSARY OF SYMBOLS

Symbol	Definition	Unit
g	Thrust Acceleration/32.17	unitless
h	Altitude	ft. or n. mi.
r	Radial Position	ft. or n. mi.
t	Time	sec. or minutes
x,y,z	Position in Rectilinear Coordinates	ft.
$\dot{x},\dot{y},\dot{z}$	Velocity in Rectilinear Coordinates	ft/sec
γ	Flight Path Angle	degrees
θ	Pitch Angle	degrees
ψ	Roll Angle	degrees
ϕ	Yaw Angle	degrees
λ	Visibility margin measured from the window lower or upper edge to the LOS to the Landing-Site or horizon	degrees
μ	Gravity constant of the moon	ft^3/sec^2
ξ	The angle between the z-Body Axis and the LOS to the horizon or to the landing-site	degrees
ρ	Slant range between LEM and the CSM	ft. or n. mi.
$\dot{\rho}$	Slant range-rate between LEM and the CSM	fps.
σ	Central angle measured in the plane of the trajectory	degrees
$\dot{\sigma}$	Rate of change of central angle measured in the plane of the trajectory	deg/sec
ω	Line-of-sight angle measured in the xz-body axis plane from the z-body axis to the projection of the LOS on the xz-body axis plane, Rendezvous Radar Trunion Angle	degrees
τ	Line-of-sight angle measured from the xz-body axis plane to the LOS, Rendezvous Radar Shaft Angle	degrees
E	Elevation angle measured between the stable member z-Axis and the LOS to the CSM	degrees
R	Surface Range	ft. or n. mi.

Glossary Of Symbols (continued)

Symbol	Definition	Unit
T	Thrust	lbs.
V	Total Velocity (speed)	fps.
	Subscripts	
SM	Stable member	
I	Indicated or measured parameter	
T	Signifies upper window edge	
B	Signifies lower window edge	
L or LEM	Lunar Excursion Module	
CM or CSM	Command Service Module	
p	pericynthion	
a	apocynthion	
	Superscripts	
*	Angles measured relative to stable member axis system	
•	Differentation with respect to time	

TABLE OF FIGURES

Table Of Figures (continued)

Table Of Figures (continued)

I. Introduction

This report on nominal trajectory characteristics supersedes the trajectory data presented in reference A-7. All trajectories presented herein were calculated using guidance laws currently planned for the Primary Navigation and Guidance System (PNGS).

These trajectory data are subject to revision with changes in the mission profile and ΔV budget. Pertinent mission ground rules which define the trajectory requirements are as follows:

1. A Hohmann coasting descent orbit is specified for transfer from an 80 n. mi. CSM circular parking orbit to a 50,000 ft. pericynthion altitude. The orbit plane will nominally contain the landing-site.

2. Requirements for pilot visibility of the landing-site during the final portions of powered descent and prior to manual take-over for the touchdown maneuver is specified.

3. A direct ascent phase to rendezvous with the CSM is specified as nominal.

4. At launch a nominal $\frac{1}{2}$ degree central angle displacement between the CSM orbit plane and the LEM launch-site is specified.

5. Nominal rendezvous is initiated 5 n. mi. from the CSM.

Included in this report are data on the likely trajectory deviations from the nominal. Current estimates on normal or in-tolerance errors in the navigation and control system performance are included in the error evaluation. Only results pertaining to errors accrued along the powered descent portion of the mission are presented in this report. Future releases of this report will include error results for all phases of the LEM mission.

II. Definitions

The definition of trajectory phases in reference A-7 apply to the discussion of trajectories in this report. For convenience, these definitions are restated with appropriate changes.

A. General

A.1 Lunar Orbit - starts after successful insertion of the CSM into lunar orbit, and terminates just prior to the LEM separation from the CSM.

B. Descent

B.1 Coasting Descent Transfer Orbit - starts with separation of the LEM from CSM, includes insertion of LEM into a coasting descent orbit and terminates at the initiation of powered descent. If any descent midcourse corrections are required during this flight phase, they will be discussed in this section.

B.2 Powered Descent - starts at the completion of the coasting descent transfer orbit and terminates at LEM touchdown on the lunar surface. For convenience, this phase is sub-divided as follows:

B.2.1 Fuel Optimum Phase (FOP) - starts at the completion of the coasting descent transfer orbit and ends just prior to the LEM rotation required to achieve visibility of the landing-site.

B.2.2 Visibility Phase (VP) - starts at initiation of LEM rotation to achieve landing-site visibility and terminates at a specified altitude, vertical velocity and horizontal velocity in the neighborhood of the landing-site.

B.2.3 Translation, Hover and Touchdown (THAT) - starts at termination of VP and includes the translation to the desired landing-site, a momentary hover and a soft landing.

C. Ascent

C.1 Powered Ascent - starts with ascent engine ignition and terminates with insertion into a coasting ascent transfer orbit or into a parking orbit. Discussion of launch window for a parking orbit ascent approach as well as that for a direct coasting ascent to rendezvous is included in this section.

C.2 Coasting Ascent Transfer Orbit - starts immediately after insertion into the coasting orbit, either by direct insertion, or from a parking orbit, and terminates when the LEM is 5 n. mi. from the CSM. Plane-change and midcourse maneuvers will be discussed in this section.

C.3 Rendezvous - starts 5 n. mi. from the CSM and terminates when the LEM is 500 ft. from the CSM.

C.4 Docking - starts at 500 ft. from the CSM and terminates at LEM-CSM contact.

In this report, most trajectory parameters are presented in the IMU stable member axis system. This axis system has its origin at the moon's center with the x-axis passing through the landing-site. The z-axis is normal to x and parallel to the plane of the CSM orbit. The positive direction of z is coincident with the forward direction of the CSM velocity when the CSM passes over the landing-site. The y-axis is orthogonal to the xz plane forming a right-handed system (figure II-1).

A selenographic axis-system is shown in figure II-2. The origin of this system is again at the moon's center. The x-axis passes through the lunar equator toward the earth's center. The z-axis is normal to x and passes through the lunar north pole. The y-axis is normal to the xz plane forming the right handed system. For this report only, the landing-site is assumed to be located on the surface of the moon on the x selenographic axis. For the discussion of the descent trajectories, the CSM is assumed to be in an equatorial orbit. In the discussion of ascent trajectories, the CSM orbit is assumed to be inclined to the equatorial plane.

Figure II-3 defines the LEM body axis system. The x-axis is along the vehicle center line and is positive in the direction of main engine thrust. The z-axis is normal to x and passes through the lower exit port. The y-axis is normal to xz in a right handed sense. Figure II-4 defines the attitude angles which rotate the stable member axes into LEM body axes. The first rotation is about y and is referred to as "pitch" (θ^*). The second rotation is about the rotated z-axis and is referred to as "roll" (ψ^*). The third rotation is about the twice rotated x-axis and is referred to as "yaw" (ϕ^*). In this report, roll and yaw are assumed zero throughout. Under this assumption, pitch is the angle between the stable member z-axis and the body z-axis. For example, during the vertical rise at initiation of powered ascent, the pitch angle is zero.

Figure II-5 shows the definition of the angles which rotate stable member axes into line-of-sight axes where, in the line-of-sight system, the z-axis lies along the line-of-sight vector. Figure II-6 defines the rotation of the LEM body axes into the line-of-sight system for the case in which yaw and roll are zero.

III. Nominal Trajectories

A. General

A.1 Lunar Orbit

From paragraph 3.1.6 of reference A-3, CSM orbit altitudes of 60-100 n.mi. are possible. The CSM orbit used to define the LEM trajectory characteristics is considered to be circular at an 80 n.mi. altitude. This CSM altitude is the same as that used in defining the nominal trajectories presented in reference A-7. The choice of the 80 n.mi. CSM parking orbit was based on trade-off studies involving superior LEM-CSM relative central angle relationships along the descent path with subsequent ΔV and ascent phase synodic time effects (reference C.1-5). The orbit characteristics associated with an 80 n. mi. altitude (reference C.1-5) are itemized in Table A.1-1.

TABLE A.1-1

CSM ORBITAL ELEMENTS *

80 N.MI. ALTITUDE

r_{CSM} Orbital Radius	=	6,188,188.97 international feet
V_{CSM} Orbital Velocity	=	5,284.699 international feet/second
P_{CSM} Orbital Period	=	122.623 minutes
$\dot{\sigma}_{CSM}$ Angular Rate	=	2.936 degrees/minute
Communication time measured from end of Translation, Hover and Touchdown phase	=	2.75 minutes
Communication time measured from horizon to horizon	=	15.6 minutes

* Lunar Constants Used

(1) r_m, Lunar Radius = 5,702,099.73 int. ft.
(2) 1 int. n. mi. = 6076.115486 int. ft.
(3) μ_m, Lunar gravitational const. = 1.72824×10^{14} int. ft3/ sec^2

Note that these constants do not agree with the constants presented in Ref. A-8.
See Nominal Trajectory Summary, Section IV.

B. Descent

Figure B-1 presents a schematic of the descent phase misssion profile. The LEM is inserted into a Hohmann orbit starting at an altitude of 80 n.mi. The pericynthion altitude of this transfer orbit is 50,000 ft above the mean lunar surface. At pericynthion, the descent engine is ignited, and thrust vector commands generated by the PNGS guide the vehicle to a point approximately 10,600 ft. above the lunar surface and 7 n.mi. from the landing-site. At this point in the trajectory, new guidance parameters affect attitude commands which rotate the LEM. If lighting conditions are proper for pilot visual surveillance, the attitude rotation provides a clear line-of-sight to the landing area. This phase of the powered descent is terminated at an altitude of 200 feet with a speed of 10 ft/sec. Although the mission plan calls for manual control for the final touchdown maneuver, a "closed loop" path adaptive guidance law is used to generate a typical translational, hover and touchdown maneuver.

B.1 Coasting Descent Transfer Orbit

The nominal coasting descent trajectory begins with separation of the LEM from the CSM. For this report, it is assumed that the impulse required for separation does not cause a difference between the LEM and CSM velocity and position at insertion. The LEM is inserted into a Hohmann orbit at the CSM orbit altitude of 80 n.mi. This Hohmann orbit has a pericynthion altitude and velocity of 50,000 ft and 5581 ft/sec respectively. From trajectory calculations using the PNGS explicit guidance law, the ΔV required for insertion into the transfer orbit is 97.33 ft/sec for a $(T/W)_o = 0.351$. The guidance-control concept directs the LEM thrust vector such that the instantaneous LEM velocity vector is driven toward an instantaneously desired velocity vector. The desired velocity vector is that velocity required to transfer to a 50,000 ft pericynthion altitude, assuming that the present LEM radial position corresponds to the apocynthion of the transfer orbit. Thrust is terminated when the LEM velocity and desired velocity vector are equal. The time of powered flight is 8.51 seconds for an insertion at full throttle (10,500 lbs).

For insertion, figure B.1-1 shows the time history of altitude and thrust acceleration. Figure B.1-2 presents the LOS angle, and the slant range and range rate of the LEM relative to the CSM. The inertial pitch angle, θ^*, and local pitch angle, θ, are presented in figure B.1-3. The relative central angle between LEM and CSM, $\sigma_{1,CM}$ and the LEM central angle, σ_{LEM}, are shown in figure B.1-4.

Figure B.1-5 is a time history of altitude and elevation angle, E, during the coasting descent. Slant range and range rate of the LEM with respect to the CSM are shown in figure B.1-6. The LEM central angle together with the relative central angle between the LEM and CSM are presented in figure B.1-7 for the interval from insertion to pericynthion.

* See reference B.1-6

B.2 Powered Descent

The powered descent trajectory is divided into three guidance phases: The Fuel Optimum Phase, the Visibility Phase, and the Translation, Hover and Touchdown Phase. The trajectories for the first two phases were computed using the PNGS terminal explicit guidance law. The guidance equations used for FOP and VP are identical except for the specified terminal conditions and the time of flight from initiation to termination of the phase. The Translation, Hover and Touchdown Phase is nominally a maneuver carried out under manual control. However, a typical trajectory for THAT has been calculated using an automatic guidance-control concept.

B.2.1 Fuel Optimum Phase. This phase of the descent trajectory was generated with the PNGS guidance equations. The guidance control commands are explicitly a function of specified terminal conditions, a predetermined initial time of flight and the instantaneous LEM position and velocity (reference B.2.1-5). The FOP starts at the 50,000 ft pericynthion altitude of the transfer orbit and ends 349.27 seconds later at an altitude of 10,621 ft. with a speed and flight path angle of 747.8 ft/sec and -12.9 deg. respectively. These terminal conditions for FOP were determined as those required as initial conditions for the Visibility Phase, during which an unobstructed visual line-of-sight to the landing-site is required.

The thrust-to-weight ratio at retrofire is 0.357 and the specific impulse is assumed a constant 301 sec. throughout the phase. Figure B.2.1-1 shows the time history of altitude and surface range. The phase starts at approximately 197 n.mi. and ends at 7 n.mi. from the landing-site. Figure B.2.1-2 presents the speed, horizontal velocity, vertical velocity and velocity increment (ΔV) as a function of time. The ΔV expended during this phase is 4979 ft/sec. Figure B.2.1-3 shows the time history of the CSM and LEM central angles. The CSM lags the LEM by 9.4 deg. at retrofire and by 3.9 deg. at the end of the phase. Figure B.2.1-4 presents time histories of the thrust acceleration and components of the thrust acceleration. Note the near linear variation in the thrust acceleration components reflecting the characteristics of the guidance equations. Figure B.2.1-5 is a time history of thrust and the inertial pitch attitude. At retrofire, thrust is at its maximum (10,500 lbs) and is at a somewhat lower level (9,875 lbs) at the end of the phase. Figure B.2.1-6 is a time history of the slant range and range rate of the LEM relative to the CSM. Included on figure B.2.1-6 is a time history of the line-of-sight angle between the LEM z- body axis and the line-of-sight vector.

B.2.2 Visibility Phase. This portion of the trajectory is flown under the same closed-loop explicit guidance law as that used in FOP. The initial conditions (the terminal conditions of FOP) are such that, when the trajectory is flown under guidance, the thrust and inertial attitude commands remain at approximately 4700 lbs and 47 degrees respectively throughout the VP. With these attitudes, a visual margin of approximately 8½ degrees is achieved. The terminal con-

ditions for this phase are:

1. Altitude = 200 feet
2. Speed = 10 ft/sec
3. Flight path angle = -10 degrees
4. Range from landing site = 1000 feet

Assuming a constant I_{sp} of 301 sec., the ΔV expended during the 114 seconds of flight is 1056 ft/sec.

Figure B.2.2-1 shows the time history of altitude and surface range. Figure B.2.2-2 presents speed, horizontal velocity, vertical velocity and ΔV as a function of time. Figure B.2.2-3 shows the time history of the CSM and LEM central angles. At the LEM terminal conditions, the CSM leads the LEM by 1.32 degrees. Figure B.2.2-4 presents time histories of the thrust acceleration and the components of thrust acceleration. Figure B.2.2-5 is a time history of thrust and inertial pitch attitude. Figure B.2.2-6 shows the slant range and range rate of the LEM relative to the CSM. Included on figure B.2.2-6 is a time history of the line-of-sight angle between the LEM z-body axis and the line-of-sight to the CSM. Figure B.2.2-7 shows the visibility angle measured from the negative x-body axis to the line-of-sight to the landing-site.

B.2.3 Translation, Hover and Touchdown - The translation, hover and touchdown trajectory shown in figure B.2.3-1 was based on a closed-loop polynominal guidance law and a signal-synthesis adaptive control technique (reference B.2.3-8). A guidance law switch was initiated at an altitude of 25 feet above the touchdown point. The switch initiates a constant attitude - constant acceleration guidance law which forces the LEM into a highly stabilized vertical descent, thereby compensating for dispersions in rotational rate and linear velocity at touchdown. The initial conditions of this trajectory correspond to the final conditions of the visibility phase. The time of flight is 121.2 seconds, the initiation altitude is 200 feet, and the range to the landing-site is 1000 ft. Visibility margins for both the landing-site and the visual horizon are shown in figure B.2.3-2. This figure shows visibility to be satisfactory. The horizon and landing-site are out of view for a total of 16 and 10 seconds respectively, early in the trajectory. The landing-site is unavoidably out of view during the final 25 seconds of flight because of the vehicle's proximity to the landing-site (within 25 ft range and altitude). The trajectory time histories are shown in figures B.2.3-3 through B.2.3-6. Figure B.2.3-7 shows the time history of the CSM central angle relative to the landing-site. At the end of the THAT maneuver, 165 seconds elapse before the CSM falls below the horizon.

The vertical and horizontal velocities, attitude, and attitude rate at touchdown are respectively, -4.99 ft/sec, 1.06 ft/sec, 89.9 deg, and zero deg/sec. These values are within the landing gear capabilities. The ΔV required to perform the trajectory is 657.6 ft/sec.

B.3 Descent Stage ΔV Summary

The total ΔV required for the nominal descent trajectory is compared with the "ΔV - Budget" adopted at the NASA/GAEC meeting on March 12, 1964 at Bethpage (reference A-9). The ΔV's computed for the nominal trajectories presented in this report are compared with the ΔV's presented under the catagory "Open Loop" in the "ΔV-Budget". The total ΔV for the nominal descent mission is 6794.9 ft/sec. The total ΔV allocated to the "Open Loop" catagory in the "ΔV-Budget" is 6952 ft/sec. The 157.1 ft/sec discrepency between the nominal trajectory ΔV and the "ΔV-Budget" is attributed to an allocation in the ΔV budget for alternate landing-site selection.

TABLE B.2.4-1

Descent Stage ΔV **

Mission Phase	Nominal Trajectory ΔV		"ΔV Budget"
B.1 Coasting Descent Transfer	102.33		102
B.1.1 Separation		5.00	5
Insertion		97.33	97
B.2 Powered Descent	6692.60		6850
B.2.1 Fuel Optimum Phase	4979	6035.00	5950
B.2.2 Visibility Phase	1056		
B.2.3 Translation, Hover & Touchdown		657.60	900
	6794.93		6952

** Only ΔV Under "Open Loop" catagory from the "ΔV-Budget" is included

C. Ascent

Figure C-1 shows the geometry of the nominal ascent mission. An out-of-plane launch displacement of ½ degree lunar central angle was assumed. The powered ascent is initiated when the CSM lags the LEM landing point by a central angle of 3.85 degrees. At burnout the LEM altitude is 50,000 ft above the mean lunar surface at a speed of 5581 ft/sec and a flight path angle of 0.892 degrees. These conditions result in an intercept with the CSM at 160.1 deg central angle, measured in the plane of the LEM trajectory and relative to the launch-site.

The coasting transfer orbit has a pericynthion altitude of 38,360. ft. The rendezvous is initiated at approximately 5 n. mi. from the CSM.

C.1 Powered Ascent

The characteristics of the LEM nominal ascent trajectory are based on an initial thrust-to-weight ratio of 0.333, a specific impulse of 306 sec. and a constant engine thrust of 3,500 lbs. The CSM is assumed to be in an 80 n. mi. circular orbit. At launch, figure C.1-1 shows the geometry of the launch-site relative to the CSM. The LEM is located at a right ascension of 3.85 degrees and at an out-of-plane (declination) of $\frac{1}{2}$ degree (8.2 nautical miles).

The nominal ascent trajectory was generated using the PNGS guidance technique (reference B.2.1-5). After a 10 sec. vertical rise ($\theta^* = 0$ deg), control commands are generated by the guidance system resulting in a rapid pitch over at -10 deg/sec. At t=15.68 seconds, an attitude null is reached ($\theta^* = -56.85$ deg). The altitude, vertical velocity, plane conditions and trajectory angular momentum required at burnout are continuously generated by the guidance system. These required burnout conditions are functions of CSM-LEM relative position and velocity. Attitude commands and an engine-cut-off time, which will guide the LEM to the proper burnout conditions for a direct transfer to CSM intercept, are "continuously" calculated.

For the nominal launch, the burnout conditions are:

1. Altitude = 50,000 ft
2. Speed = 5581 ft/sec
3. Flight path angle = 0.892 deg
4. ΔV consumed = 6062 ft/sec
5. Weight of propellent used = 4827.8 lbs
6. Time of flight = 422.09 sec.
7. Inertial pitch attitude = -108.4 deg
8. Central angle from launch = 9.94 deg.

Figure C.1-2 presents the time history of altitude and speed. Included on figure C.1-3 are the time histories of ΔV, thrust acceleration and inertial pitch angle. Figure C.1-4 shows the flight path angle and the vehicle attitude referenced to the local horizontal. Figure C.1-5 shows the geometric relationship involved in defining the line of sight vector between the CSM and the LEM. Fig. C.1-6 and C.1-7 presents the time history of the line-of-sight parameters starting when the CSM appears over the horizon and ending at LEM powered ascent burnout.

C.2 Coasting Ascent Transfer Orbit

At the 50,000 ft. altitude burnout condition, the nominal out-of-plane displacement (declination) of the LEM from the CSM orbit plane is 0.732 degrees. A burnout velocity of 5581 ft/sec and a flight path angle of 0.892 degrees result in a transfer orbit which intersects the CSM orbit 150.26 degrees central angle from burnout. This

transfer orbit is inclined to the CSM orbit by 1.46 degrees. For the nominal trajectory, no midcourse corrections are required, however, future error analyses on normal N & G performance will include the PNGS midcourse correction technique and the calculation of the likely ΔV required for midcourse corrections. Rendezvous is initiated at 141.92 degrees central angle from burnout, or equivalently 5 n. mi. from the CSM. The time of flight elapsed from burnout to rendezvous initiation is 45.89 minutes.

Figure C.2-1 presents a time history of slant range between the LEM and CSM. Figure C.2-2 presents slant range rate along the LOS between the LEM and CSM. Figure C.2-3 shows the line-of-sight rate while figures C.2-4 and C.2-5 presents the radial position and speed of the LEM respectively.

C.3 Rendezvous

Rendezvous is initiated by the LEM 5 n. mi. from the CSM. The time of flight needed to perform the nominal maneuver using the prime rendezvous guidance technique is 660 seconds. The ΔV required to perform the maneuver is 169.9 ft/sec. * which compares favorably with an impulsive rendezvous ΔV of 169.44 ft/sec. The guidance concept requires radar measurements of range, range rate, and LOS angle between LEM and the CSM as a means of estimating (i.e. by mixing radar and inertial information) the LEM orbit. At specified ranges, a time of flight for LEM-CSM interception is specified. With the specified time of flight and the estimated LEM orbit, ΔV corrections are computed. In the nominal, three such correction points are specified, at 5 n. mi., 1.5 n. mi. and .25 n. mi. Figure C.2-1 and C.2-2 show the time histories of slant range and range rate between the LEM and the CSM. Included on C.2-1 and C.2-2 are the points at which the rendezvous corrections are applied. Figure C.2-3 shows the line-of-sight rate as a function of time. Rendezvous correction points are indicated. Figure C.2-4 presents the LEM speed. It can be seen that for the nominal rendezvous, the LEM speed is increased at each correction point. Figure C.2-5 shows the radial position of the LEM during the rendezvous maneuver. Table C.3-1 shows the nominal thrust schedule followed during the nominal rendezvous. Included are the ranges at which correction is applied, the elapsed time since powered ascent burnout, the duration of the correction control period, the ΔV expended during the control period, and the thrust level applied. All maneuvers are performed by two z-body axis RCS engines, having a nominal thrust level of 100 lbs. and an I_{sp} of 295 sec. The thrust to weight ratio at the initiation of the first correction is .0365.

* Includes 2.58 ft/sec residual velocity after the last rendezvous correction.

TABLE C.3-1

NOMINAL RENDEZVOUS CORRECTION SCHEDULE

Range (n. mi.)	Time Elapsed Since Powered Ascent Burnout (sec.)	Thrusting Period (sec.)	Δ V (ft/sec)	Thrust Level (lbs)
5	2753.8	58.74	69.28	200
1.5	2947.3	71.04	81.79	200
0.25	3228.0	13.67	16.29	200
		143.45	167.36	
	Residual Velocity To Be Nulled During Docking		2.58	
	Grand Total Used To Compare With Impulsive ΔV		169.94	

C.4 Docking

The docking maneuver is nominally initiated 500 ft slant range from the CSM and at relative velocities of 2.58 ft/sec. The maneuver is performed manually with an alloted 25 ft/sec ΔV. Because docking is a manual mode of operation, trajectory data will not be available until future simulation studies have been completed.

C.5 Ascent Stage Δ V Summary

The total Δ V for the nominal ascent trajectory is compared with the Δ V allocated to the "Open Loop" catagory of the "Δ V Budget" (reference A-9) in Table C.5-1. The ΔV required to perform the nominal ascent is 6256.94 ft/sec. This ΔV consumption is 44.06 ft/sec below that indicated in the " ΔV-Budget". The discrepancy in the ΔV's can be partly attributed to an allocation in the " ΔV-Budget" for a 12 second vertical rise and that the in-plane and out-of-plane rendezvous maneuvers are performed separately.

TABLE C.5-1

Ascent Stage ΔV**

Mission Phase	Nominal Trajectory ΔV	"Open Loop" ΔV Budget
C.1 Powered Ascent	6062.00	6090.00
C.2 Midcourse Correction During Coasting Ascent Transfer Orbit	-------	
C.3 Plane Change and Rendezvous	169.94	186.00
C.4 Docking	25.00	25.00
Total Ascent	6256.94	6301.00

IV. Summary of LEM Nominal Trajectories

Table IV-1 is a summary of the nominal trajectories presented in this report. The ΔV expended is 6794.9 ft/sec for the nominal descent trajectory, and 6256.9 ft/sec for the nominal ascent trajectory. These ΔV expenditures are within the "ΔV-Budget" for the computation of nominal fuel comsumption. All ground rules dictated by mission requirements have been satisfied; however, recent operational features introduced by the performance capabilitites of the descent engine gimble trim mechanism have changed the descent trajectory. Future releases of this report will then include:

1. Insertion at reduced thrust levels.
2. Retrofire for initiation of powered ascent at decreased thrust levels for a period of approximately 25 seconds.

The next nominal trajectory report will include the orbit characteristics between separation of the LEM from the CSM and the insertion. A landing-site will be chosen and all trajectory characteristics presented in reference to this more realistic mission. The lunar constants specified in reference A-8 will be used to calculate all trajectories. The specific impulse will be assumed to be a function of the thrust levels in future trajectory calculations.

** Only ΔV Under "Open Loop" catagory from the "ΔV-Budget" is included.

TABLE IV-1

Summary Of Trajectory Characteristics

Mission Phase	Guidance Procedure	Trajectory Characteristics	Control Characteristics	ΔV Required	ΔV Available	Figures
A. Lunar Orbit		1. Orbital Parameters Altitude = 80 n. mi. Speed = 5,284.7 ft/sec. Period = 122.6 minutes Angular Rate = 2.94 deg/sec Communication Time (Horizon to Horizon) = 15.6 min.				Table A.1-1 Page 4
B. Descent Separation				5	5	
B.1 Coasting Descent Transfer Orbit	Insertion: "$\underline{V}_G \times \dot{\underline{V}}_G = 0$" MIT/IL explicit guidance equations presented in Ref. B.1-6. The velocity to gain, V_G, is a function of the LEM instantaneous velocity required to achieve a Hohmann transfer to a 50,000 ft. pericynthion altitude.	1. Insertion initial condition: Altitude = 80 n. mi. Speed = 5,284.7 ft/sec Flight Path Angle = 0.0 deg Central Angle From Landing-Site = 192.41 deg 2. Insertion "burn-out" conditions Altitude = 486,000.2 ft. Speed = 5,187.4 ft/sec Flight path angle = 0.0 deg Time of burn = 8.51 sec.	1. Thrust = const =10500 lbs 2. I_{SP} = 301 sec. 3. Attitude: Function of $\underline{V}_G \times \dot{\underline{V}}_G$ guidance with the control constraint that thrust be held constant. 4. $(T/W)_o$ = .351	97.33	97.0	Figures B.1-1 Pg 31 B.1-2 Pg 32 B.1-3 Pg 33 B.1-4 Pg 34
	Transfer Orbit: - Hohmann	3. Pericynthion condition of transfer orbit: Altitude = 50,000 ft. Speed = 5581 ft/sec Flight Path Angle = 0.0 deg Time of Flight From Insertion = 3,494.4 sec.				Figures B.1-5 pg 35 B.1-6 pg 36 B.1-7 pg 37
B.2. Powered Descent 1. Fuel Optimum Phase	Explicit guidance equations calculate thrust and attitude commands. These equations are functions of desired final velocity and position conditions and the LEM instantaneous velocity & position. Reference B.2.1-5.	1. Initial conditions same as pericynthion condition 3 above. 2. Final Conditions Altitude = 10,021 ft Speed = 747.8 ft/sec Flight path angle = -12.9 deg	1. Thrust levels determined by guidance equations. Initial value = 10,500 lbs Final value = 9876 lbs 2. $(T/W)_o$ = .357	4979	Undefined in "ΔV-Budget" (See Section II.3.3)	B.2.1-1 pg 38 B.2.1-2 pg 39 B.2.1-3 pg 40 B.2.1-4 pg 41 B.2.1-5 pg 42 B.2.1-6 pg 43

FORM G332 5-63 (ENG 72)

Mission Phase	Guidance Procedure	Trajectory Characteristics	Control Characteristics	ΔV Required	ΔV Available	Figures
B.2. Powered Descent (Cont.) 1. Fuel Optimum Phase (Cont.)		3. Time of flight (from retro-fire) = 349.2 sec.	3. I_{sp} = 301 sec. 4. Attitude determined by guidance equations. Initial Value, $\theta^* = 195^\circ$ Final Value, $\theta^* = 161^\circ$			
2. Visibility Phase	Explicit guidance equations same as for fuel optimum phase.	1. Initial Conditions Same as 2 above for B.2.1 2. Final Conditions Altitude = 200 ft Speed = 10 ft/sec. Flight path Angle = -10 deg. 3. Time of flight (from 10,621 ft altitude) = 115 sec. 4. Trajectory yields approximately 8 deg visual margin for pilot surveillance of landing-site	1. Thrust levels determined by guidance equations. Initial value = 4748 lbs Final value = 4744 lbs 2. $(T/W)_o$ = .274 3. I_{sp} = 301 sec 4. Attitude determined by guidance equations. Initial value $\theta^* = 46.7^\circ$ Final value $\theta^* = 47.0^\circ$	1056	Undefined in "ΔV Budget" (See Section II B.3)	B.2.2-1 pg 44 B.2.2-2 pg 45 B.2.2-3 pg 46 B.2.2-4 pg 47 B.2.2-5 pg 48 B.2.2-6 pg 49 B.2.2-7 pg 50
			Sub Total (POP & VP)	6035	5950	
3. Translation, Hover and Touch-down	"Polynominal Guidance", Flight path predetermined as function of initial conditions. Control system feedback on command flight; reference, B.2.3-3	1. Initial Conditions: Same as 2 above for B.2.2 2. Final Conditions Altitude = 0.0 Speed = 0.0 3. Time of flight (from 200 ft. altitude) = 121.2 sec.	1. Average thrust approximately - 2600 lbs 2. I_{sp} = 301 sec. 3. Attitude $-30^\circ \leq \theta^* \leq 30^\circ$	657.6	900	B.2.3-1 pg 51 B.2.3-2 pg 52 B.2.3-3 pg 53 B.2.3-4 pg 54 B.2.3-5 pg 55 B.2.3-6 pg 56 B.2.3-7 pg 57
C. Ascent C.1 Powered Ascent	Explicit guidance equations which determine "burn-out" conditions for an intercept with the CSM. Steering equations determine attitudes and engine cut-off times required to achieve the desired "burn-out" conditions.	1. Initial Conditions: LEM Launch-Site is ½ deg central angle out-of-the plane of the CSM orbit. At launch the CSM lags the LEM by 3.85 deg.	1. Thrust = const = 3500 lbs 2. I_{sp} = 306 sec. 3. $(T/W)_o$ = .333	6062	6090	C.1-1 pg 59 C.1-2 pg 60 C.1-3 pg 61 C.1-4 pg 62 C.1-5 pg 63 C.1-6 pg 64 C.1-7 pg 65

FORM G332 5-63 (ENG 72)

Mission Phase	Guidance Procedure	Trajectory Characteristics	Control Characteristics	ΔV Required	ΔV Available	Figures
C. Ascent (Cont.) C.1 Power Ascent (Cont.)		2. Final "burn-out" conditions Altitude = 50,000 ft. Speed = 5581 ft/sec. Flight path angle = .8917 deg Out-Of-Plane angle = .73185 3. Time-of-flight = 422.09 sec.	4. Attitude: $0 \leq t \leq 10$ sec; $\theta^* = 0$ deg $10 \leq t \leq 15.68$; $\dot{\theta}^* = 10$ deg/sec $15.68 \leq t \leq 422.09$; attitude as a function of explicit guidance law.			
C.2 Coasting Ascent Transfer Orbit		1. Initial conditions: Same as "burn-out" conditions for C.1. 2. Transfer Orbit: a. Intersects CSM Orbit 160.1 deg from launch b. Inclined to CSM Orbit by 1.46 degrees 3. Rendezvous is initiated 141.92 degrees from burn-out or equivalently 5 n. mi from the CSM 4. Time-of-flight from "burn-out" to rendezvous initiation = 45.9 min.				C.2-1 pg 66 C.2-2 pg 67 C.2-3 pg 68 C.2-4 pg 69 C.2-5 pg 70
C.4 Rendezvous	Rendezvous radar data on range, range rate, and LOS angle are used to update the PNGS. At specified ranges, a predetermined time of flight and the estimated LEM orbit is used to calculate ΔV corrections for rendezvous.	1. Rendezvous starts 5 n. mi from the CSM at which point a. Range rate = -165 ft/sec b. LOS rate = .52 mr/sec 2. Rendezvous ends 500 ft from the CSM at a closing velocity of 2.58 ft/sec. 3. Time-of-flight from initiation to termination = 474.2 minutes	1. Thrust from the RCS: Range From CSM (n.mi) / Thrust Level (lbs) / Duration (sec) 5.0 / 200 / 58.74 1.5 / 200 / 71.04 0.25 / 200 / 13.64 2. I_{sp} = 295 sec	169.94	186.0	C.2-1 pg 66 C.2-2 pg 67 C.2-3 pg 68 C.2-4 pg 69 C.2-5 pg 70
C.5 Docking	Manual			25	25	

V. LEM Normal Error Performance

Normal error performance is the likely trajectory deviations from the nominal trajectory caused by in-tolerance errors in the following catagories;

1. Initiation of the navigation system - Prior to separation of the LEM from the CSM, the command module navigation data is transferred to the LEM. The transferred information on the velocity and position is used as initial conditions to the LEM integrating inertial system. This data is only as accurate as the estimated CSM orbit via the orbital navigation technique.

2. Navigation system sensor errors - This group of error sources includes such uncertainties as the alignment of the IMU, platform drift rates and radar accuracies.

3. Errors in execution - This group of errors includes the uncertainties in the thrust and attitude from the levels commanded by the guidance system.

The combined effect of all the errors sources presented under the three catagories briefly identified above are analyzed using a linear statistical error technique developed at GAEC. References V-1 thru V-8 discuss in detail the mathematical theory used as a basis to generate the data presented in this section. At this time, only the results of an analysis performed on the powered descent trajectory are presented.* Future trajectory reports will include the results of studies on all phases of the LEM mission.

A. Error Sources

Table V-1 presents the uncertainties in the LEM inertial system's indication of the position and velocity at pericynthion. These errors are presented

TABLE V-1

COVARIANCE MATRIX OF UNCERTAINTIES AT PERICYNTHION

x	y	z	$\dot{x}$	$\dot{y}$	$\dot{z}$	
4.6519 E 05	1.7127 E 04	1.4045 E 06	-1.3300 E 03	8.0413 E 00	4.9294 E 01	x
1.7127 E 04	3.9102 E 05	3.2212 E 03	-9.4216 E 00	4.5204 E 01	-1.4251 E 01	y
1.4045 E 06	3.2212 E 03	7.9014 E 06	-7.5680 E 03	1.4930 E 02	1.4911 E 03	z
-1.3300 E 03	-9.4216 E 00	-7.5680 E 03	7.4018 E 00	-1.2291 E 01	-1.4635 E 00	$\dot{x}$
8.0413 E 00	4.5204 E 01	1.4920 E 02	-1.2291 E 01	3.5357 E 01	3.9890 E 02	$\dot{y}$
4.9294 E 01	-1.4251 E 01	1.4911 E 03	-1.4635 E 00	3.9890 E 02	5.0063 E 01	$\dot{z}$

in the form of a covariance matrix in which the diagonal terms are the variance in the components of position and velocity, and the off-diagonal terms are the covariances. The off-diagonal terms indicate the correlation between the errors on the diagonal. The matrix is referenced to the stable member axis system; that is, starting at the upper left hand element of the matrix, and in successive order, the variances in the position along the x, y and z axis, and in the velocity along the x, y

* Errors caused by IMU sensor errors, timing errors and control execution errors during descent insertion will cause increases in errors along the powered descent from those presented in this report.

and z axes of the stable member coordinate system are defined. This covariance matrix was obtained by propagating the covariance matrix, representing the orbital navigation uncertainties, from insertion to the pericynthion. The orbital navigation uncertainties at insertion were obtained through correspondence with MIT/IL. (Reference V-9). At insertion, the uncertainties were given as:

Altitude	770 ft	(1 sigma)
Down Range	2380 ft	(1 sigma)
Cross Track	673 ft	(1 sigma)
Vertical Velocity	1.71 ft/sec	(1 sigma)
Horizontal Velocity	.56 ft/sec	(1 sigma)
Cross Track Velocity	.552 ft/sec	(1 sigma)

for the MIT/IL "Model-2" orbital navigation technique. (Reference V-10).

The trajectory deviations at powered descent initiations are assumed to be slightly larger in magnitude than the errors in the navigation system and are assumed to have at least a 90% correlation with the navigation uncertainties. The high correlation asserts that trajectory deviations at pericynthion of the descent orbit are primarily due to the uncertainties in navigation. The magnitude of the trajectory deviations are assumed to be slightly larger to account for possible errors in the execution of the insertion maneuver. A detailed account of the meaning of the correlation of the navigation uncertainties with trajectory deviations can be found in reference V-7.

Table V-2 presents the IMU sensor errors considered in the analysis. The one sigma values quoted in Table V-2 were taken from an MIT/IL documentation of the inertial system performance presented in reference V-11. The methods by which sensor errors are incorporated into a linear statistical error analysis can be found in reference V-3.

TABLE V-2

IMU SENSOR ERRORS (1-Sigma Values)

Accelerometer zero bias	= .2 cm/sec^2
Accelerometer scale factor error	= 100 ppm
Accelerometer sensitivity (1st order)	
Scale factor error	= 10 ppm/g
Initial stable member	
Misalignment	= .85 mr
Fixed Drift Rate	= .15 deg/hr.

Table V-3 presents the errors in execution assumed in the analysis. A 0.1 degree (3σ) uncertainty in attitude control is attributed to the RCS dead band. A 100 lb. thrust uncertainty is attributed to engine throttle resolution.

TABLE V-3

ERROR IN EXECUTION

(3-sigma)

Attitude Errors	= .1 deg.
Thrust Errors	= 100 lbs

The errors quoted in the PNGS requirements (Reference V-12) for the landing radar were used in the analysis of the latter portions of the powered descent trajectory. The radar error in the measurement of altitude is assumed to be one percent of the vehicle altitude or 5 ft, which ever is greater. The velocity errors are assumed to one percent of the vehicle velocity or 1 ft/sec, which ever is greater. The uncertainties for the radar are calculated using the assumption of a smooth lunar surface with a radius equal to the mean. The effects of surface variations will be studied in the future.

B. N & G Operational Procedures

For powered descent, the navigation and guidance procedures assumed in the error analysis are in chronological order:

1. Alignment of the IMU using the AOT is made fifteen minutes prior to the initiation of powered descent. The uncertainty in the alignment at the initiation of powered descent is 0.82 milliradians.

2. The inertial navigation system is used to supply the descent explicit guidance equations with information required to generate control signals to the RCS.

3. At 270 seconds into the powered descent trajectory (approximately 25,000 ft), an update of the inertial system is made using information on altitude and velocity from the landing radar.

4. Radar - Inertial Mixing is terminated at t = 290 seconds into the powered descent.

5. From 290 seconds to the end of FOP, inertial information is used exclusively.

6. From the beginning of the VP to 430 seconds, mixing of radar - and inertial information is again made.

7. From t = 430 seconds to the end of VP, inertial information is used exclusively.

C. Error Results

When discussing the errors in position and velocity, a subscript "I" denotes an uncertainty in the navigation system and a variable without a subscript denotes a trajectory deviation from the nominal. All errors in state (e.g. velocity and position) are referenced to the stable member axis system.

Figure V.C-1 is a time history of the one sigma uncertainty in navigation information and of one sigma trajectory deviations in the x-axis direction. As the landing-site is approached, the x-axis errors closely approximate errors in altitude. For the first 270 seconds into the powered descent, the trajectory deviation is approximately equal to the uncertainties in the inertial system. This should be expected since the guidance law is using information from the navigation system to generate the vehicle control commands. At 270 seconds (or approximately 25,000 ft), and update is made by mixing landing-radar and inertial information. An improvement in the navigation accuracy is immediately introduced, however, the trajectory deviation slowly reduces to the accuracy of the navigation system at the end of the Fuel Optimum Phase. At the beginning of the Visibility Phase, an improvement in the indicated state is again made resulting in an altitude uncertainty and trajectory deviation at the hover of approximately 25 ft (1σ). The final error in altitude can be improved if the updating procedure is continued futher into the trajectory than was done for this analysis.

Figure V.C-2 presents the navigation uncertainties and trajectory deviations in velocity along the stable member x-axis. After the first update period, an increase in velocity deviation of 14.5 ft/sec is expected due to the guidance response to a detected error in altitude. A less severe velocity response can be expected during the second update phase.

Figure V.C-3 presents the errors in the y and z direction. The y-axis corresponds to cross track at the landing-site, and the z-axis corresponds to down range. No improvement in down range or cross track accuracy can be expected due to an update. However, the rate of increase in the likely position errors is stopped. The update in velocity along the y and z axes prevents any further increase in position uncertainties.

Figure V.C-4 shows the navigation uncertainties and trajectory deviations in the velocities along the y and z axes. The increase in z-axis velocity trajectory deviations is due to the thrust uncertainties.

Figure V.C-5 is a time history of the expected deviations in the thrust command signal from the nominal. At each discontinuity point in navigation information, a corresponding discontinuity in thrust commands is likely. A maximum thrust deviation of 260 lbs (1-sigma) can be expected to occur at initiation of VP. Figure V.C-6 shows the expected deviation in attitude command signals. The maximum likely attitude deviation occurs at 320 seconds into the powered descent trajectory. The 2.4 deg (3-sigma) likely deviation in pitch attitude is attributed to the update of altitude.

Figure V.C-7 presents the expected deviation in fuel consumption along the descent trajectory. At this time, methods of analyzing the error

characteristics of the last 10 seconds of the trajectory are not available. However, the total deviation in fuel consumption required for correction of guidance errors should be approximately equal to the last value recorded on figure V.C-6. The additional fuel required for correction of guidance errors, assuming normal error performance, is 30 lbs. (3 sigma).

Figure V.C-8 thru V.C-15 present the weighting factors used during the two update periods. ($270 \leq t \leq 290$, $\leq 350 \leq t \leq 430$) These weighting factors were generated using an optimum technique for minimizing the variance in a linear combination of inertial and radar information. (see Reference V.C-8). This technique is sometimes referred to as "Linear Filtering" or "Kalman Filtering."

VI. Summary of Normal Error Performance

Only errors accrued along the powered descent trajectory have been presented in this report. The likely errors in the LEM position, velocity and fuel consumption at the hover point are:

Altitude = 25 ft (1σ)
Downrange = 2850 ft (1σ)
Cross track = 785 ft (1σ)
Vertical velocity = 1.5 ft/sec (1σ)
Horizontal velocity = 1.8 ft/sec (1σ)
Cross track velocity = 1.5 ft/sec (1σ)
Fuel consumption = 10 lbs (1σ)

Future errors studies on the powered descent trajectory will include the primary navigation and guidance update procedure and the errors caused by sensor errors during the insertion. Other phases of the LEM mission will also be treated.

VII. Bibliography

III. A. General

A-1 Trajectory Analysis Group, Dynamics - Systems Engineering, Trajectory Characteristics During LEM Mission, I, L500-M03-10, March 8, 1963 (C)

A-2 Trajectory Analysis Group, Dynamics - Systems Engineering, Trajectory Characteristics During LEM Mission, II, LMO-500-48, May 22, 1963 (C)

A-3 Project Apollo/Lunar-Landing Mission Design Plan, NASA/MSC, March 15, 1963 (C)

A-4 Speiser, K., LEM ΔV Budget Resulting from NASA/GAEC/MIT Δ V Budget Meeting at Houston, April 29, 1963, LMO-500-37, Revision A, May 8, 1963 (C)

A-5 Nathan, A., LEM ΔV Budget, LMO-500-37 Revision D February 8, 1964 (C)

A-6 Munter, P., Adornato, R., and Patterson, G., Trajectory Documentation for Lunar Landing Operational Mission Plan, LMO-500-98, October 7, 1963 (C)

A-7 Trajectory Analysis Group, Dynamics - Systems Engineering, Trajectory Characteristics During Then LEM Mission, Revision III, LMO-500-141, January 23, 1964 (C)

A-8 Yagi, F., Speiser, K., Constants To Be Used For Trajectory Computations, LAV-500-44, April 27, 1964 (U)

A-9 R. Fleisig, Minutes Of NASA/MSC - GAEC Meeting On RCS And Δ V Budget On 12 March 1964, At Bethpage, LMO-500-167, March 25, 1964 (C)

A-10 A. Nathan, LEM ΔV Budget, LMO-500-37E, March 30, 1964 (C)

III. B. Descent

B.1 Coasting Descent Transfer Orbit

B.1-1 Adornato, R., Error Coefficients of Synchronous Orbit, PDM-323A-98, October 4, 1962 (U)

B.1-2 Nathan, A., Mapping of Synchronous Orbit Characteristics, L500-M03-6, February 28, 1963 (U)

B.1-3 Nathan, A., Mapping of Hohmann Descent Orbit Characteristics, LMO-500-96, October 1, 1963 (U)

B.1-4 F. Yagi, A. Nathan, Error Analysis of LEM Trajectories. Part 2. Results of Linear and Non-Linear Error Analysis of the Synchronous Descent Transfer Orbit, LMO-500-91, September 17, 1963 (U)

B.1-5 Nathan, A., Yagi, F., Comparison of Hohmann and Synchronous Pericynthion Condition Uncertainties, LMO-500-104, October 21, 1963 (C)

B.1-6 J. McNamara, F. Yagi, The Hohmann Descent Orbit Insertion Using The MIT/IL Guidance Equations, LMO-500-187, May 8, 1964 (U)

III. B.2 Powered Descent

B.2.1 Fuel Optimum Phase

B.2.1-1 Nathan, A., Fully Powered Descents from Circular Orbital Altitude, L500-M03-5, February 18, 1963 (U)

B.2.1-2 Nathan, A., Powered Descents from Various LEM Pericynthion Conditions, LMO-500-8, April 2, 1963 (C)

B.2.1-3 Weber, L,, Powered Descents Initiated Along Synchronous Orbits, LMO-500-46, May 24, 1963 (C)

B.2.1-4 Taenzer, E., Trajectory Analysis for Powered Descent, LTM-(B)-7005-24, October 1, 1963 (C)

B.2.1-5 G. Cherry, A Unified Explicit Technique For Performing Orbital Insertion, Soft Landing and Rendezvous With a Throttleable Rocket-Propelled Space Vehicle, MIT/IL R417, August 1963 (U)

B.2.1-6 J. McNamara, F. Yagi, A Powered Descent Trajectory Using The MIT/IL Guidance Law, LMO-500-145, February 20, 1964 (U)

III. B.2.2 Visibility Phase

B.2.2-1 Sperling, H., Preliminary Study of the Proportional Navigation Phase of the LEM Powered Lunar Descent, PDM-323A-88, September 11, 1962 (U)

B.2.2-2 Taenzer, E., Guidance With Constant Inertial Acceleration Vector, LTM-(B)-7005-19, May 3, 1963 (C)

B.2.2-3 Weber, L. and Nathan, A., Analysis of the Effects of the Line-of-Sight and Visual Bounds on the Powered Descent Trajectory, LMO-500-42, May 3, 1963 (C)

III. B.2.3 Translation, Hover, and Touchdown

B.2.3-1 Gebhard, D., Piloted Descent and Landing Techniques

and Trajectories for Use in LEM Simulator Design, L570-M03-12, February 20, 1963 (U)

B.2.3-2 Nathan, A., An Automatic Guidance Technique for Performing the Lunar Hover to Touchdown Maneuver, LMO-500-17, March 19, 1963 (C)

B.2.3-3 Sperling,H.,Rimer, M., Derivation of a Guidance-Control Technique for Automatic Lunar Landing-Hover-to-Touchdown, LMO-500-109, December 16, 1963 (U)

B.2.3-4 Munter, P., Equations for Phase A Lunar-Landing Simulation, L500-M03-7, February 17, 1963. (U)

B.2.3-5 Wood, F., Interim Report, Phase A Lunar-Hover and Landing Simulation, LMO-570-55, May 2, 1963 (C)

B.2.3-6 Freeberg, N. and Wolf, H., Lunar-Landing Simulation-Phase A - Report # 1, LED 480-5, August 19, 1963 (C)

B.2.3-7 Rimer, M., Sperling, H., Wood F., Analysis of LEM Lunar Landing Touchdown Conditions Derived for GAEC Simulator Results, LMO-500-136, February 12, 1964 (U)

B.2.3-8 Sperling,H., Rimer, M., Analysis And Performance Of An Automatic Lunar Landing System Including A Guidance And Navigation Equipment Error Study, LMO-500-110, June 23, 1964 (U)

III. C. Ascent

C.1 Powered Ascent

C.1-1 Speiser, K., The Relative Positions of the LEM-to-Apollo During the 24-Hour Period After a Delay In Hohmann Transfer, PDM-323A-91, September 13, 1962 (U)

C.1-2 Dunn, S., Fully Powered Ascent of the LEM to Low Altitude CSM Orbits, LMO-500-21, March 23, 1963 (C)

C.1-3 Dunn, S., ΔV and Burning Time for Powered Ascent, LMO-500-52, May 28, 1963 (C)

C.1-4 Dunn, S., Nominal Ascent Pitch Program and Corresponding Error Analysis, LMO-500-54, June 14, 1963 (C)

C.1-5 Murra, F., A Generalized Study of Elliptic Transfer Orbits Between LEM and CSM Lunar Parking Orbits, LMO-500-30, April 17, 1963 (C)

C.1-6 Dunn, S., The Sensitivity of Ascent Trajectories to Attitude Limit Cycles, LMO-500-53, June 13, 1963 (C)

C.1-7 Dunn, S., Relation of Ascent ΔV To Vertical Rise Time, LMO-500-57, June 17, 1963 (C)

C.1-8 Dunn, S., Revised Nominal Ascent Pitch Programs and Manual Execution Error Analysis, LMO-500-63, August 19, 1963 (C)

III. C. 2 Coasting Ascent

C.2-1 Rothstein, H., Sullivan, G. and Cook, J., Effects of Ascent Injection Errors and Time of Midcourse Corrections on ΔV Requirements, L500-M03-9, March 30, 1963 (C)

C.2-2 Adornato, R., A Comparison of Lunar Ascent Using a Parking Orbit vs. Direct Ascent, LMO-500-107, October 23, 1963 (C)

III. C. 3 Rendezvous

C.3-1 Greene, S., LEM Rendezvous Trajectory Analysis, LMO-500-22, April 1, 1963 (C)

C.3-2 Tucker, L, and Cook, J., Digital Program for the Analysis of Automatic Rendezvous and Docking, LMO-500-32, April 17, 1963 (C)

C.3-3 Hamilton, T. and Greene, S., Rendezvous ΔV Requirements for the Reaction Control Subsystem, LMO-500-45, May 15, 1963 (C)

C.3-4 Hamilton, T., Nominal Rendezvous Trajectories, LMO-500-61, July 3, 1963 (C)

C.3-5 Hamilton, T., Effects of Thrust Misalignment and Thrust Variation Errors on Rendezvous, LMO-500-81, August 8, 1963 (C)

C.3-6 Hamilton, T., Characteristics of Nominal Rendezvous Trajectories, LMO-500-102, October 14, 1963 (C)

III. C. 4 Docking

C.4-1 Greene, S., Equations of Motion for LEM Docking Simulation, L500-M03-3 February 16, 1963 (U)

C.4-2 Russo, J., NAA Docking Simulation Study, LMO-570-48, April 23, 1963 (C)

C.4-3 Tucker, L. and Cook, J., Results of Preliminary Automatic Docking Analysis, LMO-500-36, April 22, 1963 (C)

V. Error Analysis

1. Yagi, F., Nathan, A., Error Analysis Of LEM Guidance System. Part 1. Mathematical Theory And Techniques For Synchronous Descent Portion, LMO-500-72, July 22, 1963 (U)

2. Yagi, F., Nathan, A., Error Analysis Of LEM Trajectories. Part 2. Results Of Linear and Non-Linear Error Analysis Of The Synchronous Descent Transfer Orbit, LMO-500-91, September 17, 1963 (C)

3. Yagi, F., McNamara, J., Error Analysis of LEM Guidance System. Part 3. Linear Error Analysis Of The Inertial Measurement Unit During Powered Descent - Mathematical Theory, LMO-500-117, November 5, 1963 (U)

4. McNamara, J., Yagi, F., Error Analysis of LEM Guidance System. Part 4 Linear Analysis of the Inertial Measurement Unit (IMU)During Descent-Results, LMO-500-126, June 25, 1964

5. Nathan, A., Yagi, F., Error Analysis of LEM Trajectories. Part 5. Linear Statistical Analysis Of Powered Flight Trajectories Under Explicit Guidance - Mathematical Tehory, LMO-500-125, December 30, 1963 (U)

6. Nathan, A., Error Analysis Of LEM Trajectories. Part 6. Typical Trajectory Dispersions During Powered Descent Using The MIT/IL Explicit Guidance Law, LMO-500-139, January 9, 1964 (C)

7. Nathan, A., Error Analysis Of LEM Trajectories. Part 7. Mathematical Theory For The Analysis Of the Effects Of Correlation Between Navigation System Uncertainties With Trajectory Deviations. LMO-500-195, to be issued. (U)

8. Nathan, A., Error Analysis Of LEM Trajectories. Part 8. A Method For Mixing Inertial Navigation And Landing Radar Data And The Associated Error Analysis. LMO-500-196, to be issued. (U)

9. Felleman, P., Transmittal of Initial Covariance Matrices, MIT Correspondence AG (79-64), January 25, 1964. (U)

10. Monthly Technical Progress Report, MIT-E 1306, Jan. - Feb. 1963 (C)

11. Grant, F., IMU Error Data For Apollo Trajectories, MIT Report E-1212 (Preliminary), September 1962. (C)

12. MIT/IL, Radar Requirements For Primary Guidance And Navigation Operation, R-404, April 1963. (C)

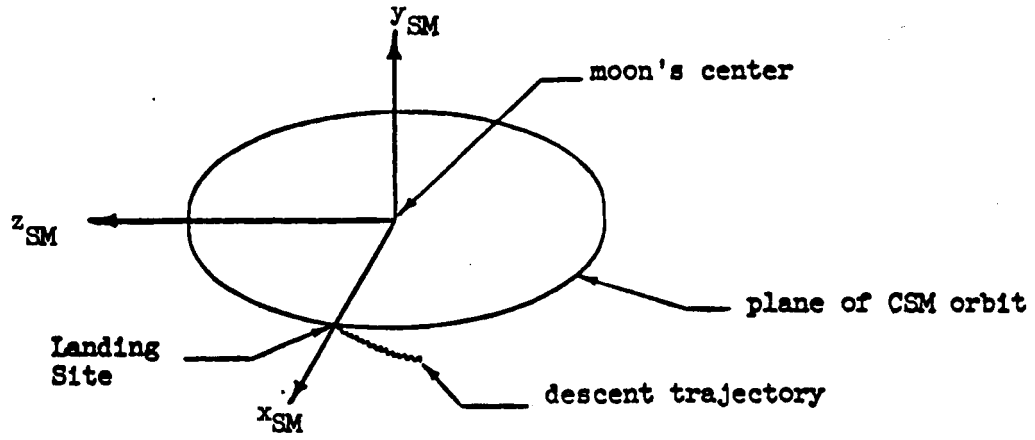

FIGURE II-1

STABLE MEMBER AXIS SYSTEM

σ = Longitude
λ = Latitude
r = Radial Position

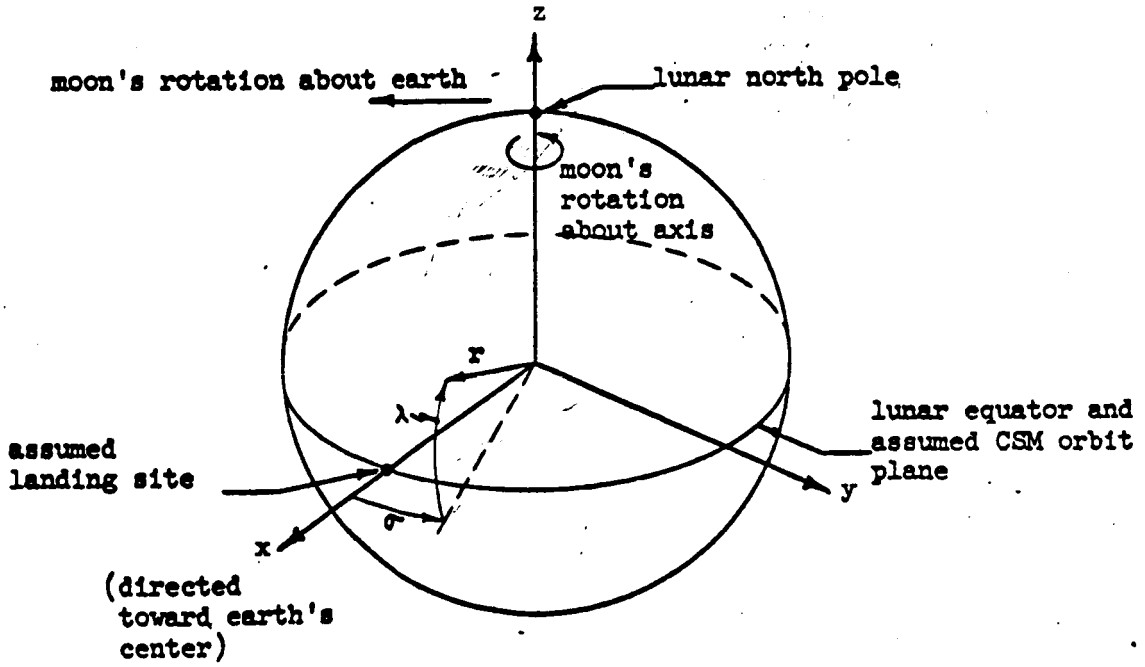

FIGURE II-2

SELENOGRAPHIC AXIS SYSTEM

FIGURE II-3

LEM BODY AXIS SYSTEM

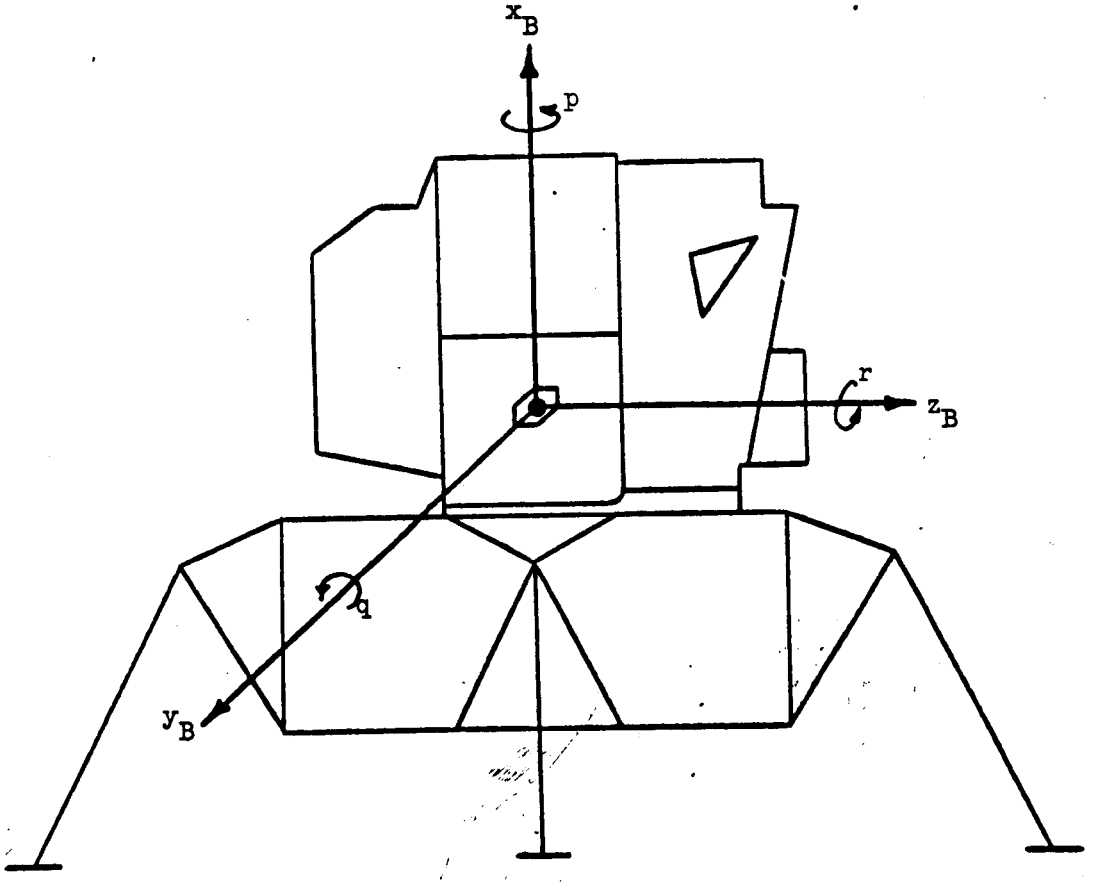

Body Axis Angular Rates

q pitch rate

r pilot roll rate

p pilot yaw rate

FIGURE II-4

STABLE MEMBER AXES ROTATED
INTO LEM BODY AXES

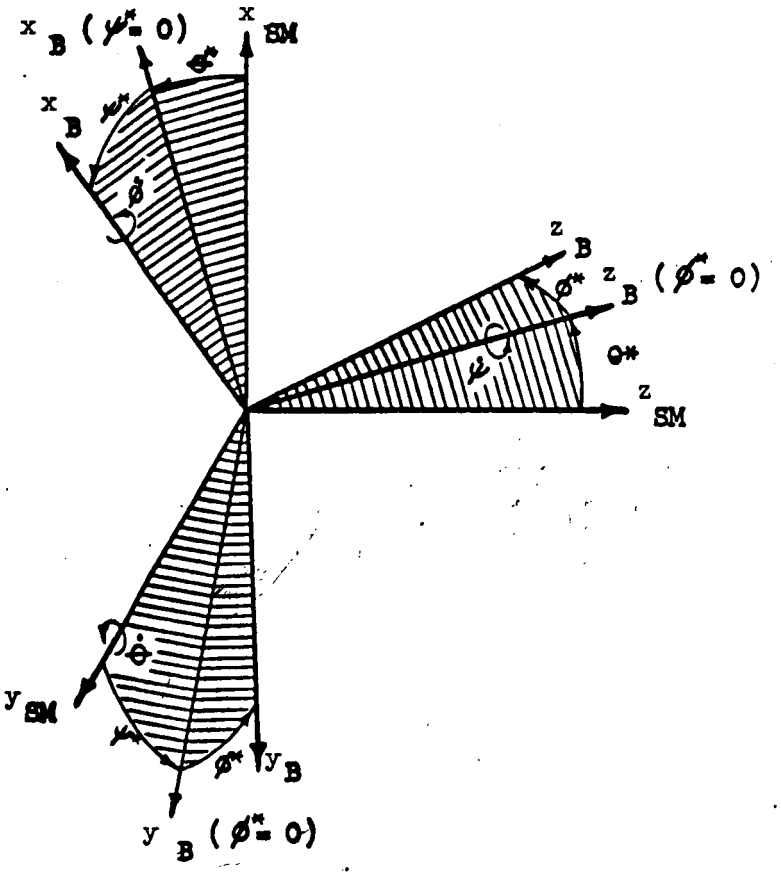

FIGURE II-5

ROTATION OF STABLE MEMBER AXES INTO LOS AXES

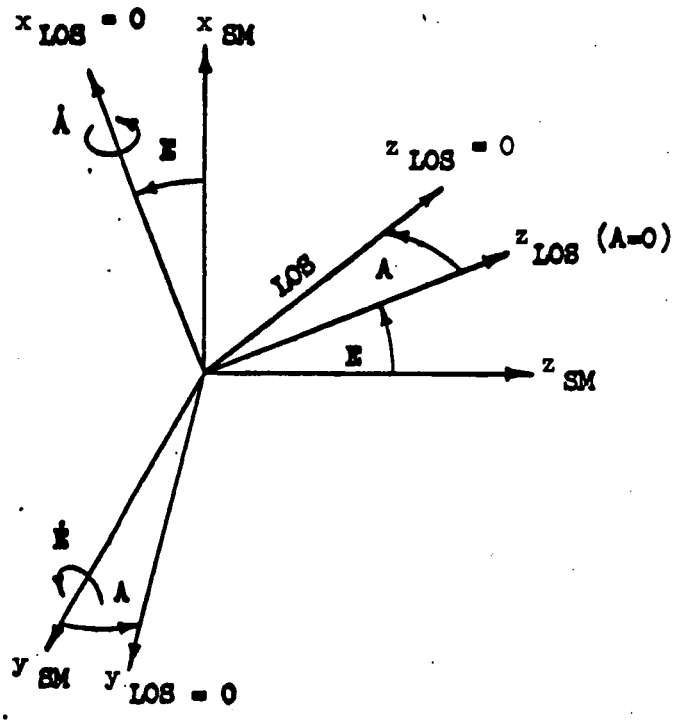

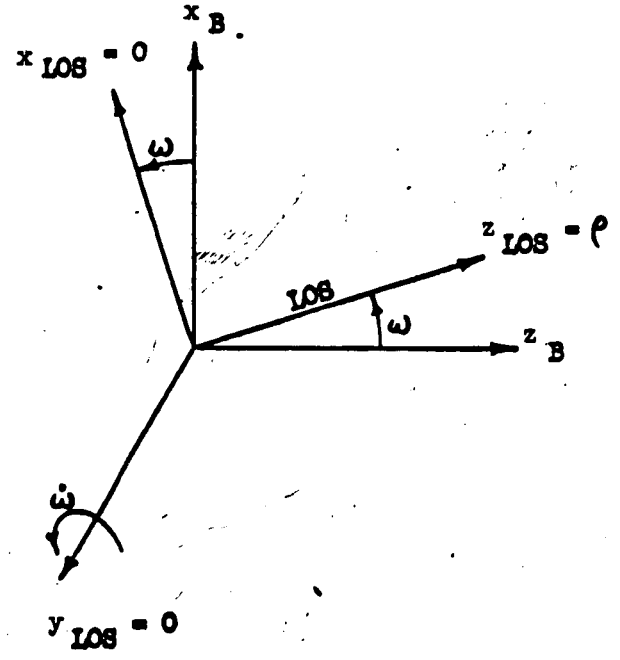

Assume
($\psi = 0, \phi = 0$)

FIGURE II-6

ROTATION OF LEM BODY AXES INTO LOS AXES

SECTION III

FIGURE B-1

DESCENT PHASE

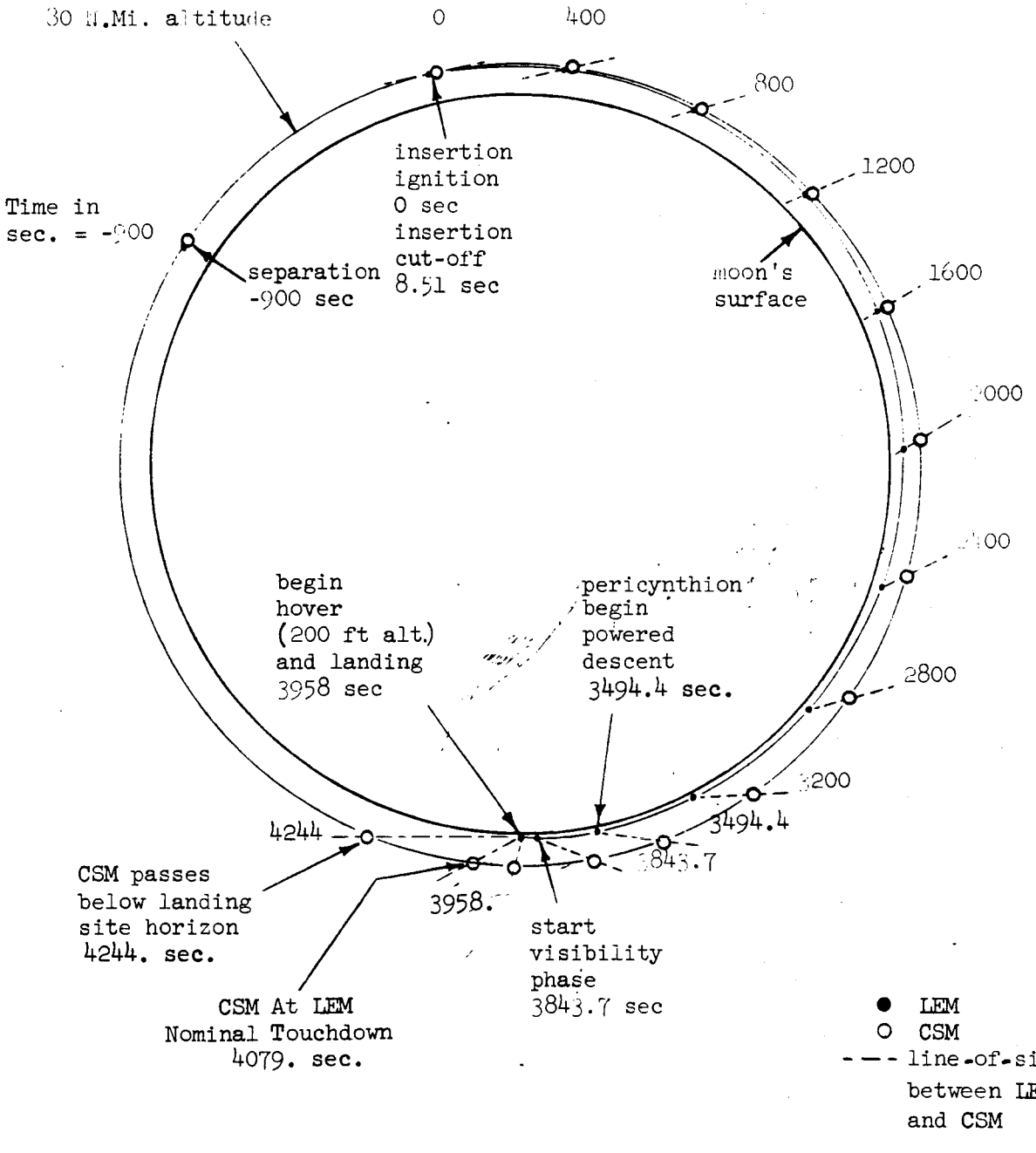

SECTION III FIGURE B.1-1

INSERTION INTO HOHMANN ORBIT

AT BURNOUT
T = 8.51 SEC
ΔV = 97.33 FT/SEC
THRUST ACCEL. = 11.495 FT/SEC²
ALT. = 486090.2 FT

THRUST ACCELERATION (FT/SEC²)

11.500
11.490
11.480
11.470
11.460
11.450
11.440
11.430
11.420
11.410
11.400
11.390
11.380

THRUST ACC.

ALT.

8.51 SEC

ALTITUDE ABOVE MOON SURFACE (FT)

.2
.1
486090.0
486089.9
.8
.7
.6
.5
.4
486089.3

CSM ORBIT = 80 NM
PERICYNTHION = 50,000 FT

I_{SP} = 301 SEC
CONSTANT THRUST = 10,500 LB
$(T/W)_o$ = .851

0 2 3 4 5 6 7 8 9

TIME (SEC)

INSERTION INTO HOHMANN ORBIT

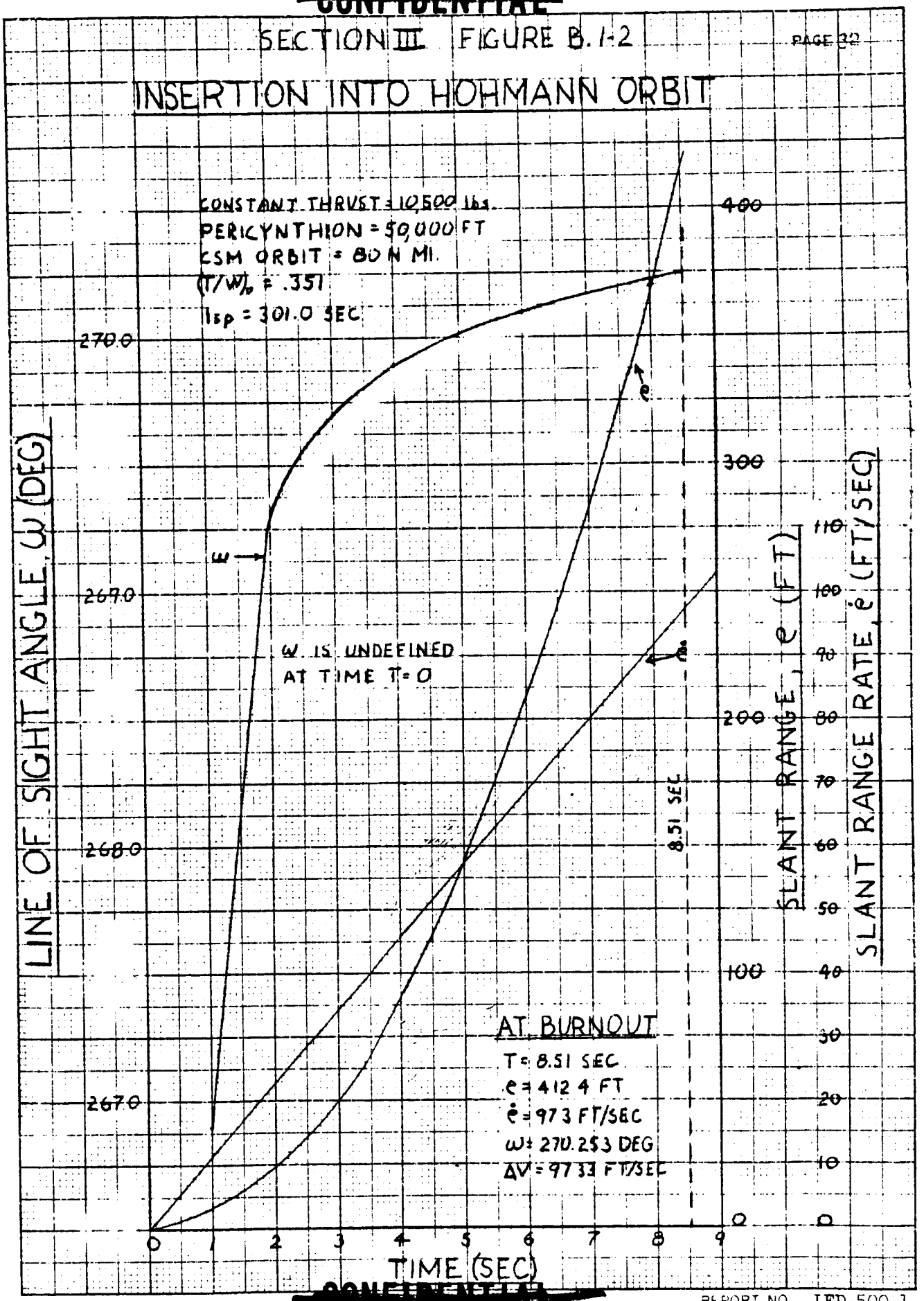

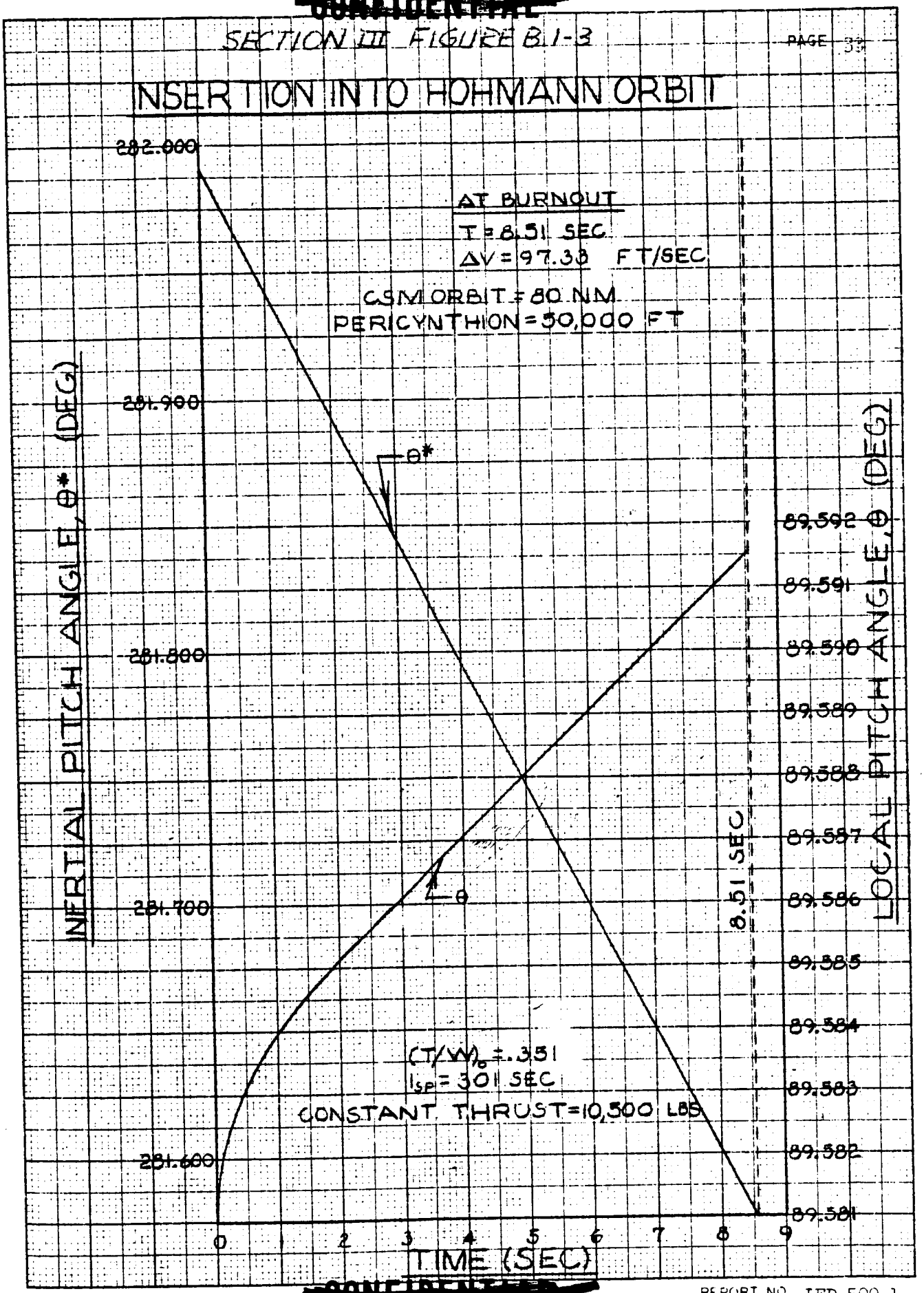
INSERTION INTO HOHMANN ORBIT
AT BURNOUT
T = 8.51 SEC
ΔV = 97.38 FT/SEC
CSM ORBIT = 80 NM
PERICYNTHION = 50,000 FT
282.000
281.900
281.800
281.700
281.600
INERTIAL PITCH ANGLE, θ* (DEG)
θ*
θ
8.51 SEC
89.592
89.591
89.590
89.589
89.588
89.587
89.586
89.585
89.584
89.583
89.582
89.581
LOCAL PITCH ANGLE, Φ (DEG)
(T/W)o = .351
Isp = 301 SEC
CONSTANT THRUST = 10,500 LBS
0
2
3
4
5
6
7
8
9
TIME (SEC)

COASTING DESCENT HOHMANN ORBIT

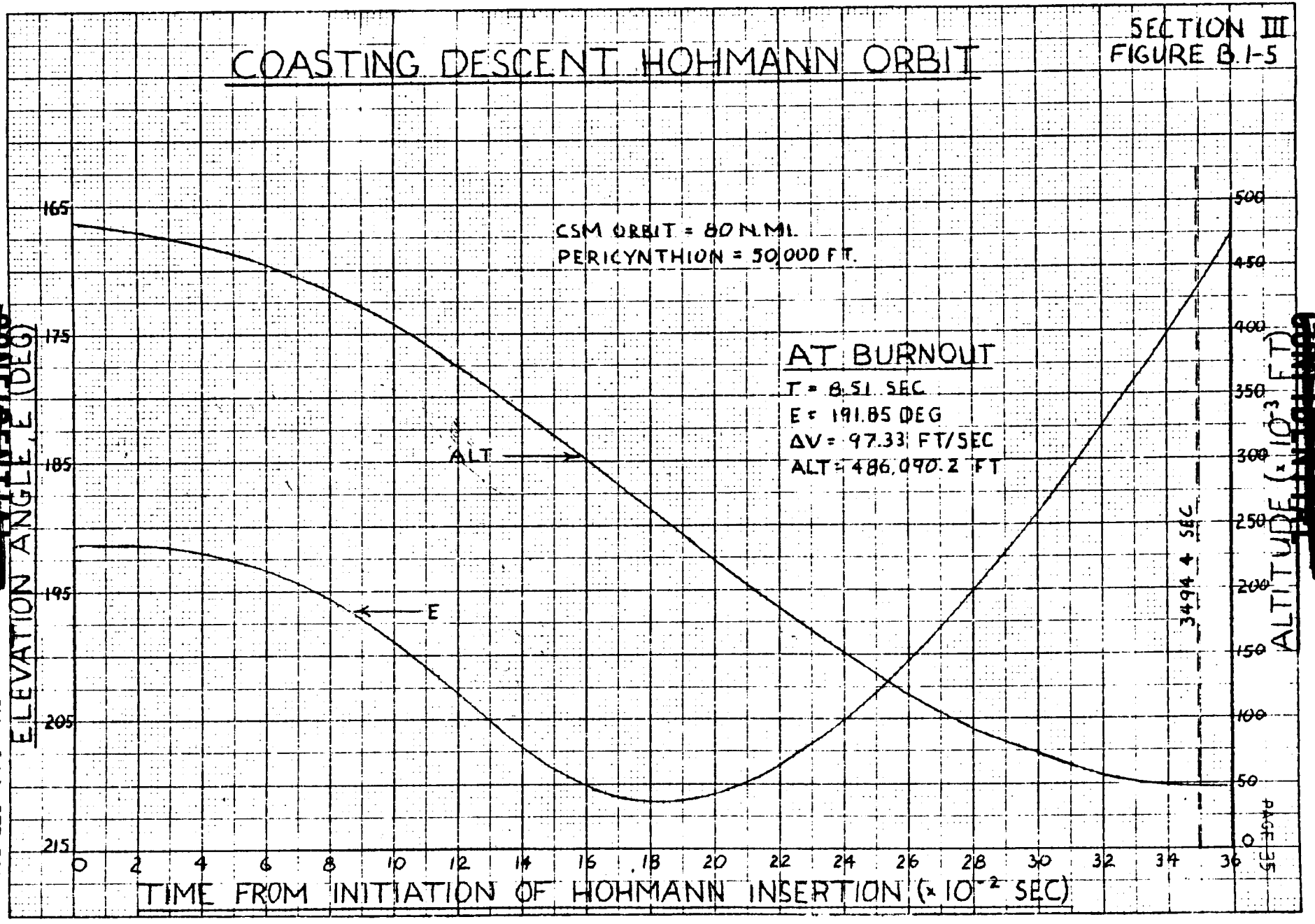

COASTING DESCENT HOHMANN ORBIT

AT BURNOUT
T = 8.51 SEC
ΔV = 97.33 FT/SEC
ρ = 412.4 FT
$\dot{\rho}$ = 97.3 FT/SEC

CSM ORBIT = 80NM
PERICYNTHION = 50,000 FT (AT 3494.4 SEC)

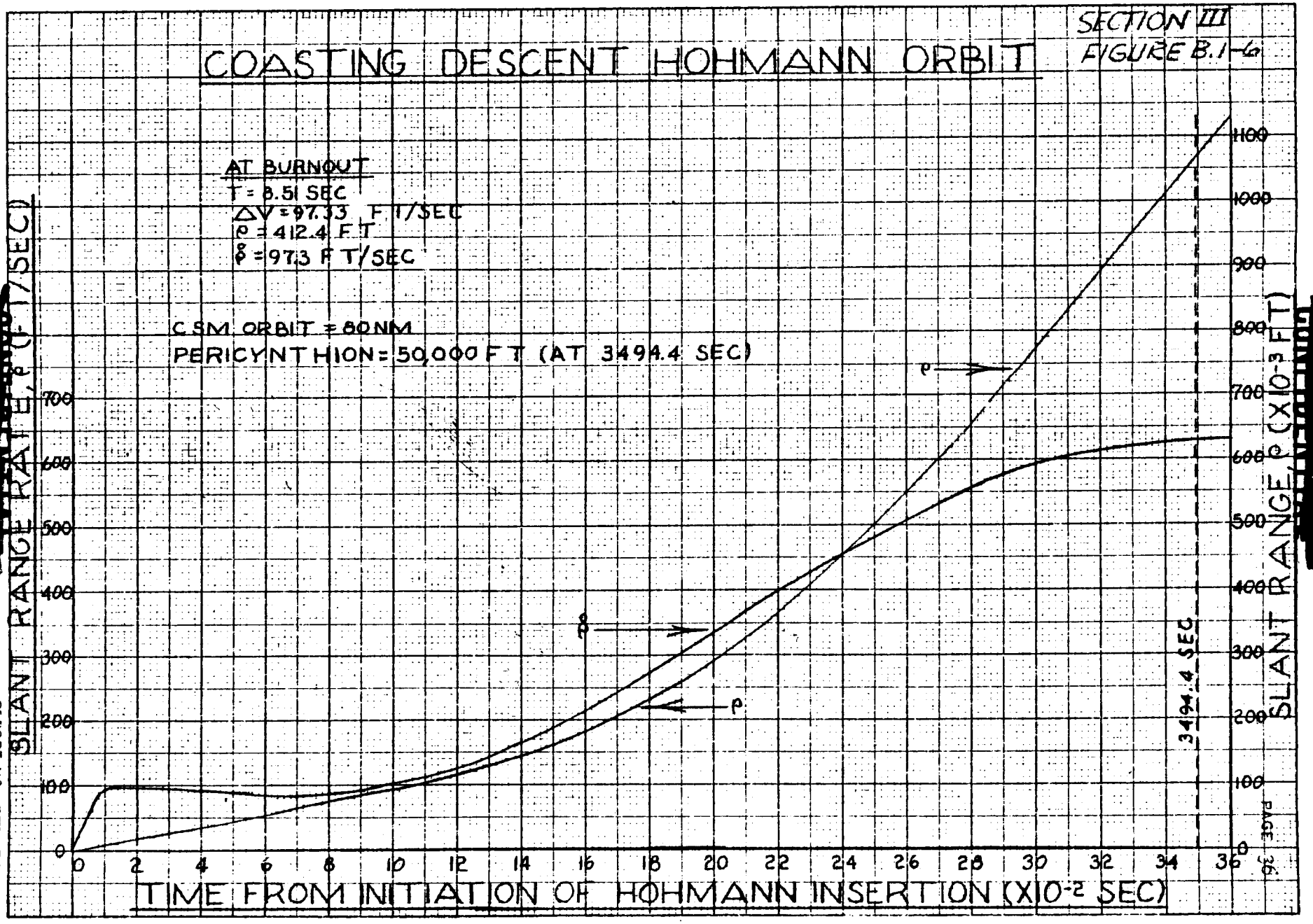

COASTING DESCENT HOHMANN ORBIT

AT BURNOUT
T = 8.51 SEC
ΔV = 97.33 FT/SEC
$\sigma_{L,CM}$ = 191.997 DEG
$\sigma_{L,CM}$ = .00382 DEG

CSM ORBIT = 80 NM
PERICYNTHION = 50,000 FT (AT 3494.4 SEC)

NEGATIVE $\sigma_{L,CM}$ INDICATES THAT CSM LEADS LEM

σ_{LEM}

$\sigma_{L,CM}$

3494.4 SEC

RELATIVE CENTRAL ANGLE, σ_{rel} (DEG)

LEM CENTRAL ANGLE σ_{LEM} (DEG)

TIME FROM INITIATION OF HOHMANN INSERTION (X10^{-2} SEC)

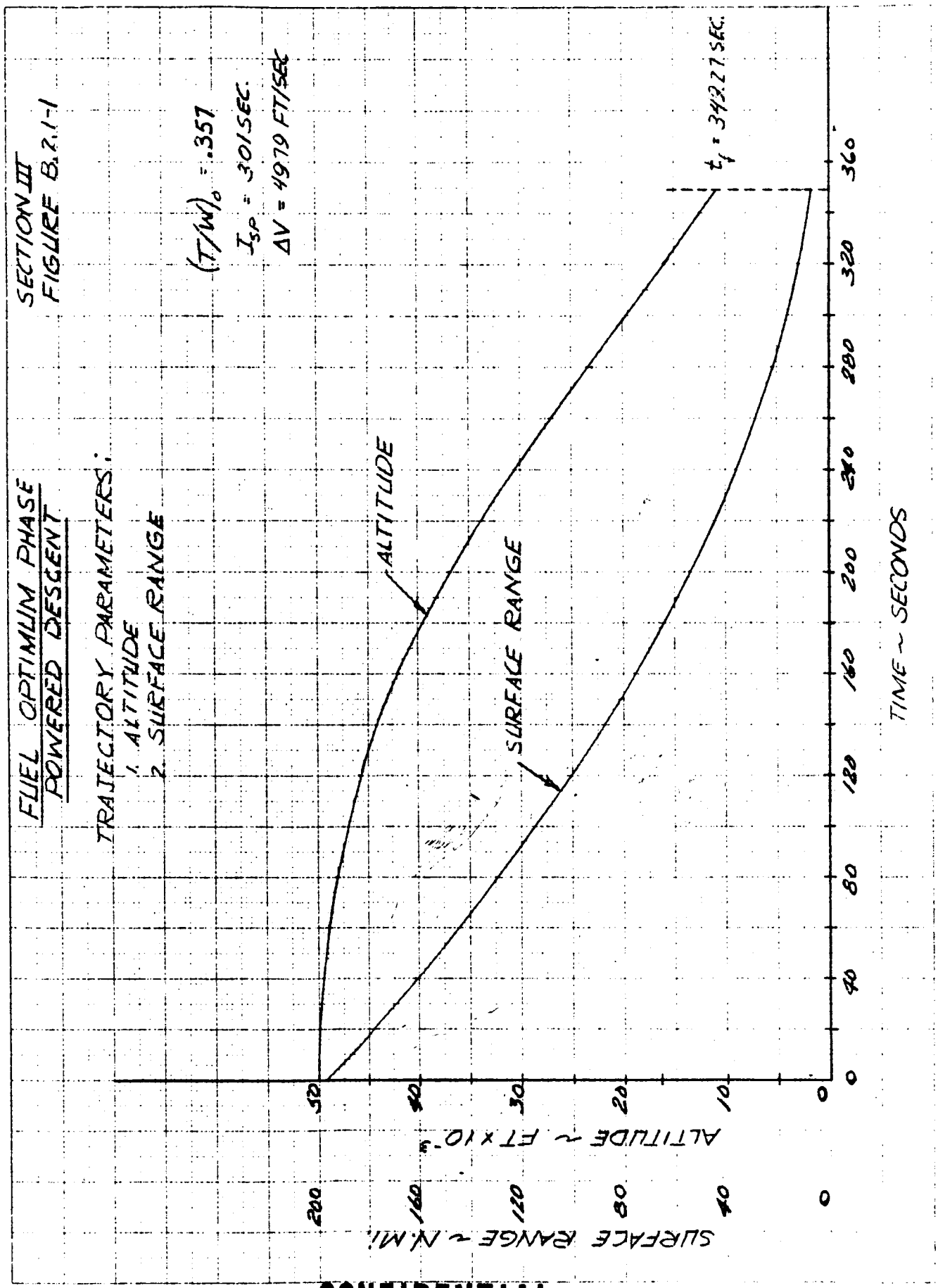
SECTION III
FIGURE 8.2.1-1
FUEL OPTIMUM PHASE
POWERED DESCENT
TRAJECTORY PARAMETERS:
1. ALTITUDE
2. SURFACE RANGE
$(T/W)_o$ = .357
I_{sp} = 301 SEC.
ΔV = 4979 FT/SEC
t_f = 342.27 SEC.
ALTITUDE
SURFACE RANGE
SURFACE RANGE ~ N.MI.
ALTITUDE ~ FT x 10⁻³
TIME ~ SECONDS
0
40
80
120
160
200
0
10
20
30
40
0
40
80
120
160
200
240
280
320
360

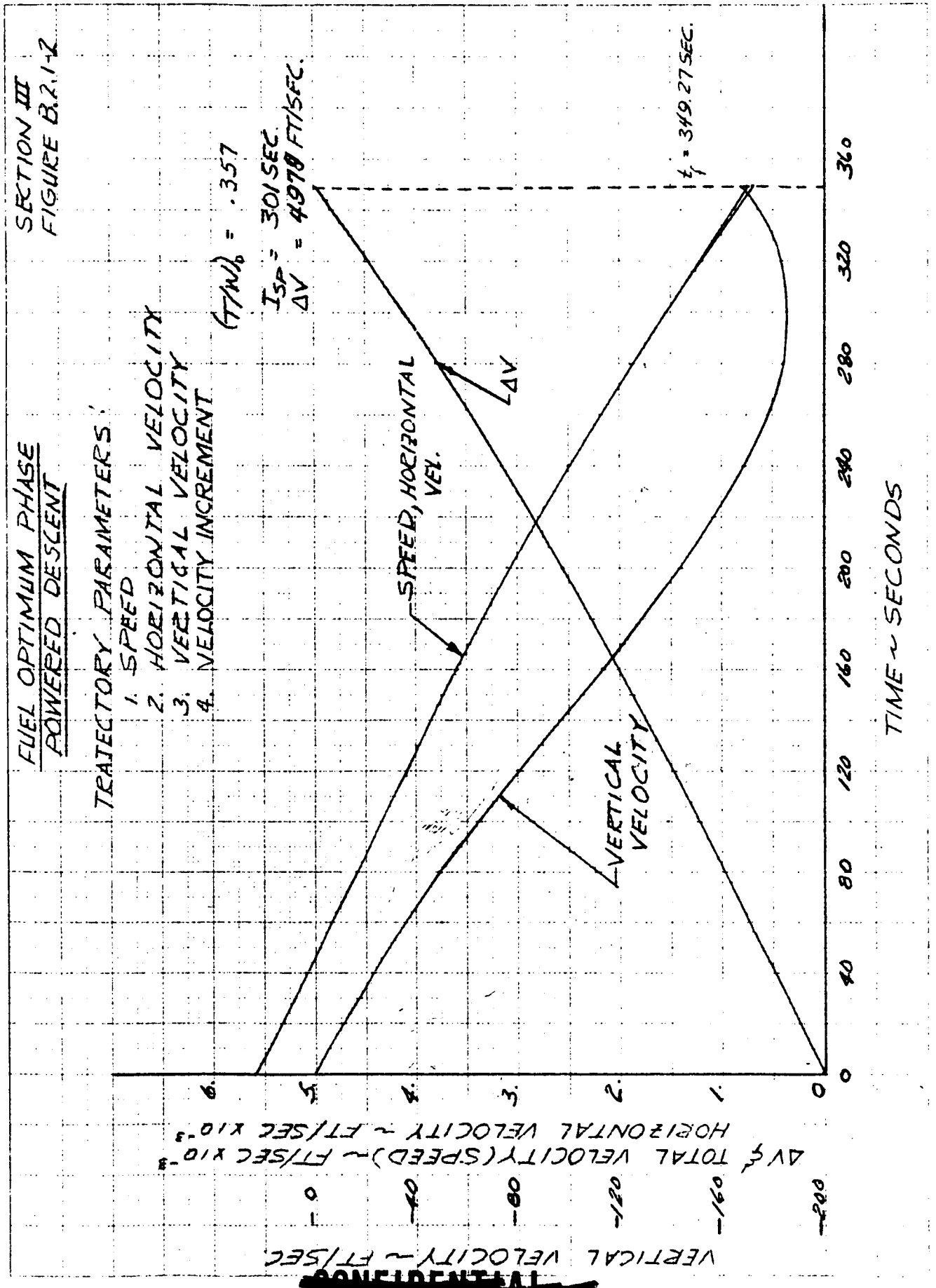
SECTION III
FIGURE 8.2.1-2
FUEL OPTIMUM PHASE
POWERED DESCENT
TRAJECTORY PARAMETERS
1. SPEED
2. HORIZONTAL VELOCITY
3. VERTICAL VELOCITY
4. VELOCITY INCREMENT
(T/W)o = .357
Isp = 301 SEC.
ΔV = 4978 FT/SEC.
tf = 349.27 SEC.
SPEED, HORIZONTAL VEL.
ΔV
VERTICAL VELOCITY
TIME ~ SECONDS
ΔV & TOTAL VELOCITY (SPEED) ~ FT/SEC x10⁻³
HORIZONTAL VELOCITY ~ FT/SEC x10⁻³
VERTICAL VELOCITY ~ FT/SEC
0
40
80
120
160
200
240
280
320
360
1.
2.
3.
4.
5.
6.
-0
-40
-80
-120
-160
-200

SECTION III
FIGURE 8.2.1-3
FUEL OPTIMUM PHASE
POWERED DESCENT
TRAJECTORY PARAMETERS
1. LEM CENTRAL ANGLE
2. CSM CENTRAL ANGLE
$(T/W)_o$ = .357
I_{sp} = 301 SEC
ΔV = 4979 FT/SEC
CSM
LEM
LANDING SITE
θ_{CM}
θ_L
t_f = 349.27 SEC
θ_{CM}
θ_L
θ_L, θ_{CM} - CENTRAL ANGLE - DEGREES
-24
-20
-16
-12
-8
-4
0
4
0
40
80
120
160
200
240
280
320
360
TIME - SECONDS

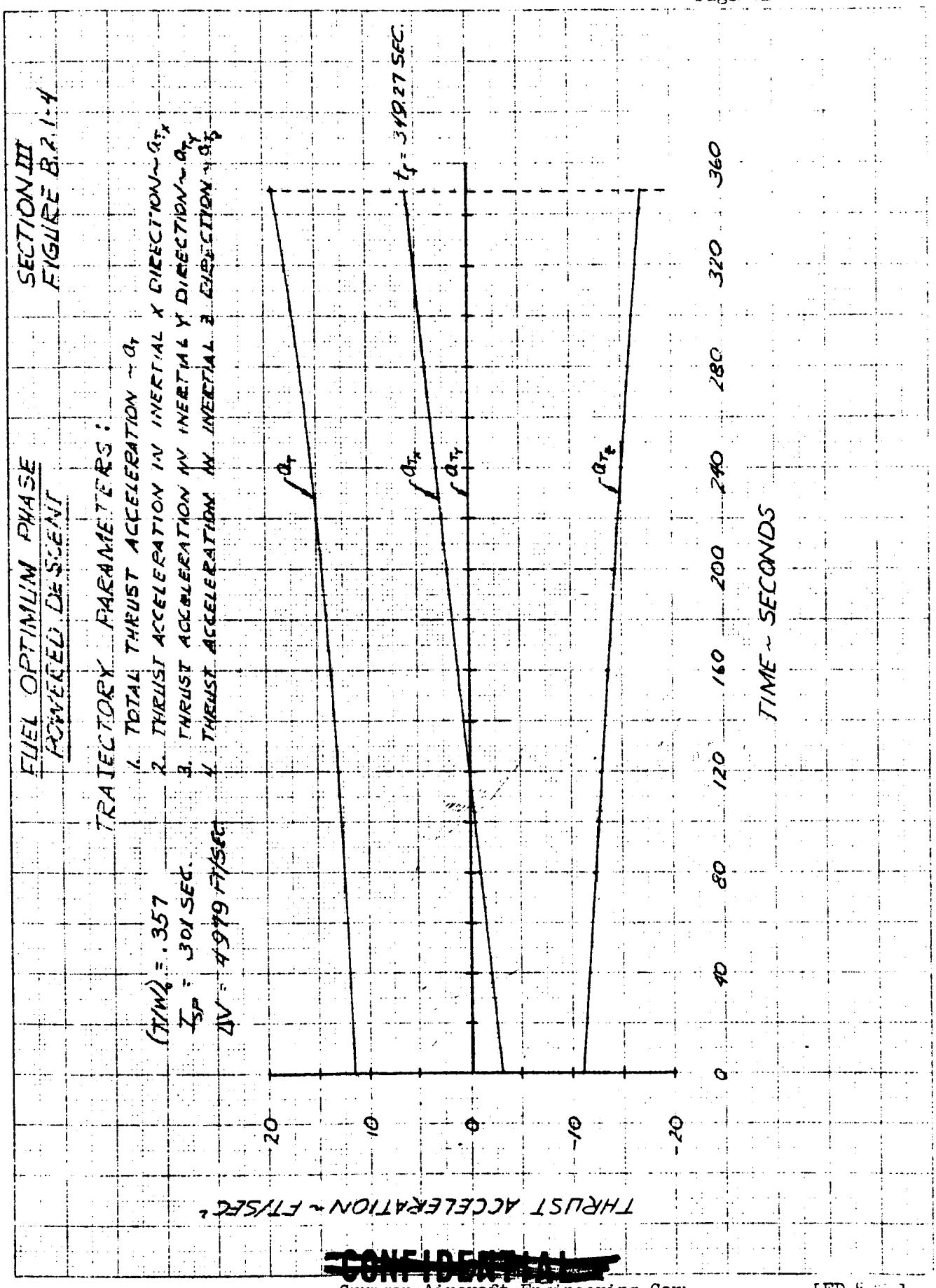

~~CONFIDENTIAL~~

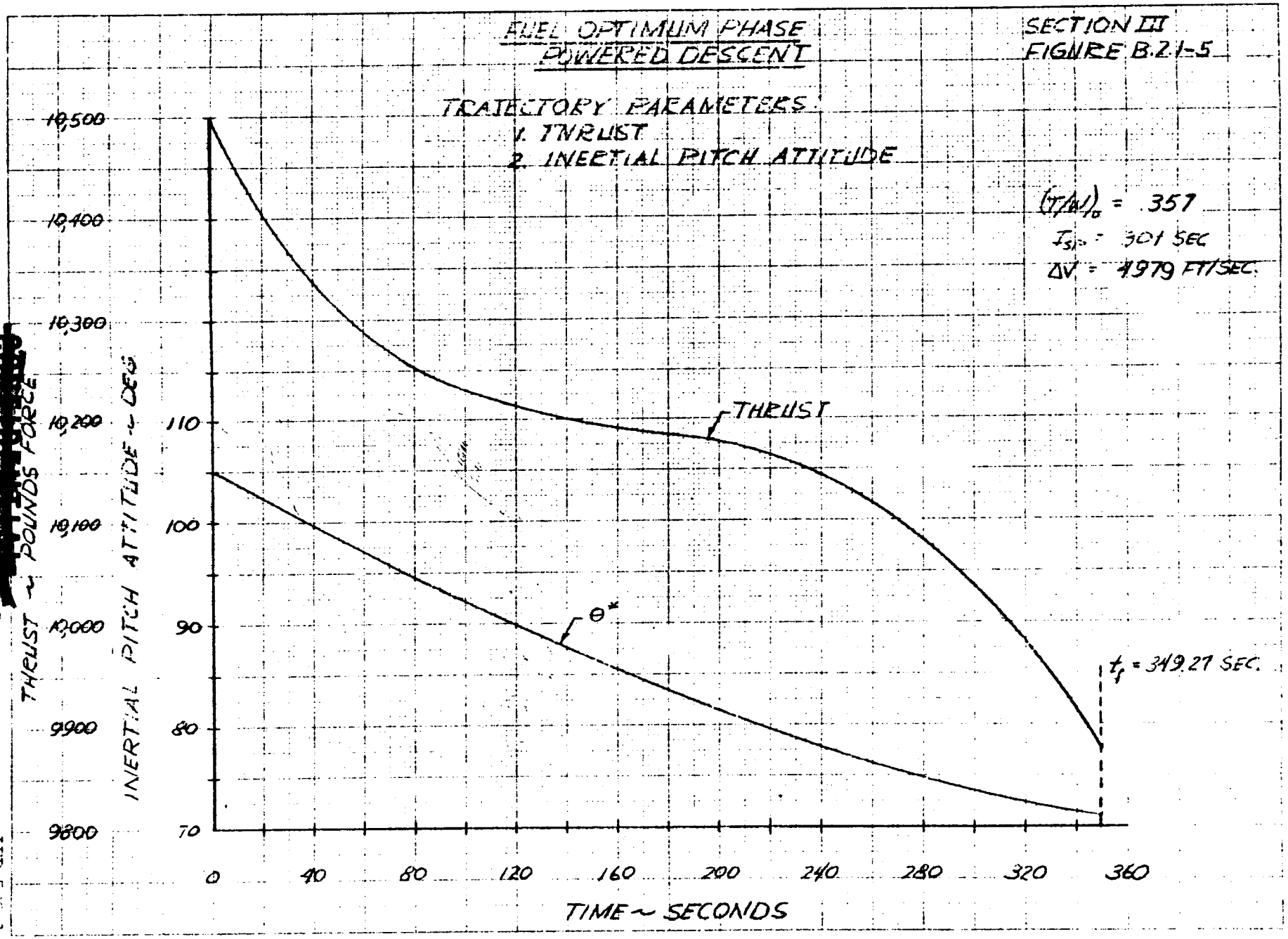

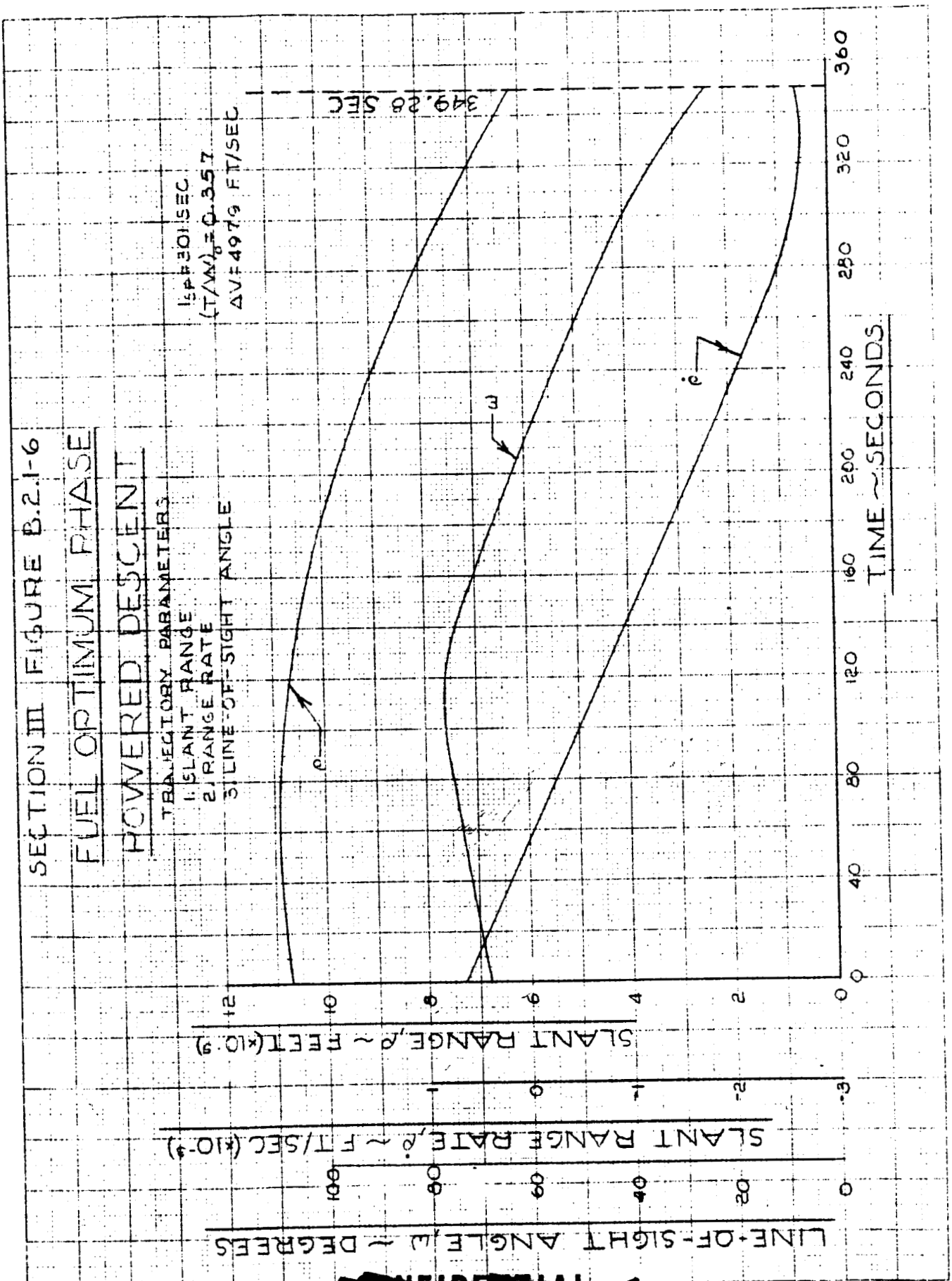
SECTION III FIGURE B.2.1-6
FUEL OPTIMUM PHASE
POWERED DESCENT
TRAJECTORY PARAMETERS
1. SLANT RANGE
2. RANGE RATE
3. LINE-OF-SIGHT ANGLE
Isp=301 SEC
(T/W)o=0.357
ΔV=4979 FT/SEC
349.28 SEC
TIME ~ SECONDS
SLANT RANGE ρ ~ FEET (×10⁻⁵)
SLANT RANGE RATE ρ̇ ~ FT/SEC (×10⁻⁴)
LINE-OF-SIGHT ANGLE ω ~ DEGREES

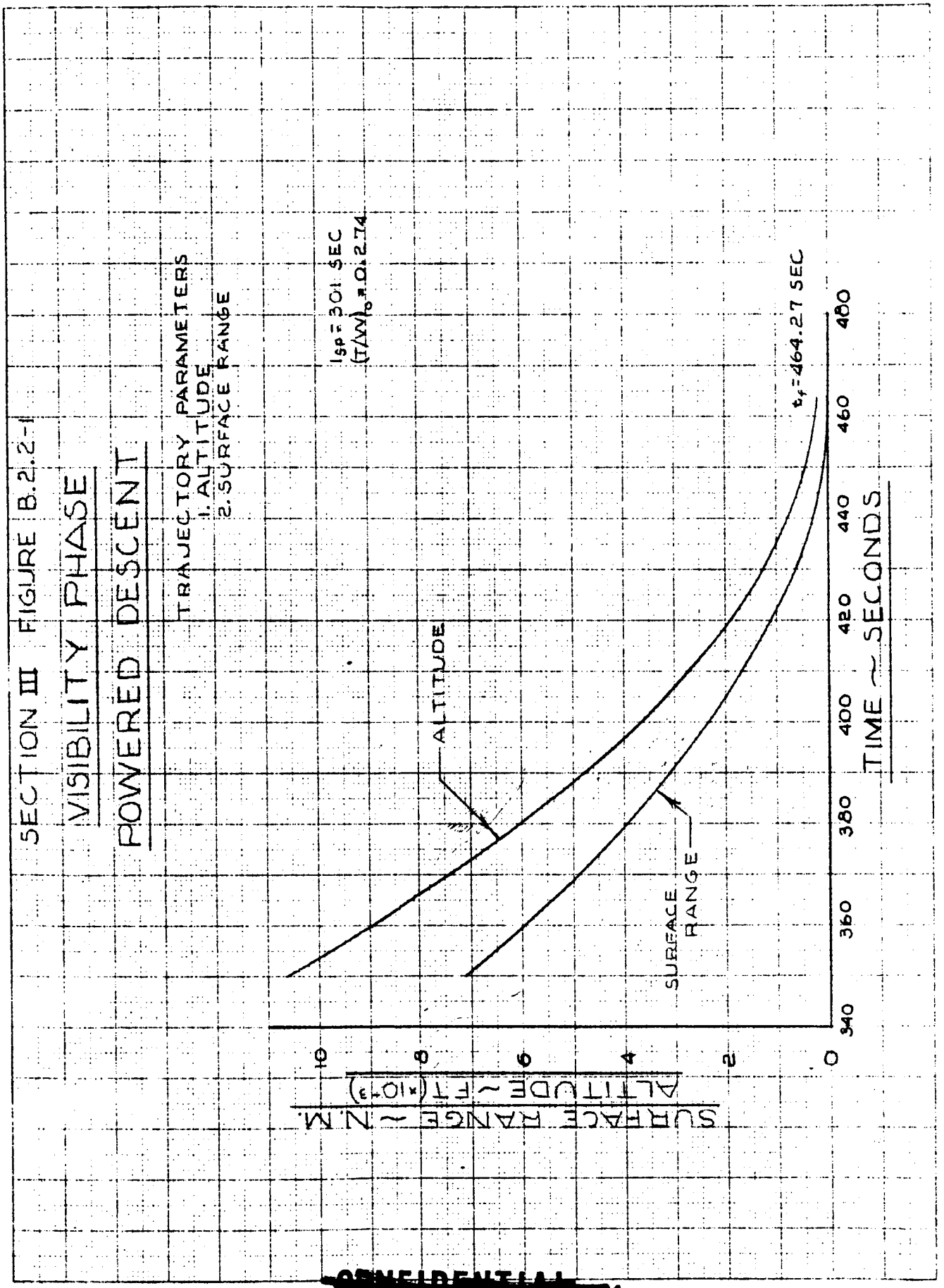
SECTION III FIGURE B.2.2-1
VISIBILITY PHASE
POWERED DESCENT
TRAJECTORY PARAMETERS
1. ALTITUDE
2. SURFACE RANGE
I_{sp} = 301 SEC
$(T/W)_o$ = 0.274
t_f = 464.27 SEC
ALTITUDE
SURFACE RANGE
TIME ~ SECONDS
340
360
380
400
420
440
460
480
0
2
4
6
8
10
SURFACE RANGE ~ N.M.
ALTITUDE ~ FT (×10⁻³)

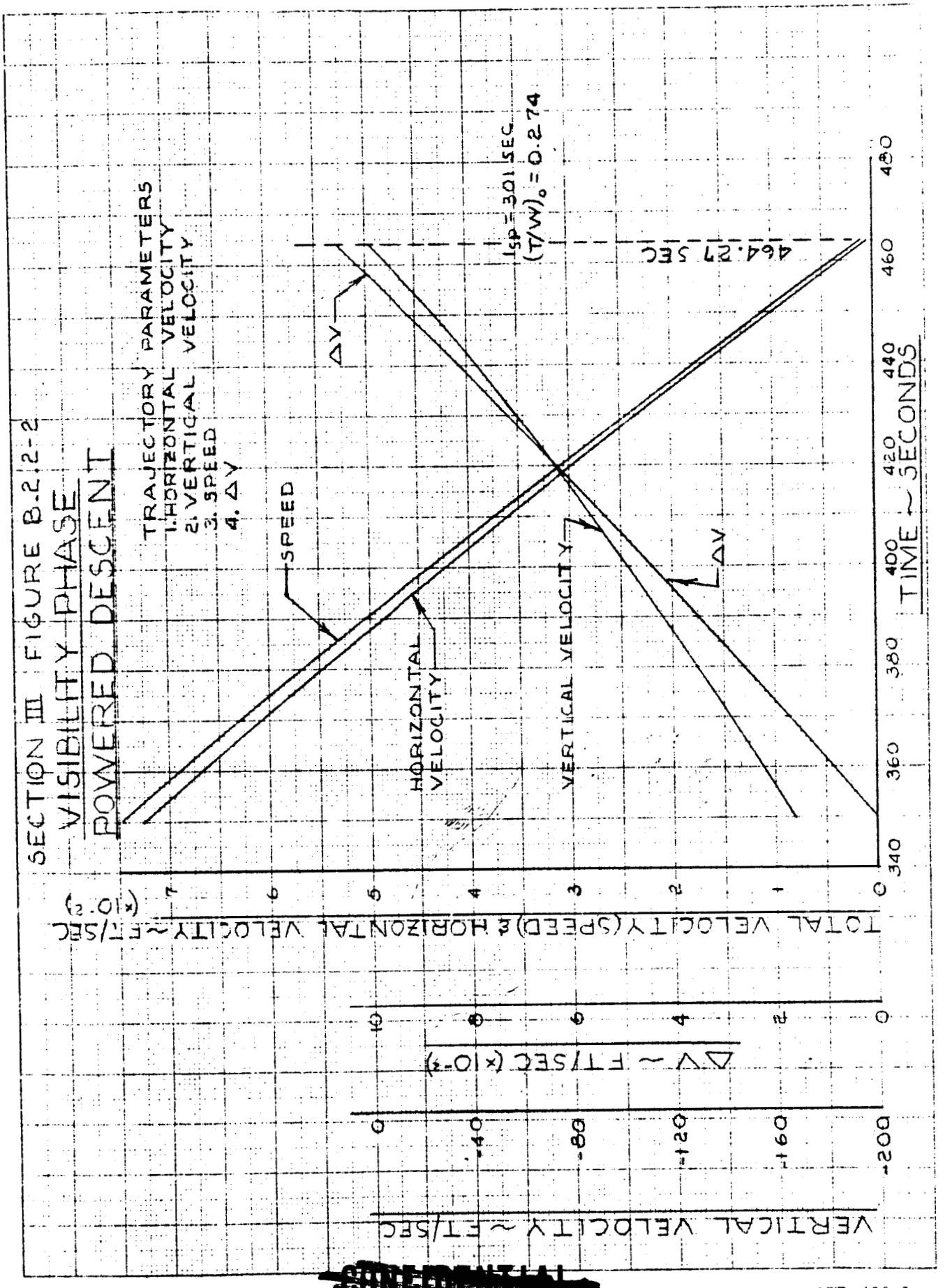
SECTION III FIGURE B.2.2-2
VISIBILITY PHASE
POWERED DESCENT
TRAJECTORY PARAMETERS
1. HORIZONTAL VELOCITY
2. VERTICAL VELOCITY
3. SPEED
4. ΔV
SPEED
HORIZONTAL VELOCITY
VERTICAL VELOCITY
ΔV
ΔV
Isp = 301 SEC
(T/W)o = 0.274
464.27 SEC
TIME ~ SECONDS
340
360
380
400
420
440
460
480
TOTAL VELOCITY (SPEED) & HORIZONTAL VELOCITY ~ FT/SEC (×10²)
0
1
2
3
4
5
6
7
ΔV ~ FT/SEC (×10⁻²)
0
2
4
6
8
10
VERTICAL VELOCITY ~ FT/SEC
0
-40
-80
-120
-160
-200

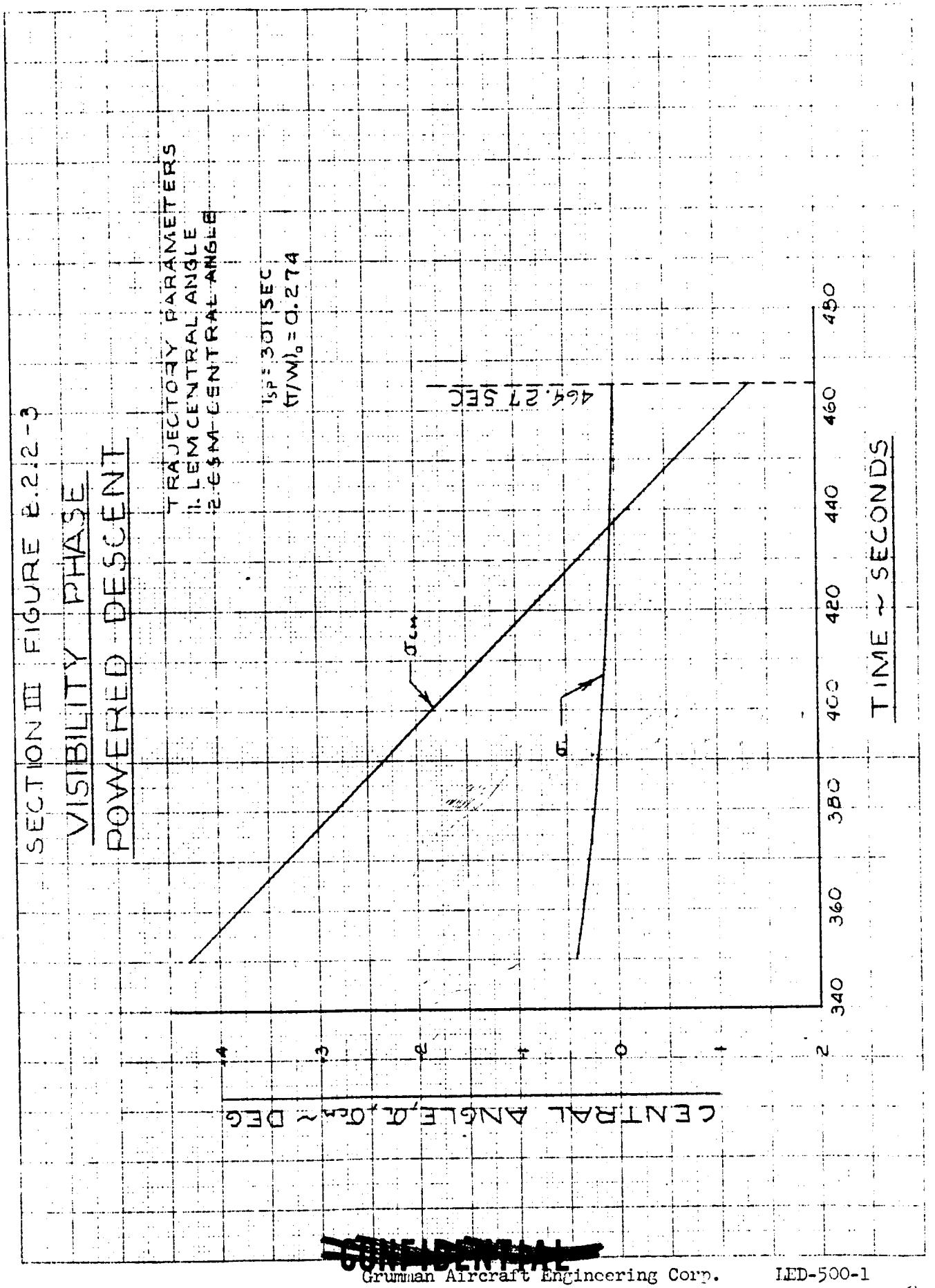
SECTION III FIGURE 2.2.2-3
VISIBILITY PHASE
POWERED DESCENT
TRAJECTORY PARAMETERS
1. LEM CENTRAL ANGLE
2. CSM CENTRAL ANGLE
I_{SP} = 301 SEC
$(T/W)_o$ = 0.274
464.27 SEC
σ_{CSM}
σ_L
CENTRAL ANGLE, σ_L, σ_{CSM} ~ DEG
TIME ~ SECONDS
-4
-3
-2
-1
0
1
2
340
360
380
400
420
440
460
480

SECTION III FIGURE B.2.2-4

VISIBILITY PHASE

POWERED DESCENT

TRAJECTORY PARAMETERS

1. TOTAL THRUST ACCELERATION $\sim A_T$.
2. THRUST ACCELERATION IN INERTIAL X DIRECTION $\sim A_{T_X}$
3. THRUST ACCELERATION IN INERTIAL Y DIRECTION $\sim A_{T_Y}$
4. THRUST ACCELERATION IN INERTIAL Z DIRECTION $\sim A_{T_Z}$

$I_{sp} = 301$ SEC

$(T/W)_o = 0.274$

464.27 SEC

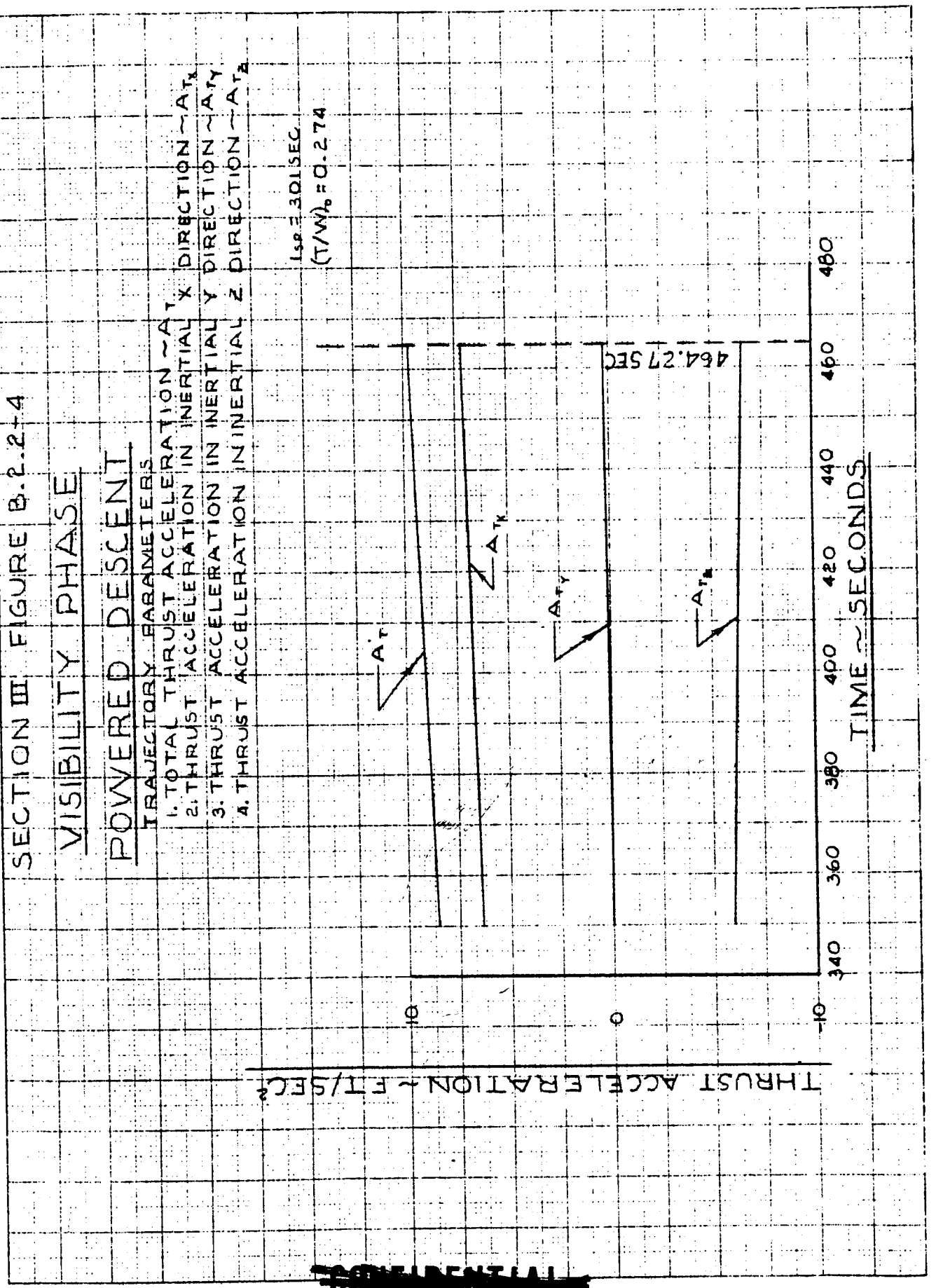

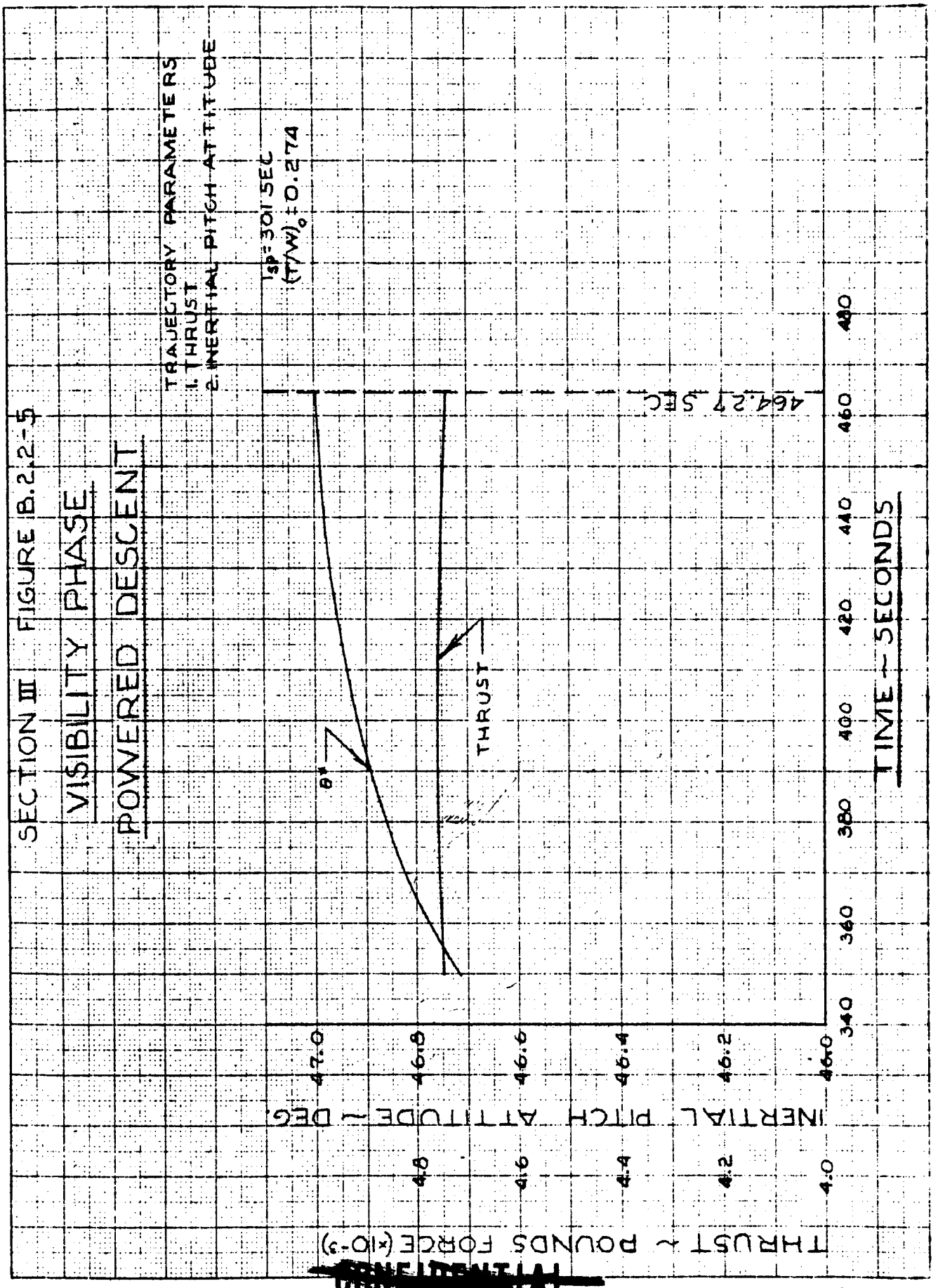

~~CONFIDENTIAL~~

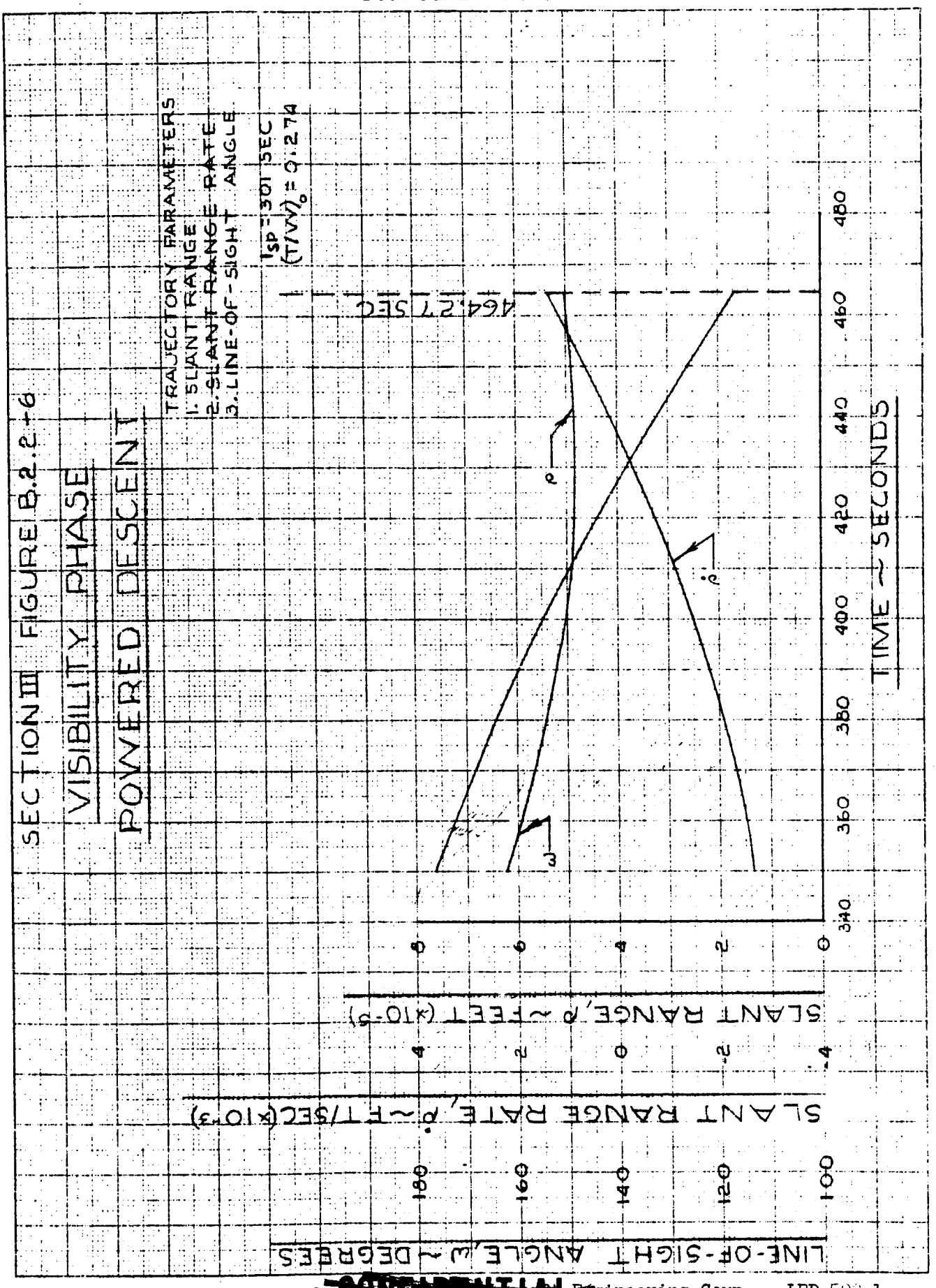
SECTION III FIGURE B.2.2-6
VISIBILITY PHASE
POWERED DESCENT
TRAJECTORY PARAMETERS
1. SLANT RANGE
2. SLANT RANGE RATE
3. LINE-OF-SIGHT ANGLE
I_{sp} = 301 SEC
$(T/W)_o$ = 0.274
464.27 SEC
TIME ~ SECONDS
SLANT RANGE, ρ ~ FEET (x10⁻⁵)
SLANT RANGE RATE, ρ̇ ~ FT/SEC (x10⁻³)
LINE-OF-SIGHT ANGLE, ε ~ DEGREES

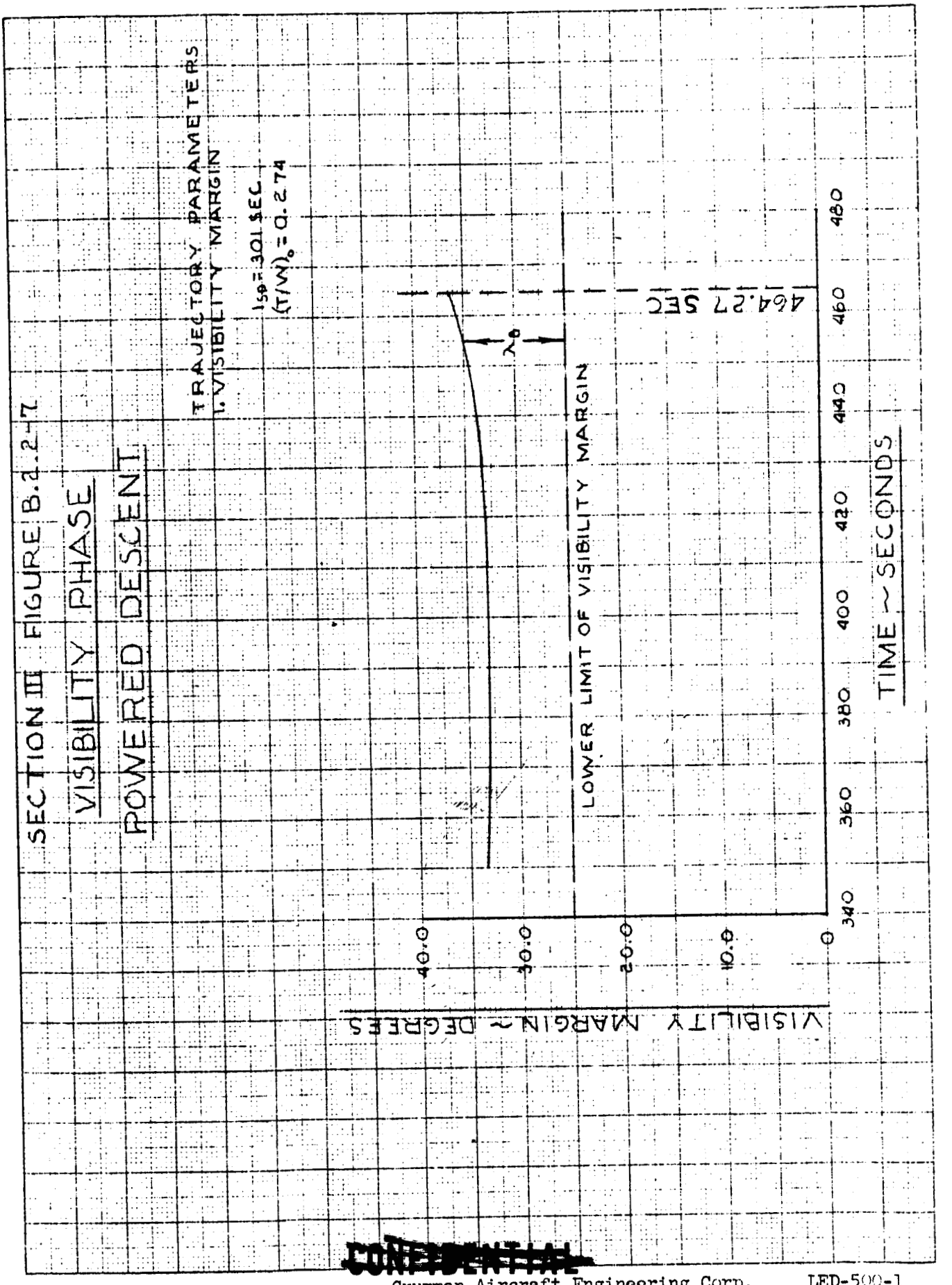
SECTION III FIGURE B.4.2-17
VISIBILITY PHASE
POWERED DESCENT
TRAJECTORY PARAMETERS
1. VISIBILITY MARGIN
I_{sp} = 301 SEC
$(T/W)_o$ = 0.274
λ_o
464.27 SEC
LOWER LIMIT OF VISIBILITY MARGIN
VISIBILITY MARGIN ~ DEGREES
40.0
30.0
20.0
10.0
0
340
360
380
400
420
440
460
480
TIME ~ SECONDS

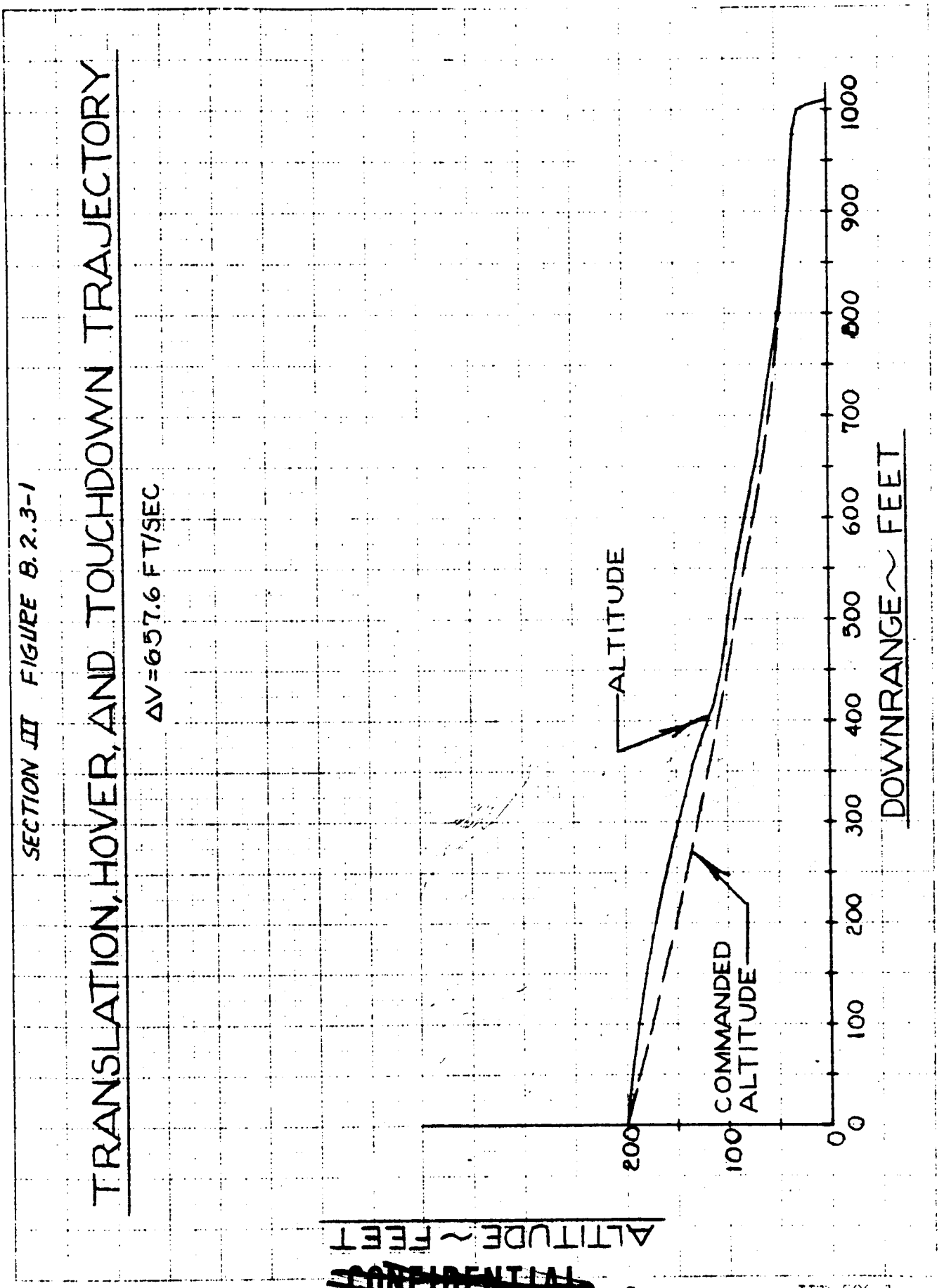
SECTION III FIGURE 8.2.3-1
TRANSLATION, HOVER, AND TOUCHDOWN TRAJECTORY
ΔV=657.6 FT/SEC
ALTITUDE
COMMANDED ALTITUDE
ALTITUDE ~ FEET
DOWNRANGE ~ FEET
200
100
0
0
100
200
300
400
500
600
700
800
900
1000

SECTION III FIGURE B.2.3-2 PAGE 52

TRANSLATION, HOVER, AND TOUCHDOWN TRAJECTORY

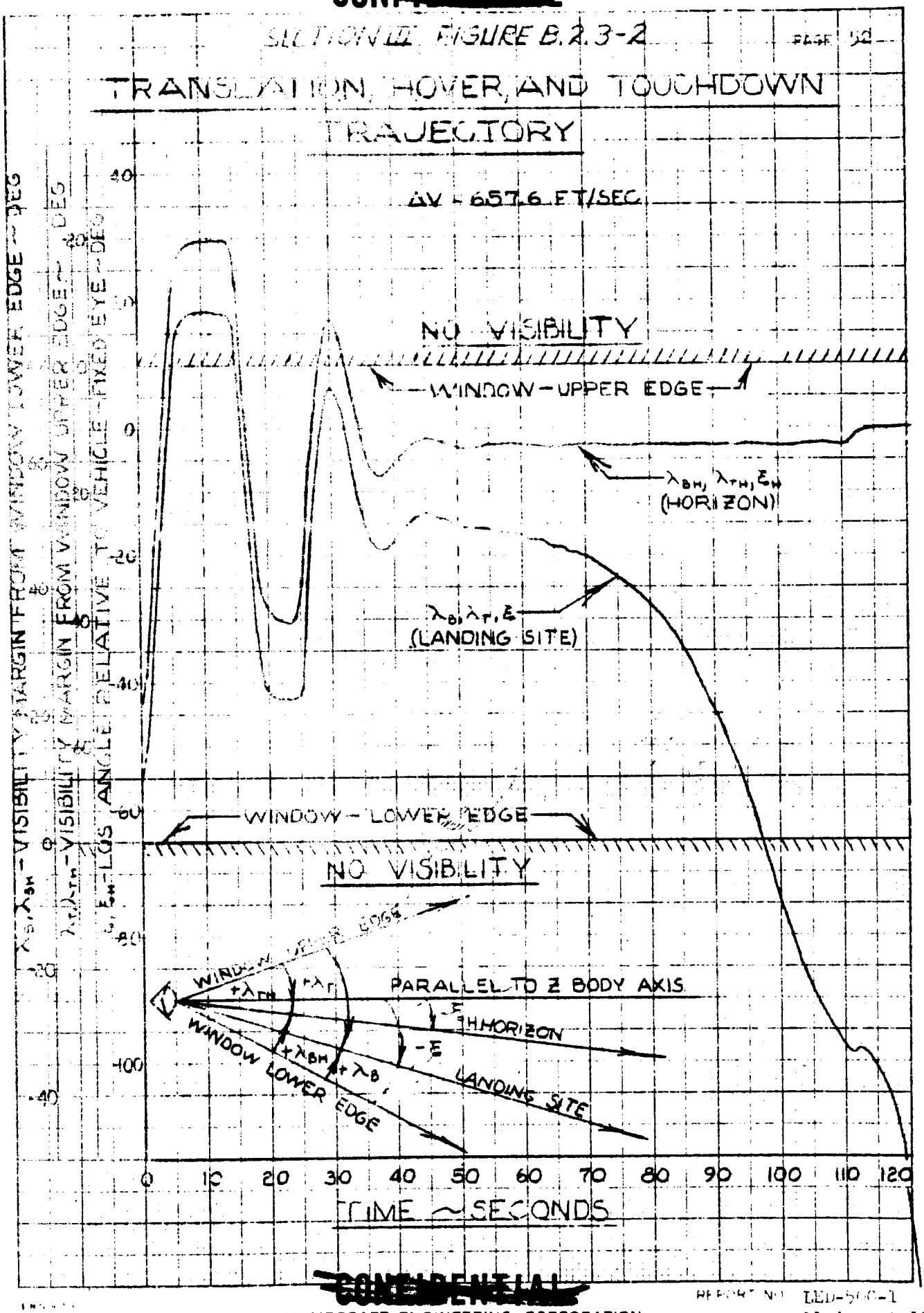

TRANSLATION HOVER, AND TOUCHDOWN TRAJECTORY

ΔV = 657.6 FT/SEC

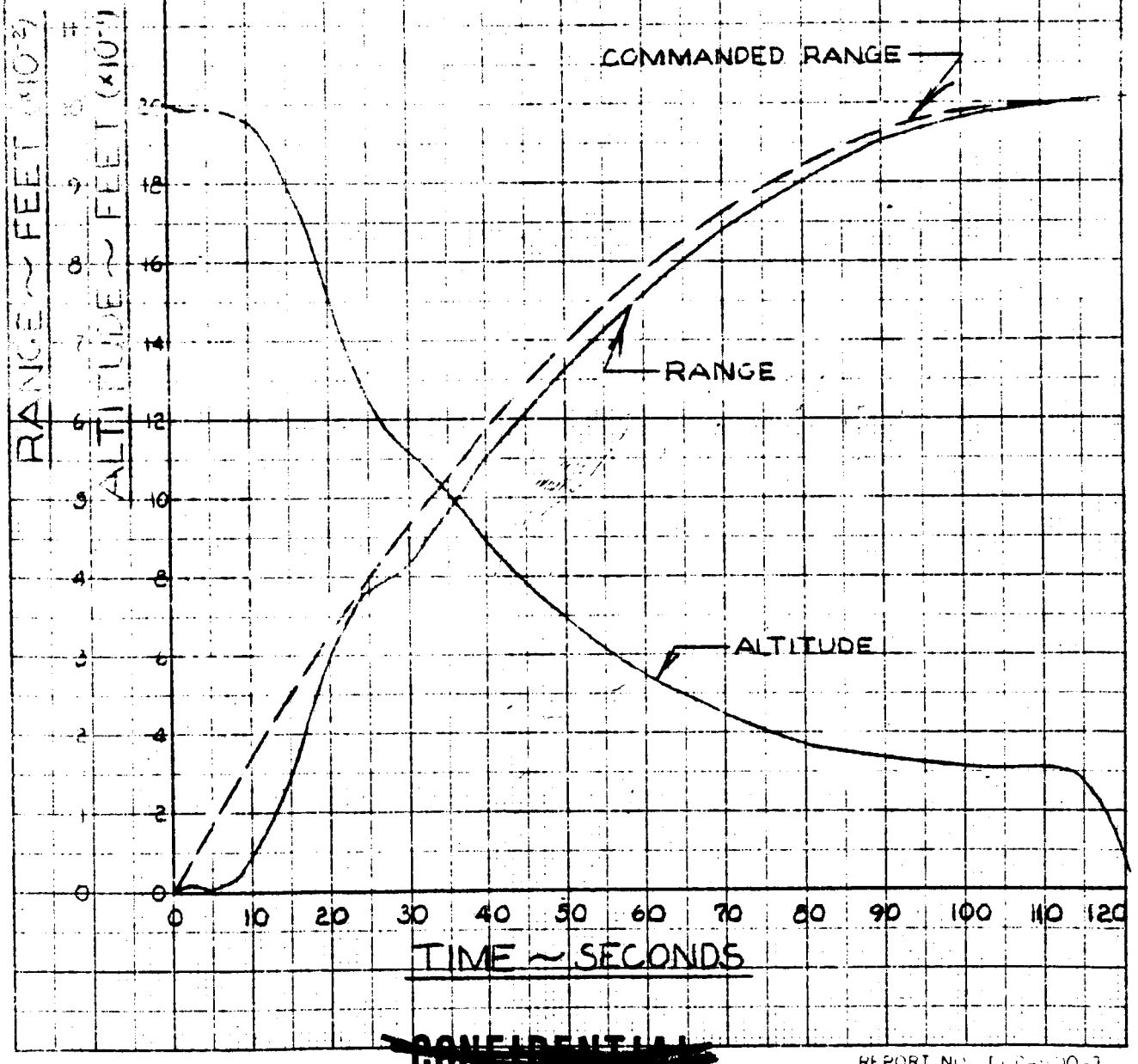

SECTION III FIGURE B.2.3-4

TRANSLATION, HOVER, AND TOUCHDOWN TRAJECTORY

ΔV = 657.6 FT/SEC

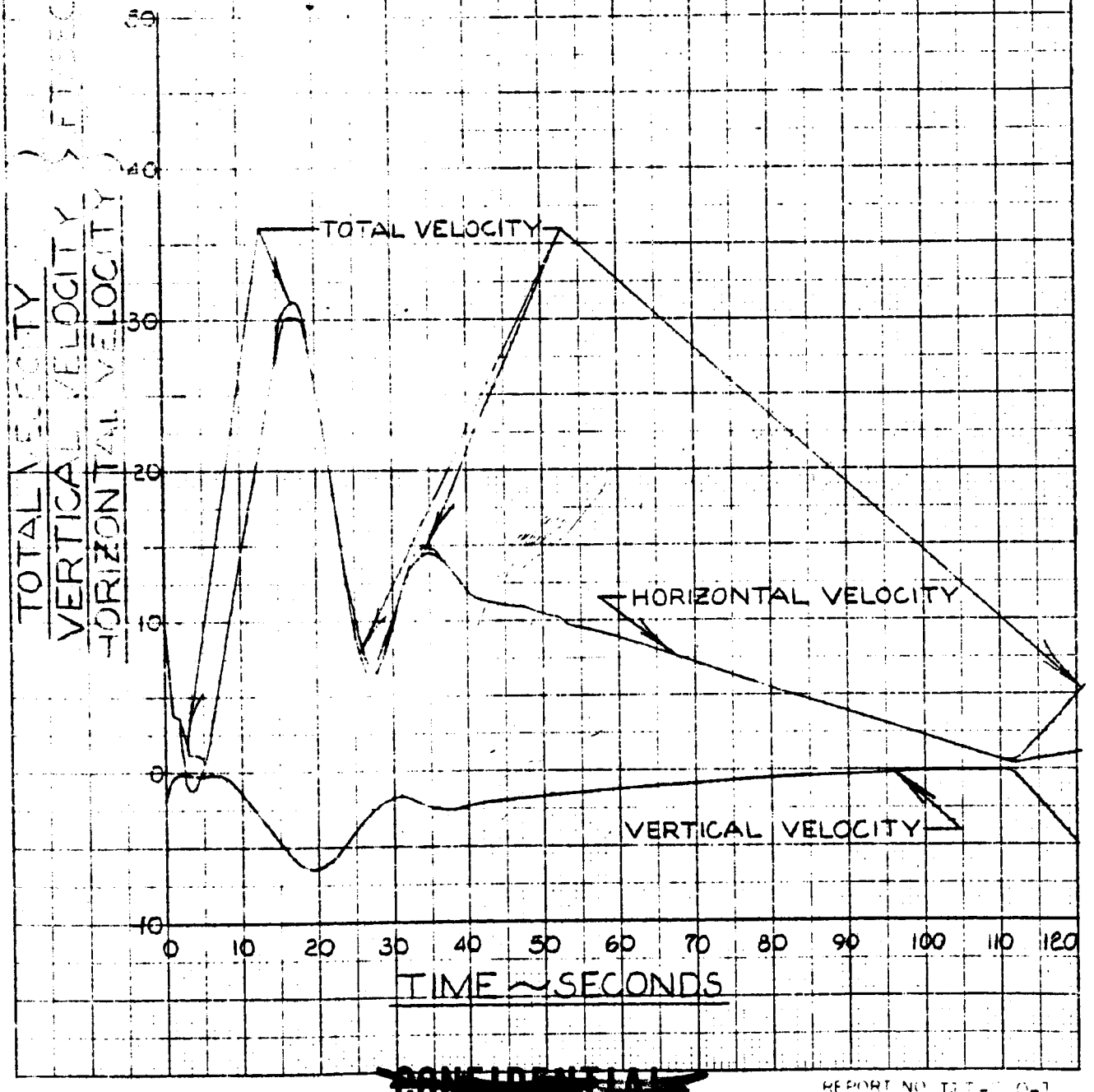

ENG 335
6 62

GRUMMAN AIRCRAFT ENGINEERING CORPORATION

REPORT NO. IM-2-0-1
1 August 1964

SECTION III FIGURE B.2.3-5

TRANSLATION, HOVER, AND TOUCHDOWN TRAJECTORY

ΔV = 657.6 FT/SEC

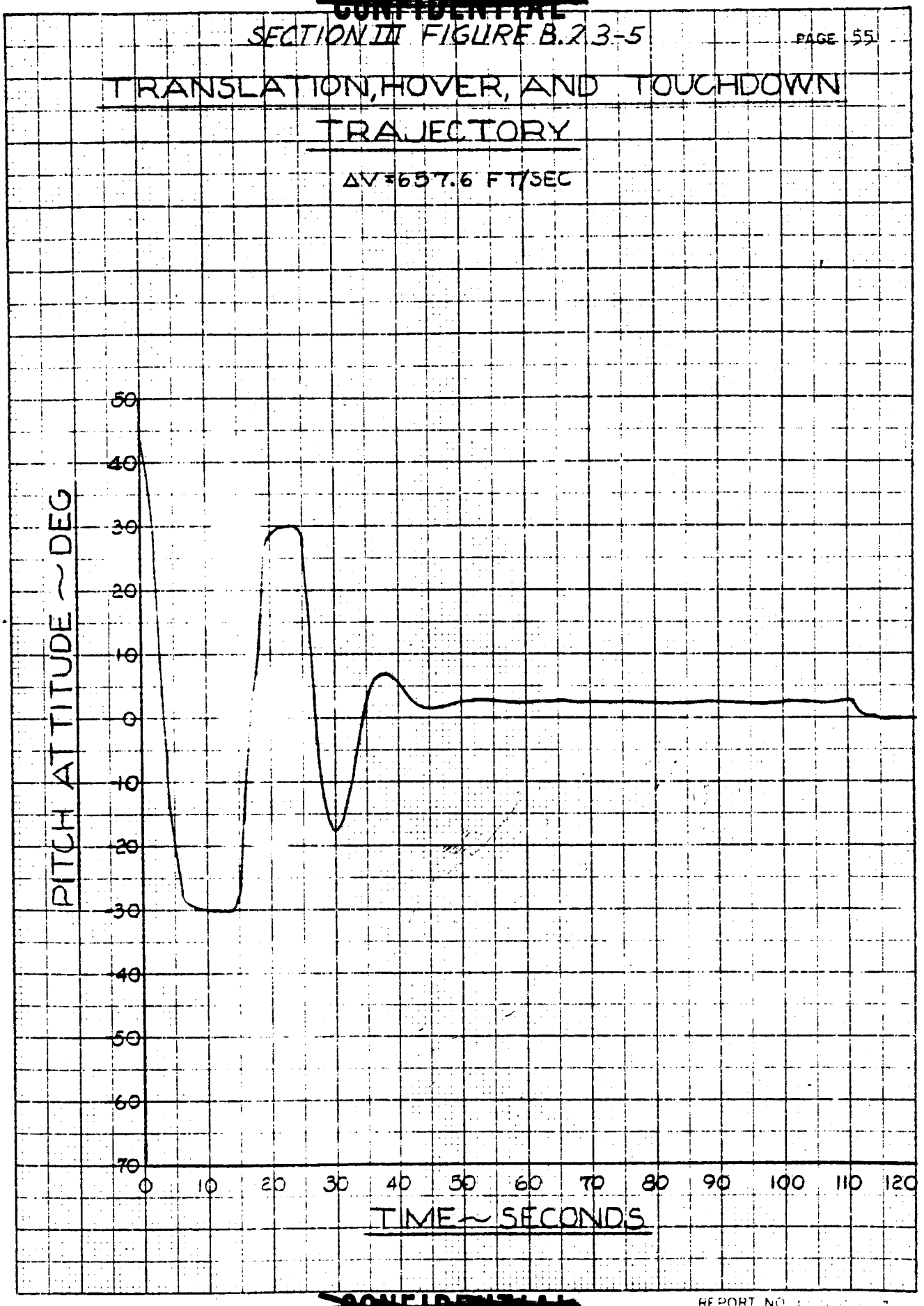

SECTION III FIGURE B.2.3-6

TRANSLATION, HOVER, AND TOUCHDOWN TRAJECTORY

ΔV = 657.6 FT/SEC

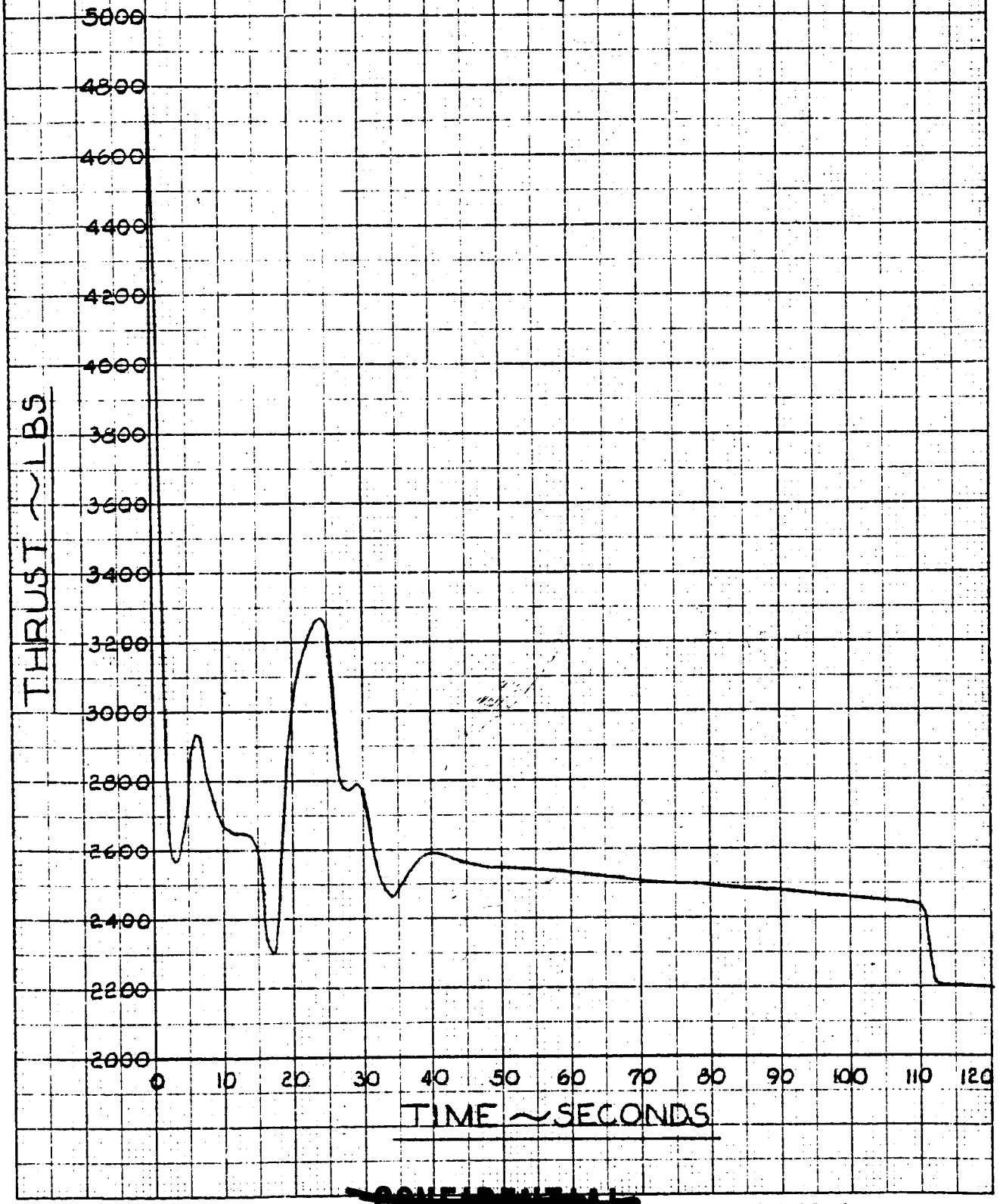

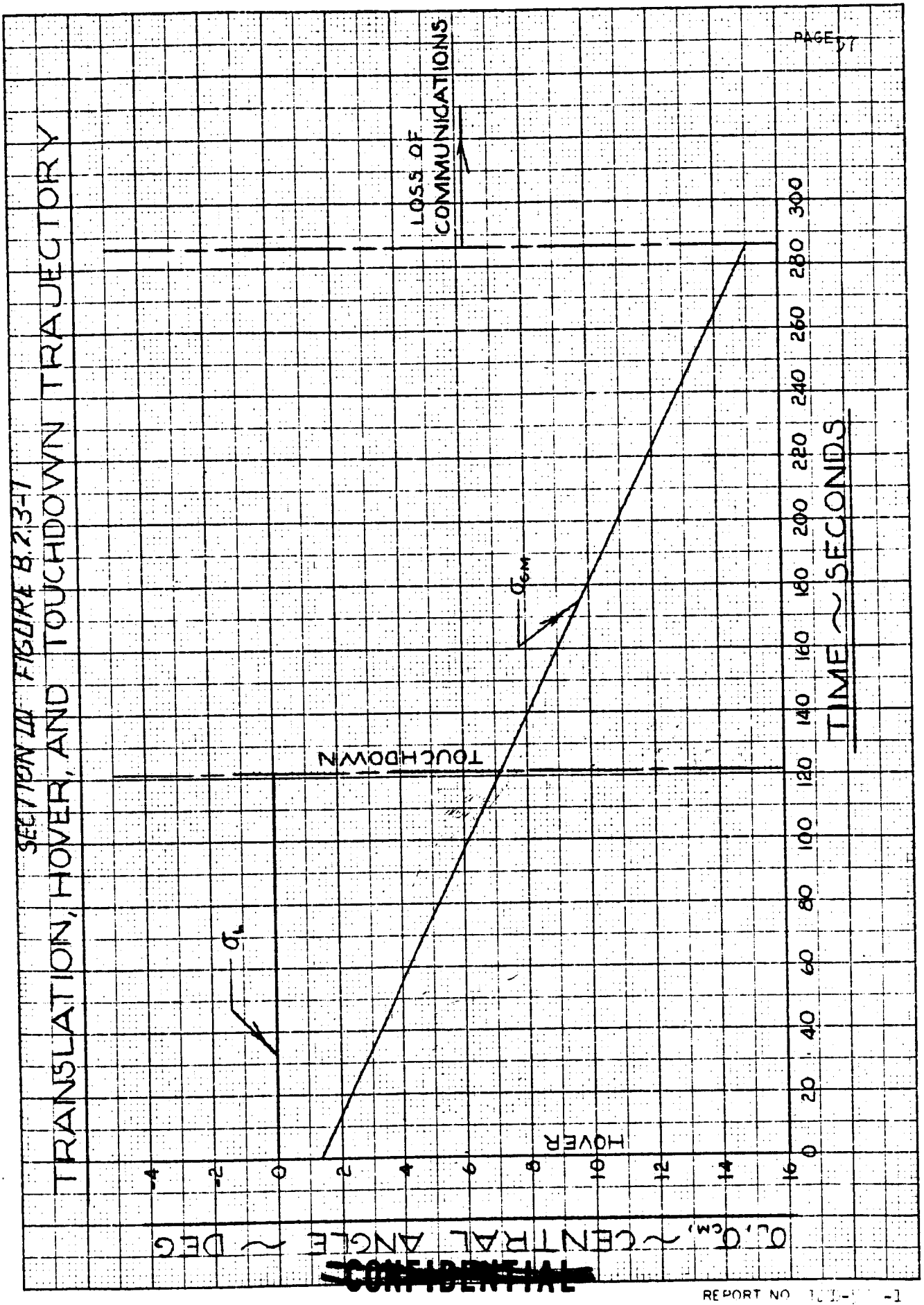
SECTION III FIGURE 3.2.13-17
TRANSLATION, HOVER, AND TOUCHDOWN TRAJECTORY
LOSS OF COMMUNICATIONS
TOUCHDOWN
HOVER
σ_{cm}
σ_L
σ, σ_{cm} ~ CENTRAL ANGLE ~ DEG
TIME ~ SECONDS
-4
-2
0
2
4
6
8
10
12
14
16
0
20
40
60
80
100
120
140
160
180
200
220
240
260
280
300

FIGURE C-1

ASCENT PHASE

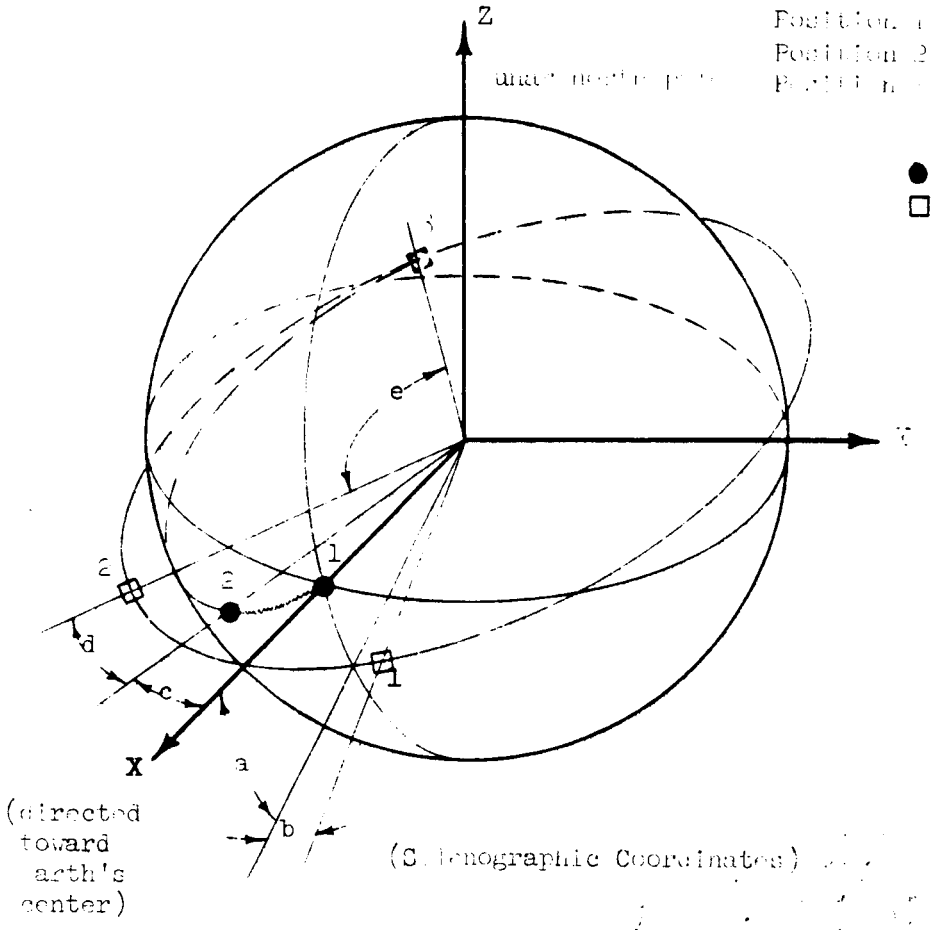

ANGLE	DEFINITION
a	CSM orbit displacement from launch-site = [illegible] deg.
b	CSM [illegible] angle at launch = 3.89 deg.
c	Central angle traversed by LEM during powered ascent = [illegible] deg.
d	CSM lead angle at LEM burnout = [illegible].38 deg.
e	LEM central angle traversed from launch to rendezvous = 190.1 deg.

SECTION III
FIGURE C.1-1

GEOMETRY AT LANDING SITE

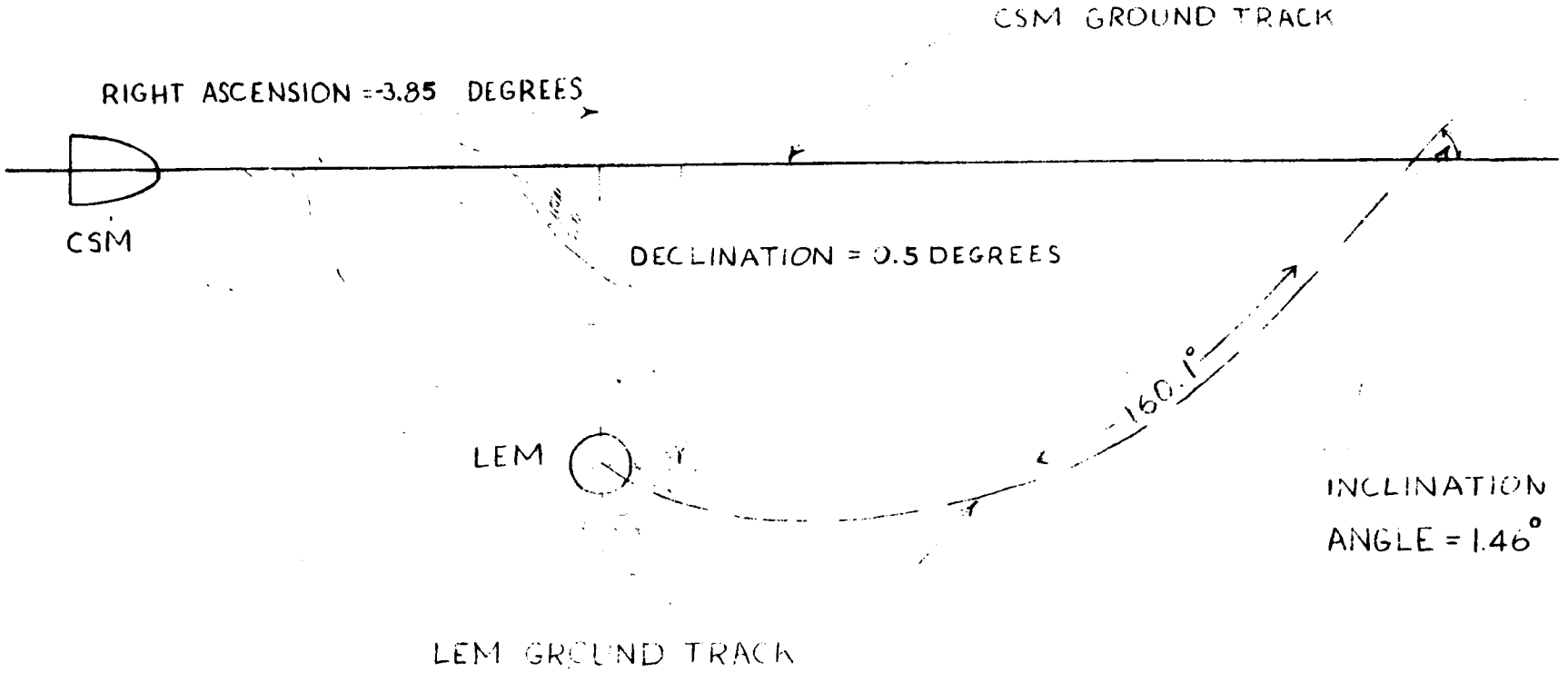

CONFIDENTIAL

SECTION III FIGURE C. 1-2

ALTITUDE AND TOTAL SPEED TIME HISTORY POWERED ASCENT TRAJECTORY

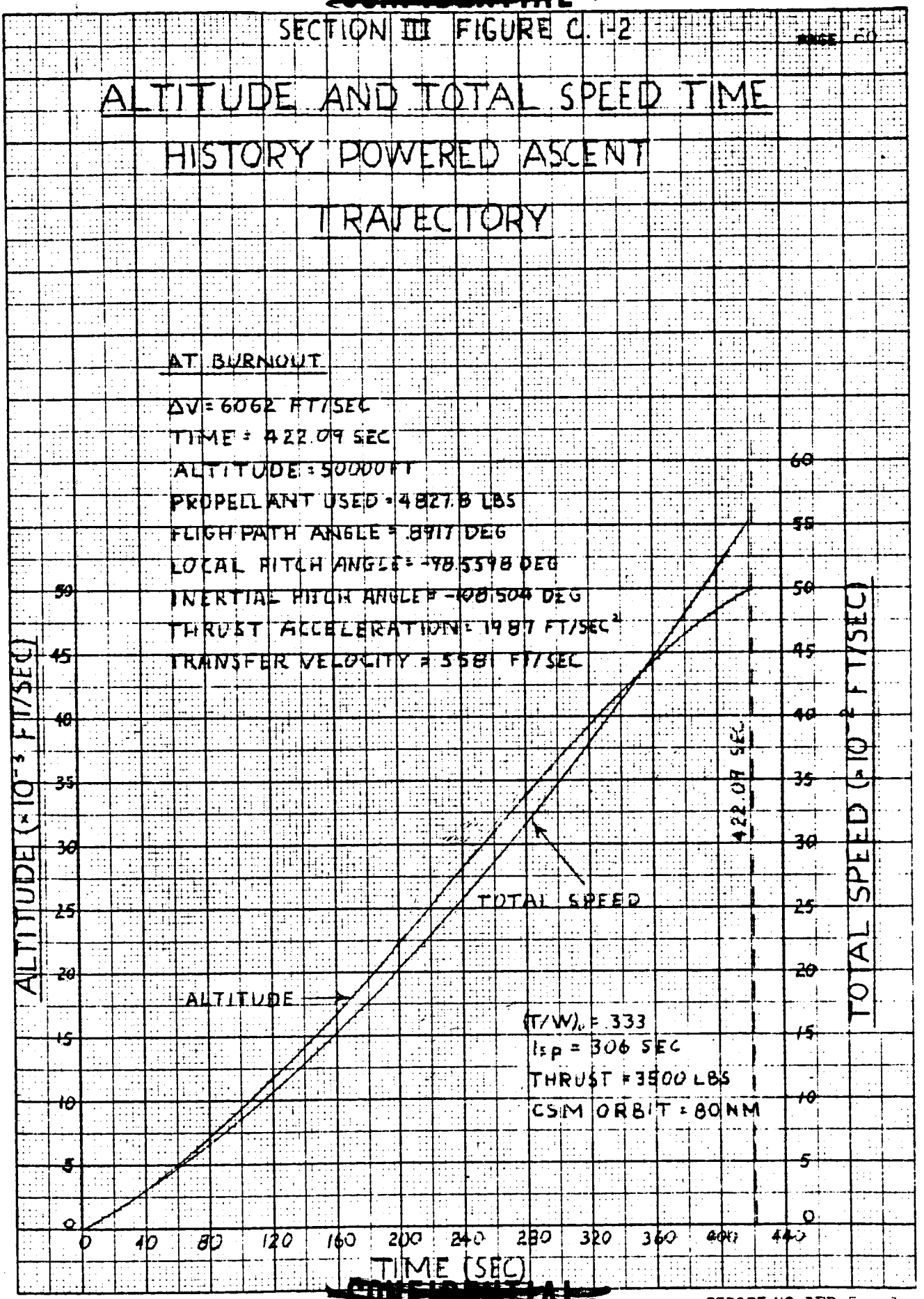

ENG 435
9 62

GRUMMAN AIRCRAFT ENGINEERING CORPORATION

REPORT NO. LED-5 -1
11 August 64

SECTION III FIGURE C.1-3

TIME HISTORY

POWERED ASCENT TRAJECTORY

AT BURNOUT

ΔV = 6062 FT/SEC
TIME = 432.99 SEC
ALTITUDE = 50,000 FT
PROPELLANT USED = 4827.8134 LBS
TRANSFER VELOCITY = 5581 FT/SEC
LOCAL PITCH ANGLE = 48.5598 DEG
FLIGHT PATH ANGLE = .8917 DEG
INERTIAL PITCH ANGLE = -108.504 DEG
THRUST ACCELERATION = 19.87 FT/SEC²

(T/W)₀ = .333
Isp = 306 SEC
THRUST = 3500 LBS
CSM ORBIT = 80 NM

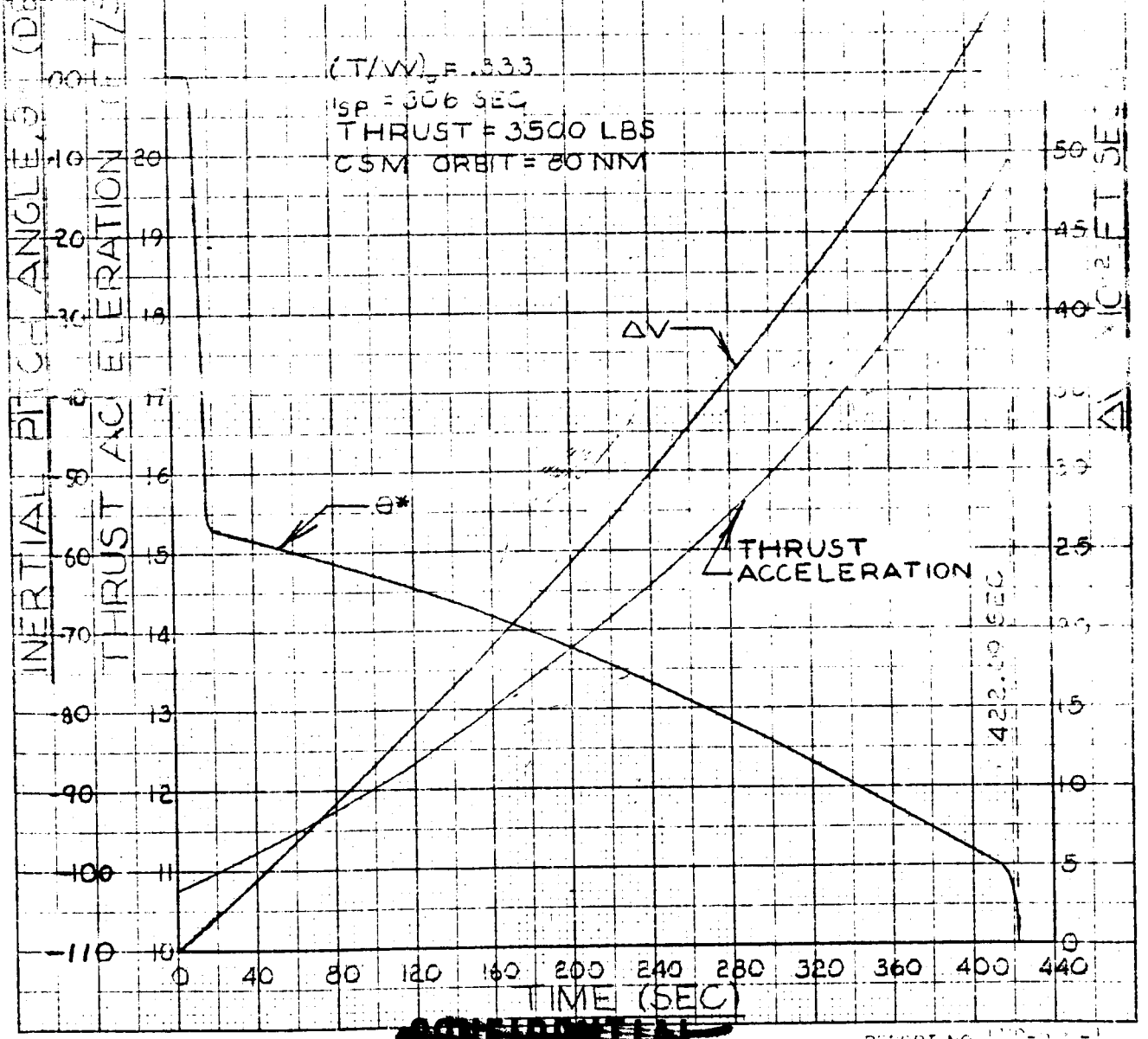

ENG 335
9 62

GRUMMAN AIRCRAFT ENGINEERING CORPORATION

REPORT NO

SECTION III FIGURE C.1-4

FLIGHT PATH ANGLE AND LOCAL PITCH ANGLE – TIME HISTORY POWERED ASCENT TRAJECTORY

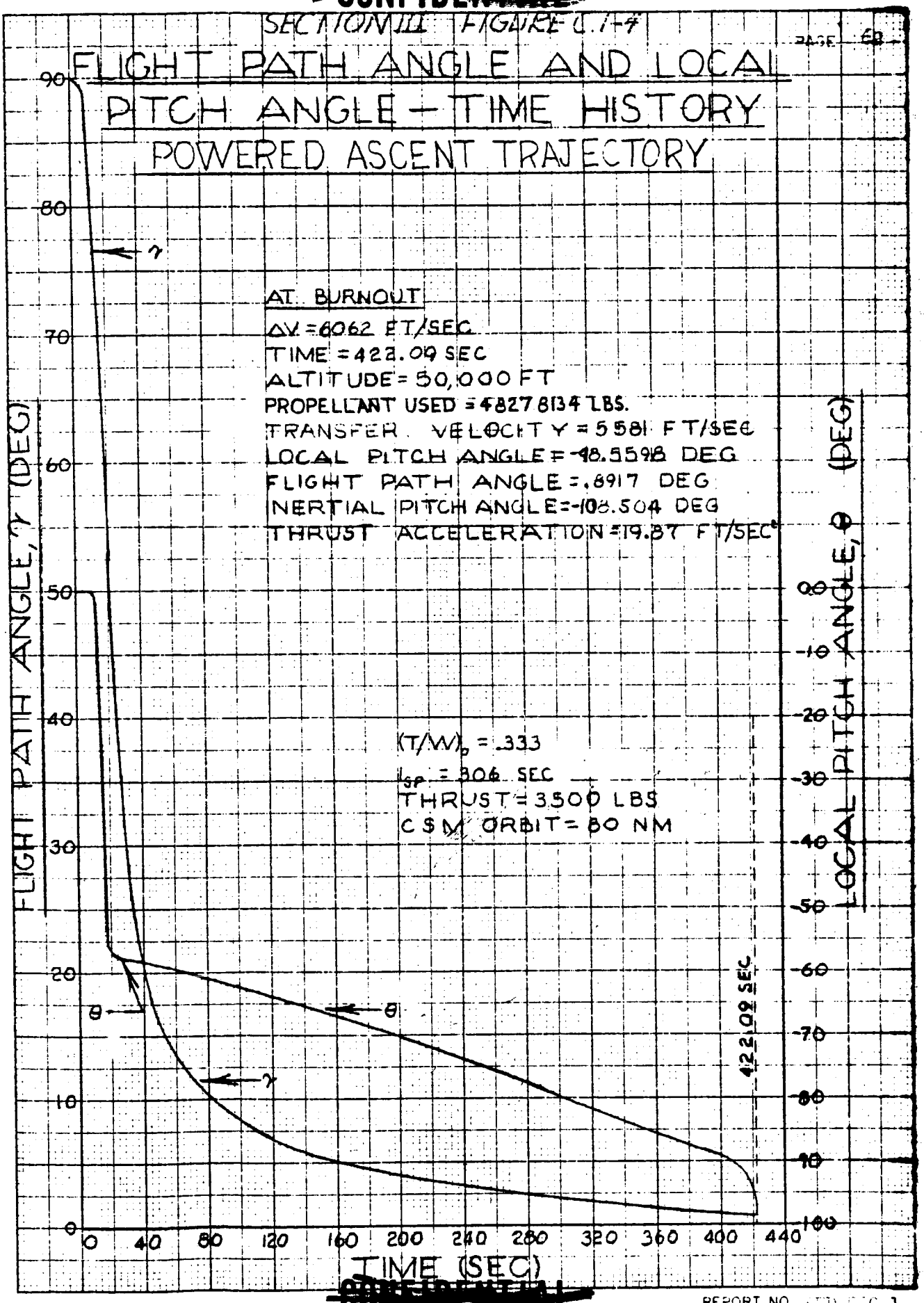

SECTION III FIGURE C.1-5

GEOMETRY FOR LINE OF SIGHT ANGLES

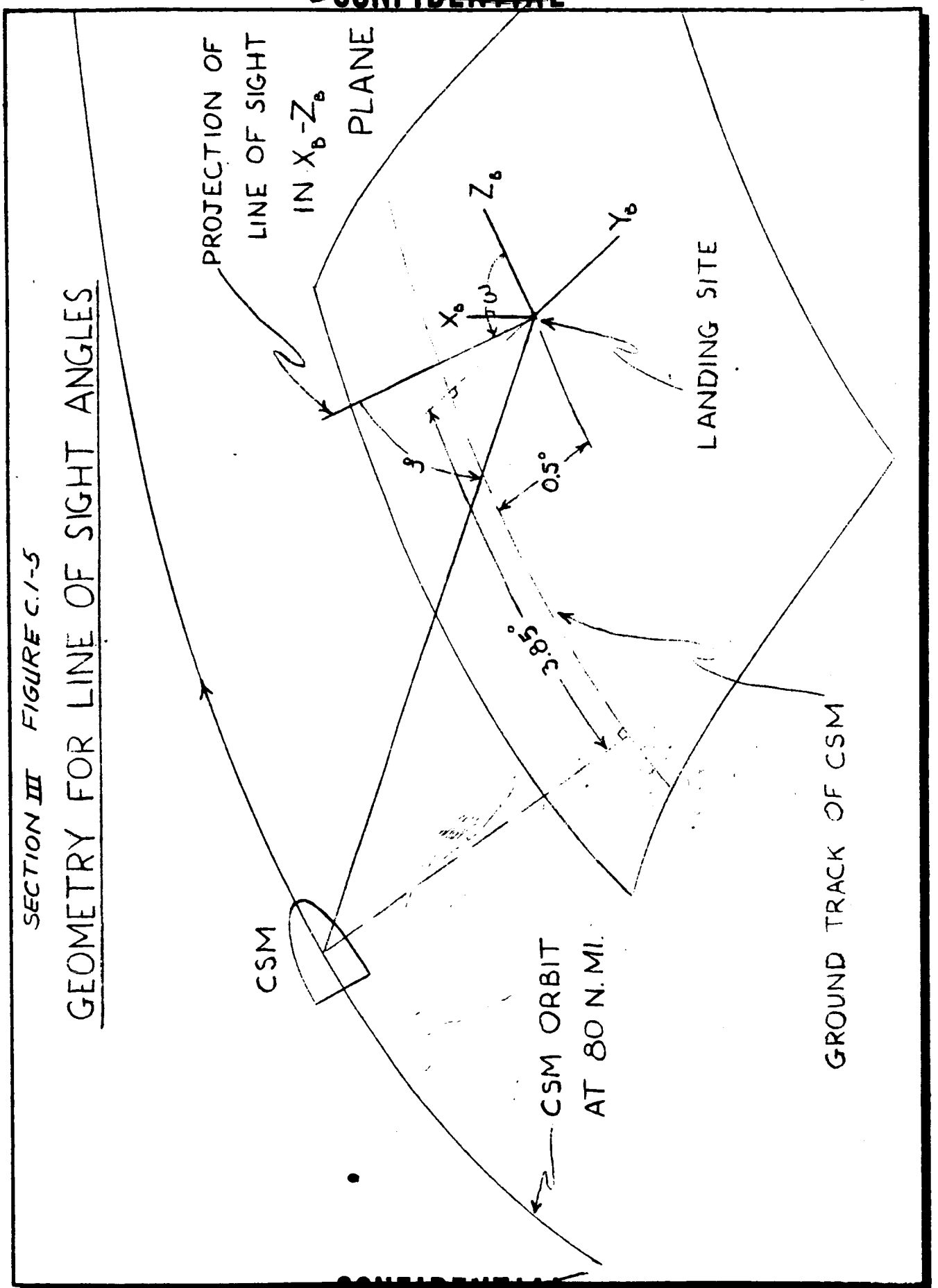

SECTION III FIGURE 6.1-6

LINE OF SIGHT TIME HISTORY - POWERED ASCENT TRAJECTORY

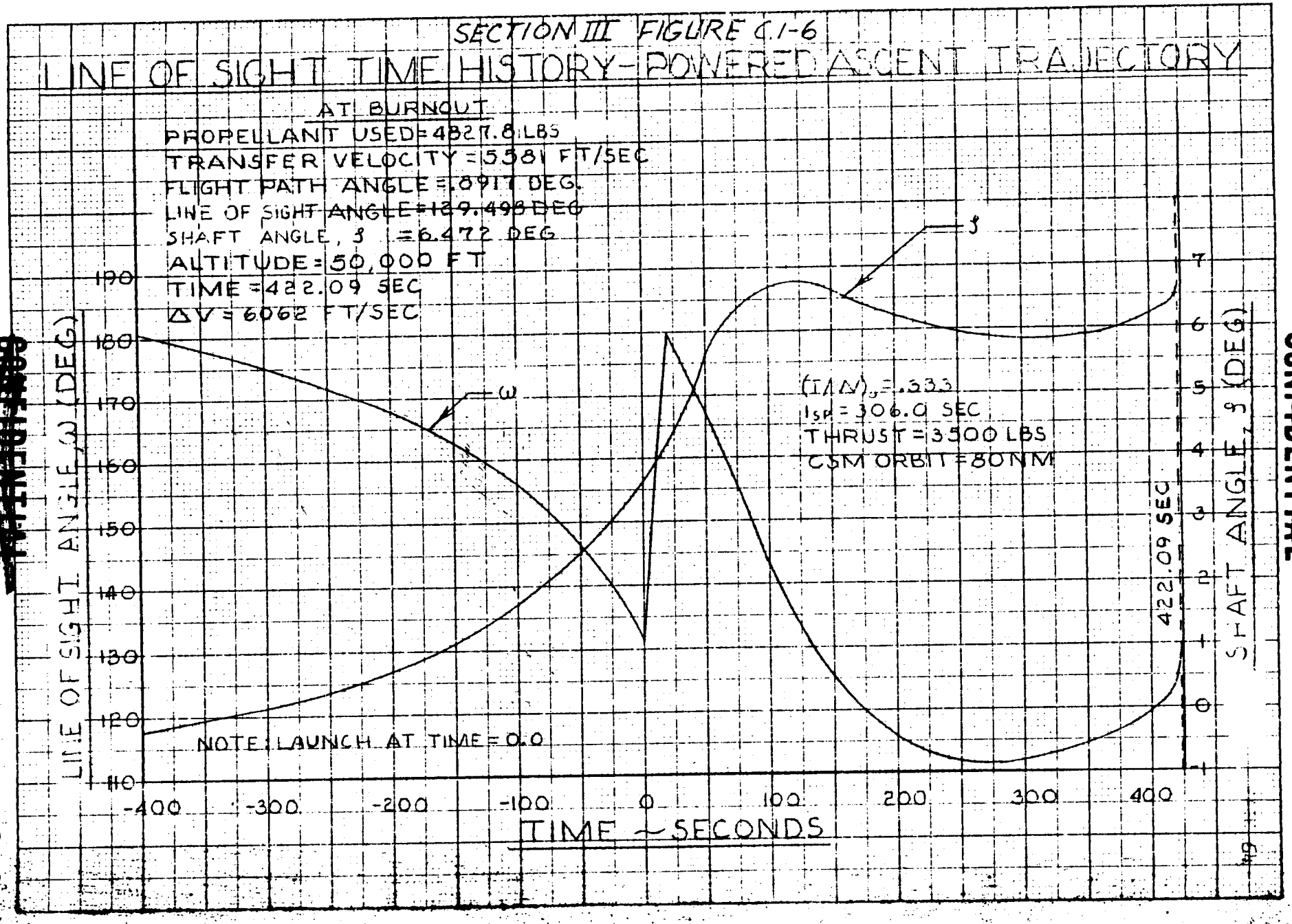

SECTION III FIGURE C.1-7

RANGE AND RANGE RATE TIME HISTORY -- POWERED ASCENT TRAJECTORY

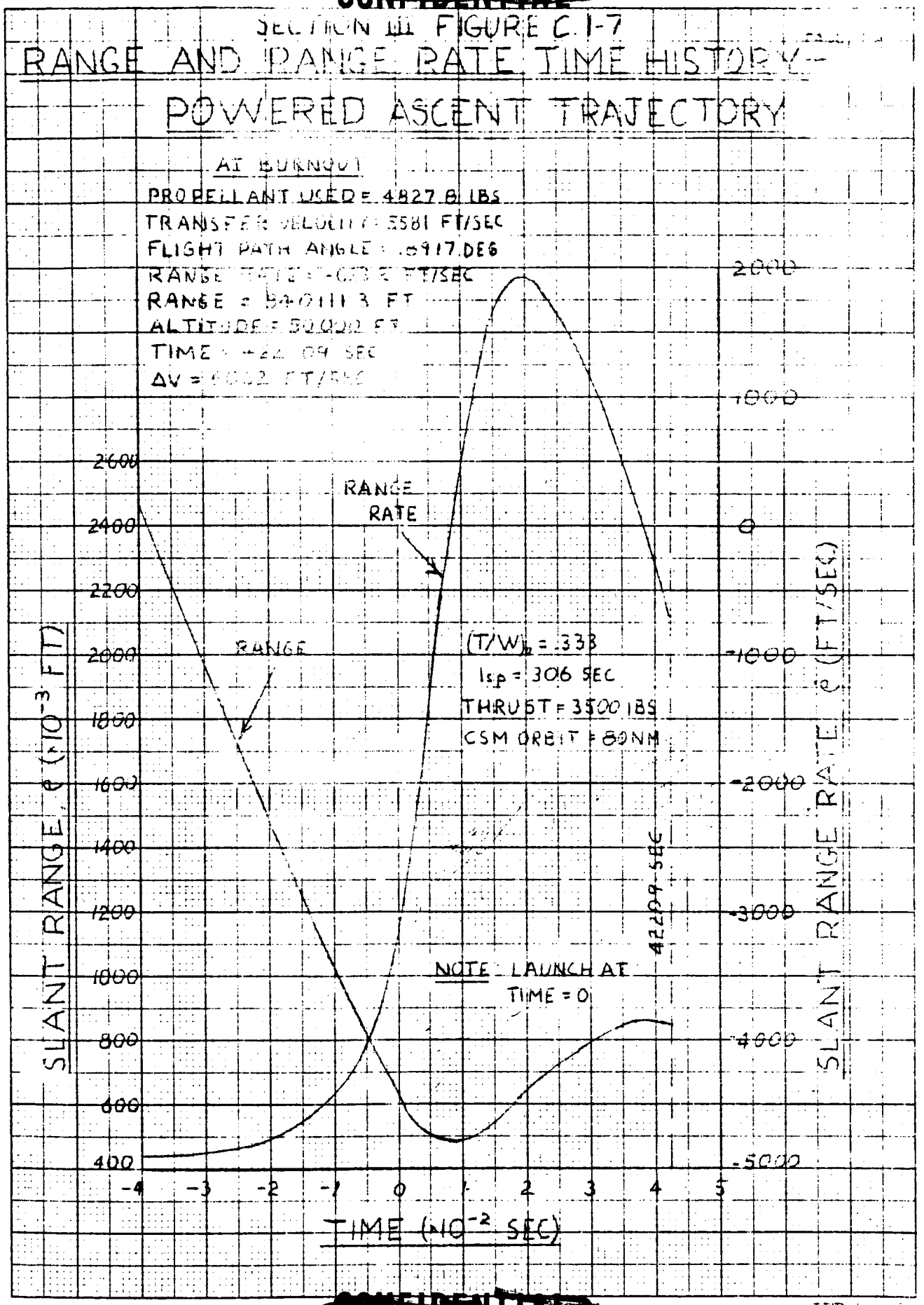

ENG 435
9 62

GRUMMAN AIRCRAFT ENGINEERING CORPORATION

REPORT NO LED-500-1
11 August 1964

SECTION III FIGURE C.2-1

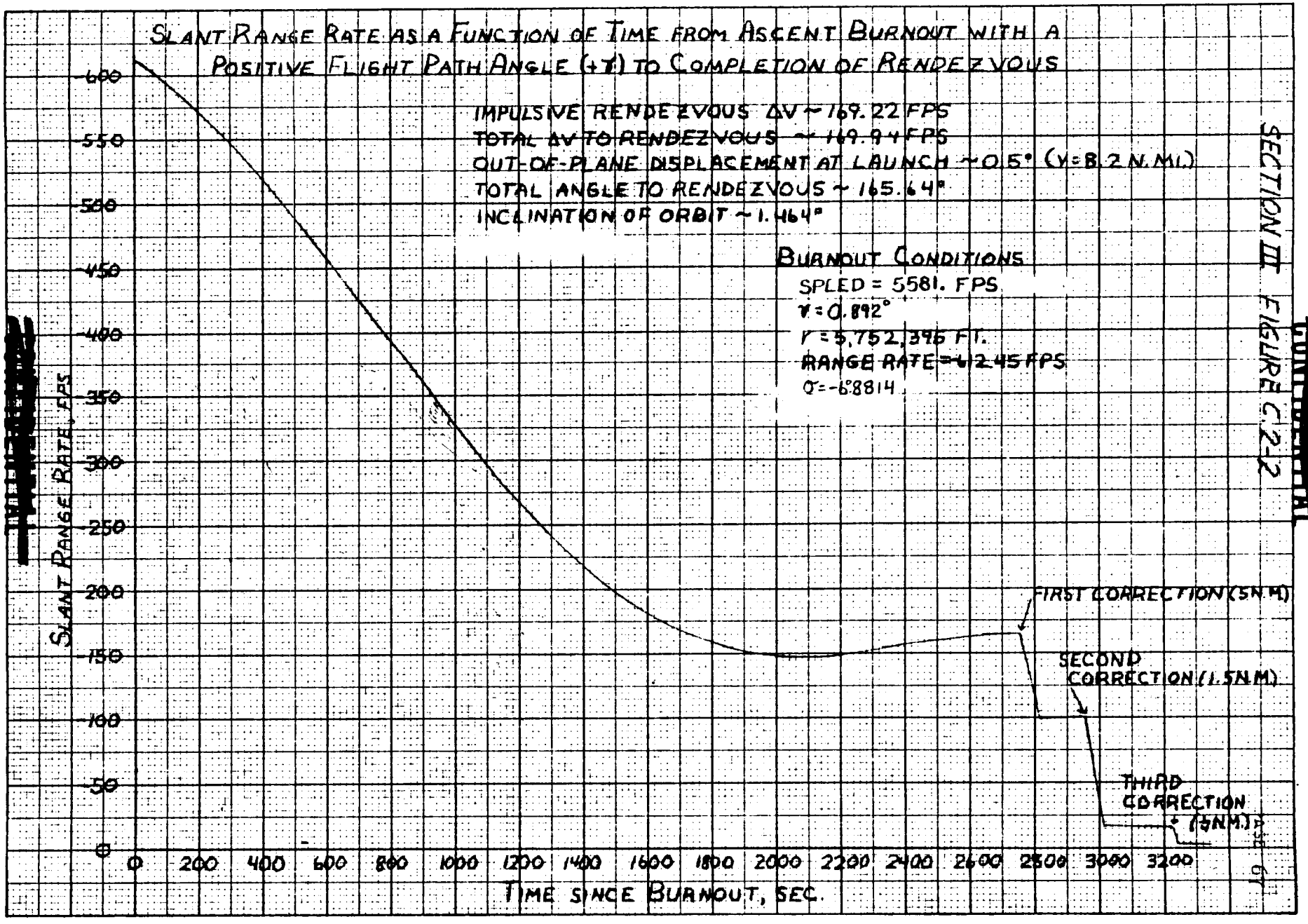
SLANT RANGE RATE AS A FUNCTION OF TIME FROM ASCENT BURNOUT WITH A POSITIVE FLIGHT PATH ANGLE (+γ) TO COMPLETION OF RENDEZVOUS
IMPULSIVE RENDEZVOUS ΔV ~ 169.22 FPS
TOTAL ΔV TO RENDEZVOUS ~ 169.94 FPS
OUT-OF-PLANE DISPLACEMENT AT LAUNCH ~ 0.5° (Y = 8.2 N.MI.)
TOTAL ANGLE TO RENDEZVOUS ~ 165.64°
INCLINATION OF ORBIT ~ 1.464°
BURNOUT CONDITIONS
SPLED = 5581. FPS
γ = 0.892°
r = 5,752,396 FT.
RANGE RATE = 4245 FPS
σ = -6.8814
FIRST CORRECTION (5 N.M.)
SECOND CORRECTION (1.5 N.M.)
THIRD CORRECTION (1 N.M.)
SLANT RANGE RATE, FPS
TIME SINCE BURNOUT, SEC.
600
550
500
450
400
350
300
250
200
150
100
50
0
0
200
400
600
800
1000
1200
1400
1600
1800
2000
2200
2400
2600
2800
3000
3200

SECTION III FIGURE C.2-3

LINE-OF-SIGHT RATE AS A FUNCTION OF TIME FROM ASCENT BURNOUT TO COMPLETION OF RENDEZVOUS

IMPULSIVE RENDEZVOUS $\Delta V \sim 169.22$ FPS
TOTAL ΔV TO RENDEZVOUS ~ 169.94 FPS
OUT-OF-PLANE DISPLACEMENT ~ 0.5
TOTAL ANGLE TO RENDEZVOUS ~ 165.64
INCLINATION OF ORBIT ~ 1.164
$(T/W)_0 = .0365$

BURNOUT CONDITIONS
SPEED = 5581. FPS
$\gamma = 0.892°$
$r = 5,1752,395$ FT
$\omega = 0.6101$
$\sigma = -6.8314$

A -- FIRST CORRECTION (5 N.MI.)
B -- SECOND CORRECTION (1.5 N.MI.)
C -- THIRD CORRECTION (0.25 N.MI.)

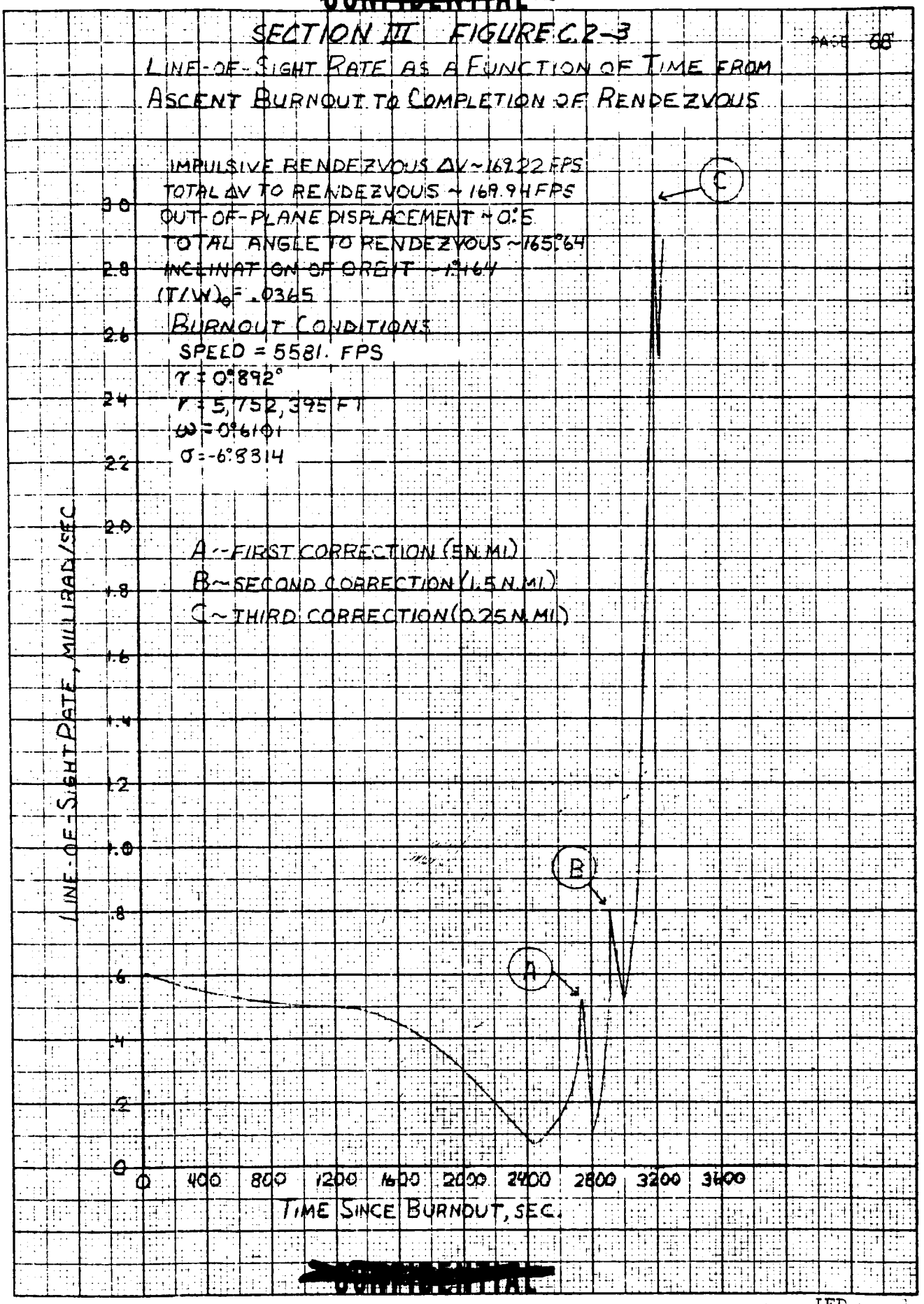

SECTION III FIGURE C.2-4

LEM TOTAL VELOCITY AS A FUNCTION OF TIME FROM ASCENT BURNOUT TO COMPLETION OF RENDEZVOUS

IMPULSIVE RENDEZVOUS $\Delta V \sim 169.22$ FPS
TOTAL ΔV TO RENDEZVOUS ~ 169.94 FPS
OUT-OF-PLANE DISPLACEMENT AT LAUNCH ~ 0.5 ($\gamma = 8.2$ N.MI.)
TOTAL ANGLE TO RENDEZVOUS ~ 165.64
INCLINATION OF ORBIT ~ 1.464
$(T/W)_0 = .0365$

BURNOUT CONDITIONS

SPEED = 5591 FPS
$\gamma = 0.892°$
$r = 5,752,395$ FT.
$\sigma = -6.8814$

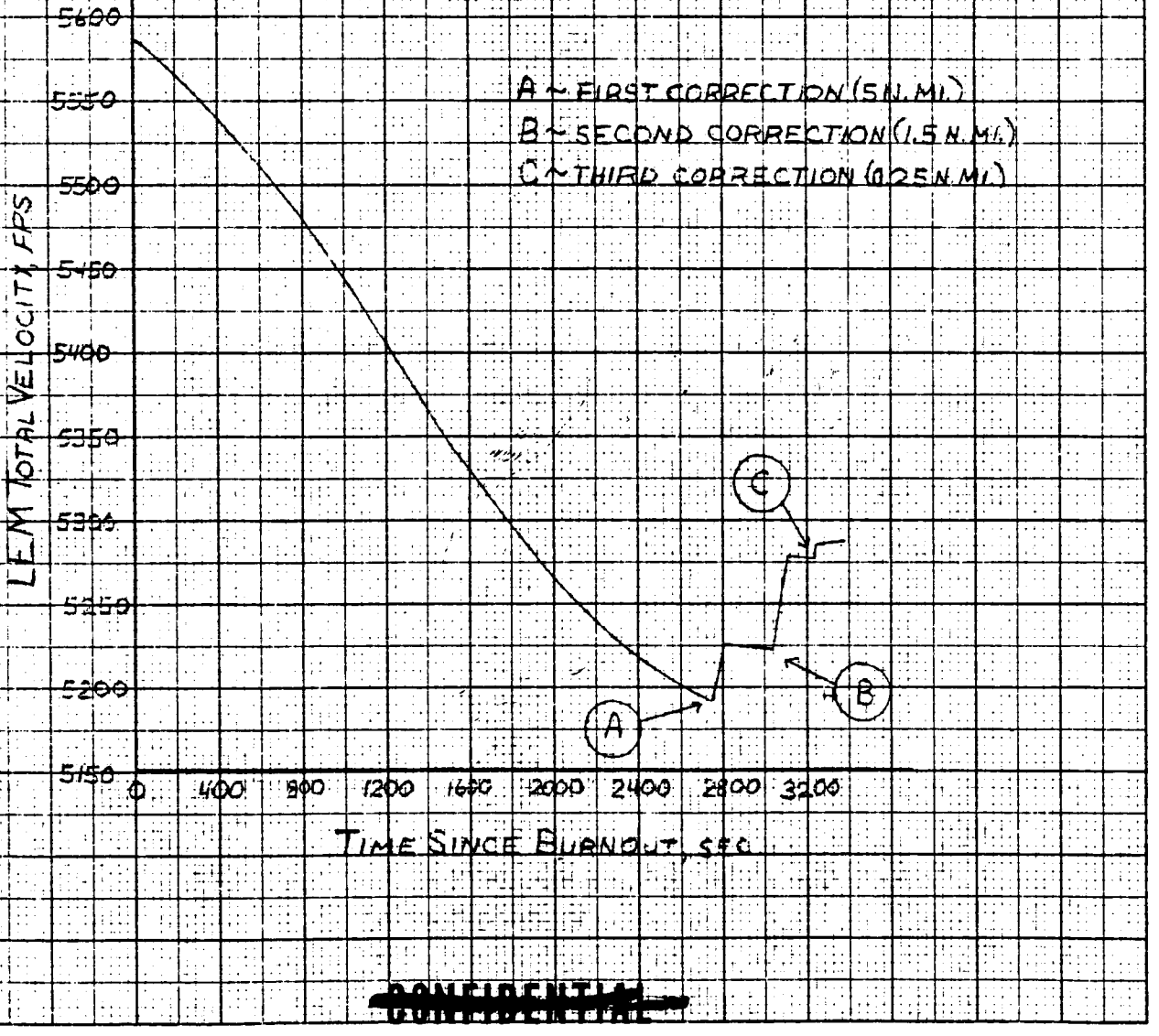

SECTION III FIGURE C.2-5

LEM RADIUS FROM CENTER OF MOON AS A FUNCTION OF TIME

A ~ FIRST CORRECTION (5 N.MI.)
B ~ SECOND CORRECTION (1.5 N.MI.)
C ~ THIRD CORRECTION (0.25 N.MI.)

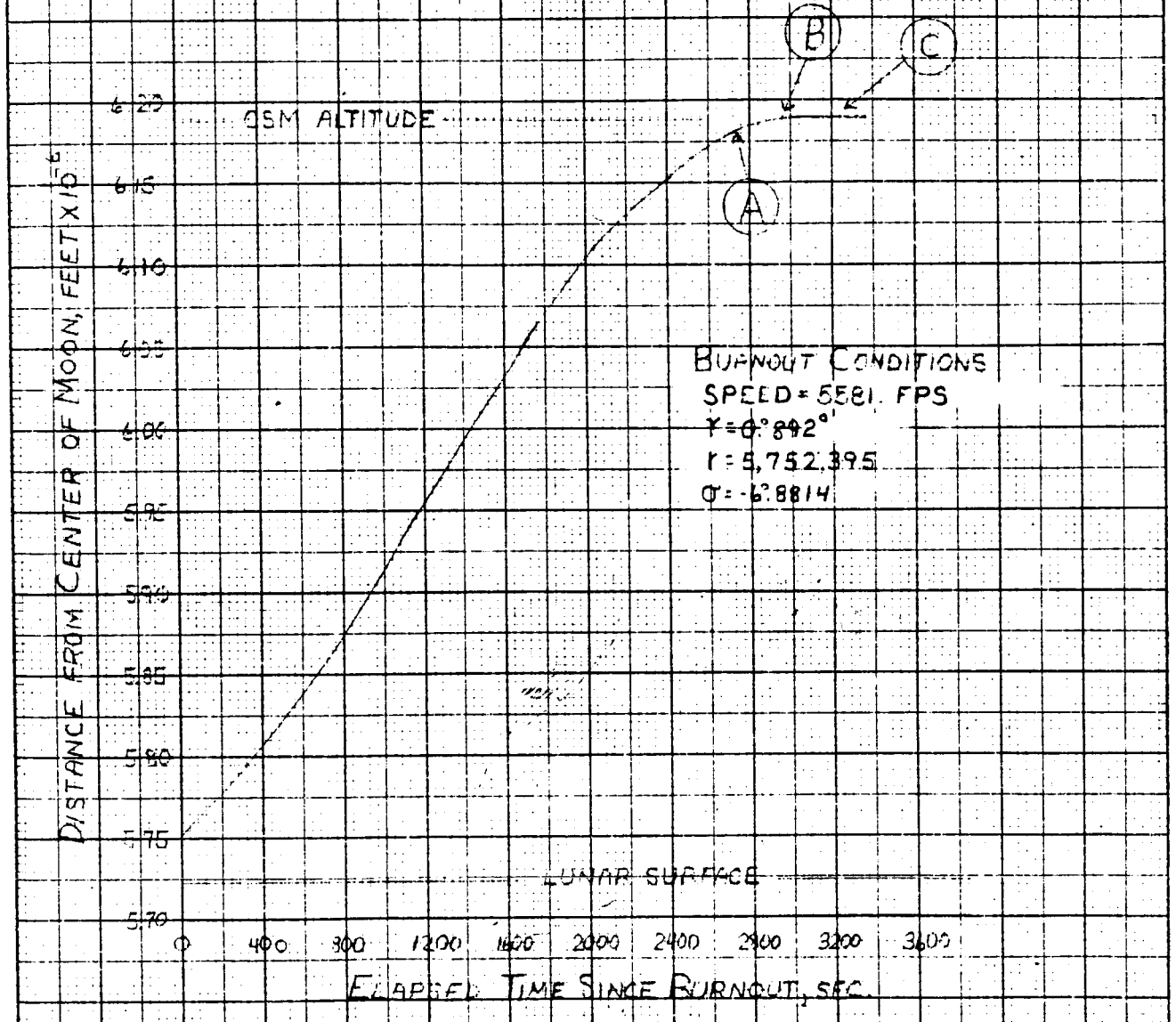

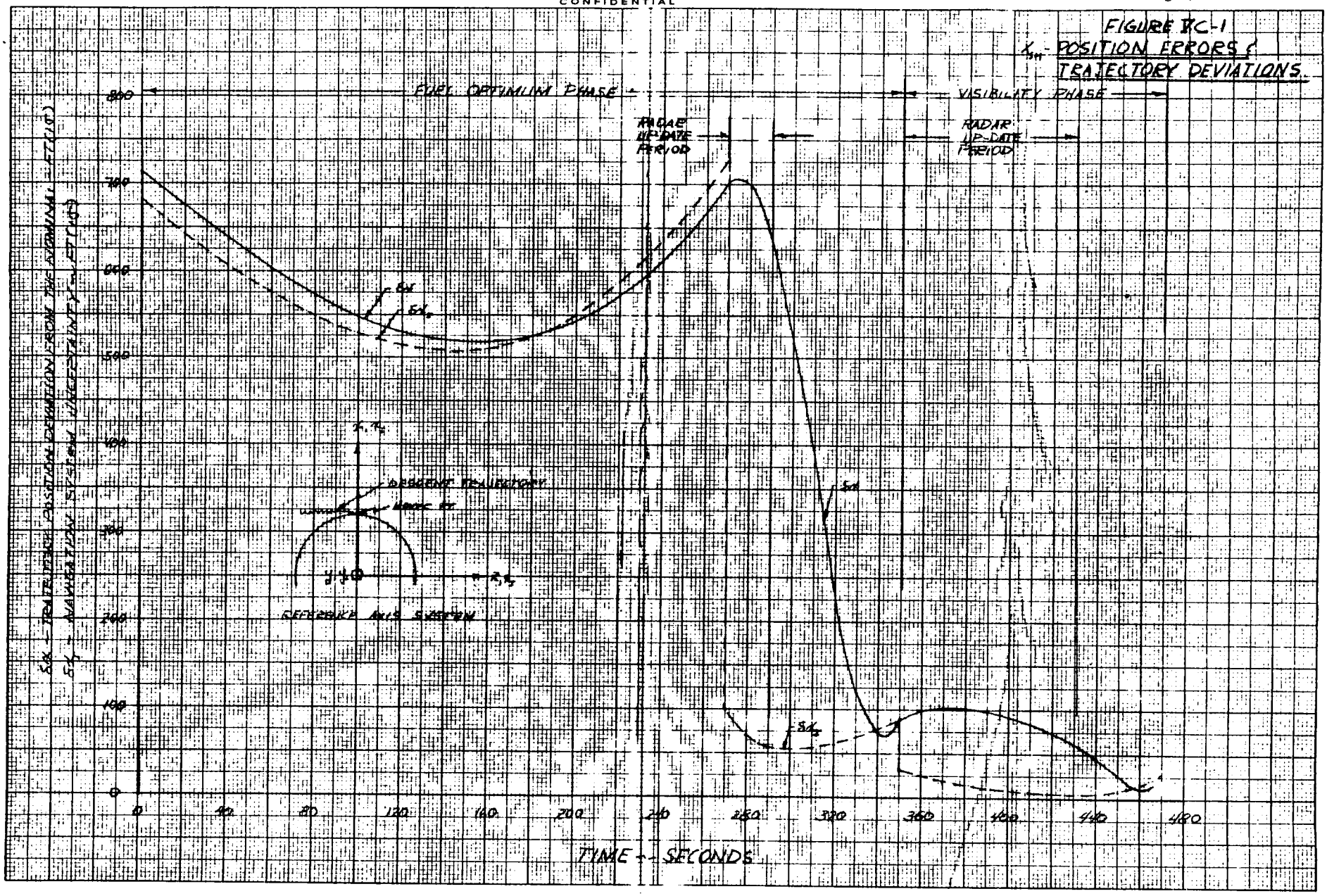

FIGURE IC-1
X_{sm} - POSITION ERRORS & TRAJECTORY DEVIATIONS.

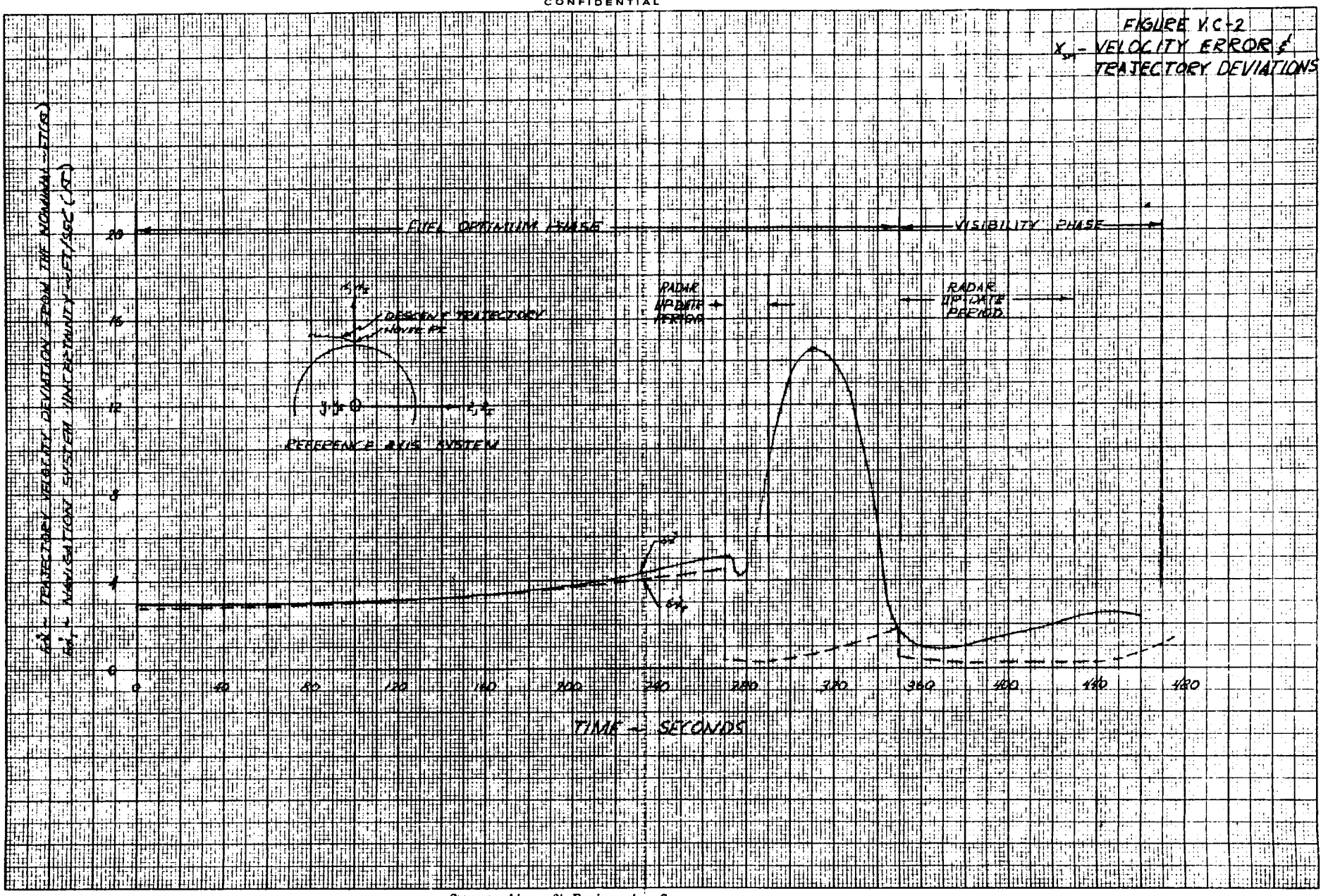
FIGURE V.C-2
X_{sm} - VELOCITY ERROR & TRAJECTORY DEVIATIONS
$\delta\dot{R}$ - TRAJECTORY VELOCITY DEVIATION FROM THE NOMINAL (FPS)
δR - NAVIGATION SYSTEM UNCERTAINTY (FT/SEC)
FUEL OPTIMUM PHASE
VISIBILITY PHASE
RADAR UPDATE + ITERATION
RADAR UPDATE PERIOD
DESIRED TRAJECTORY
ABOVE R_2
PERTURBANCE AXIS SYSTEM
20
15
12
8
4
0
0
40
80
120
160
200
240
280
320
360
400
440
480
TIME - SECONDS

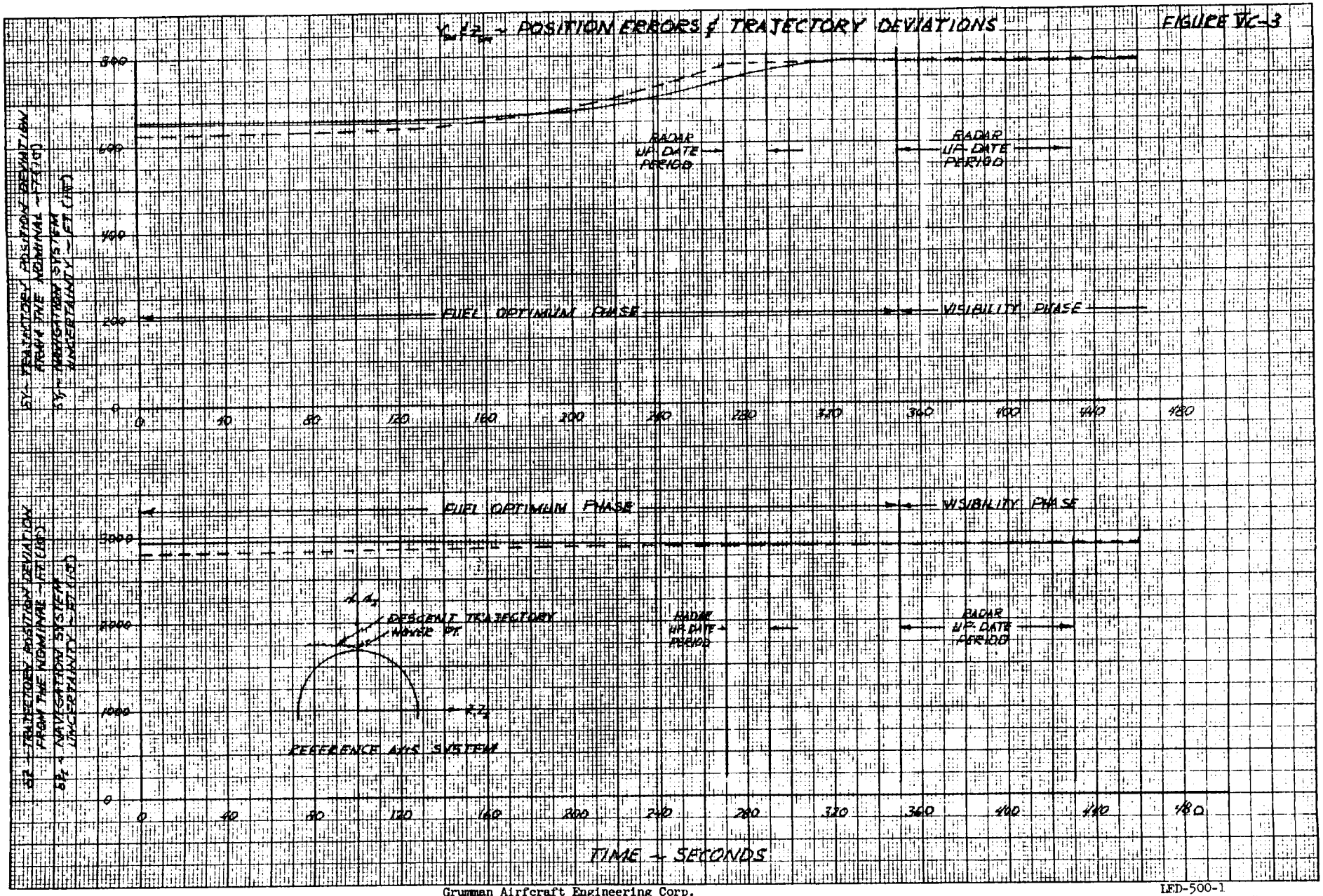
FIGURE VC-3
Y_{nr} & Z_{nr} - POSITION ERRORS & TRAJECTORY DEVIATIONS
δY - TRAJECTORY POSITION DEVIATION FROM THE NOMINAL - (FT) (M)
δy - NAVIGATION SYSTEM UNCERTAINTY - (FT) (M)
δZ - TRAJECTORY POSITION DEVIATION FROM THE NOMINAL - (FT) (M)
δz - NAVIGATION SYSTEM UNCERTAINTY - (FT) (M)
RADAR UP-DATE PERIOD
RADAR UP-DATE PERIOD
FUEL OPTIMUM PHASE
VISIBILITY PHASE
FUEL OPTIMUM PHASE
VISIBILITY PHASE
RADAR UP-DATE PERIOD
RADAR UP-DATE PERIOD
DESCENT TRAJECTORY
NOMINAL PT.
REFERENCE AXIS SYSTEM
TIME - SECONDS

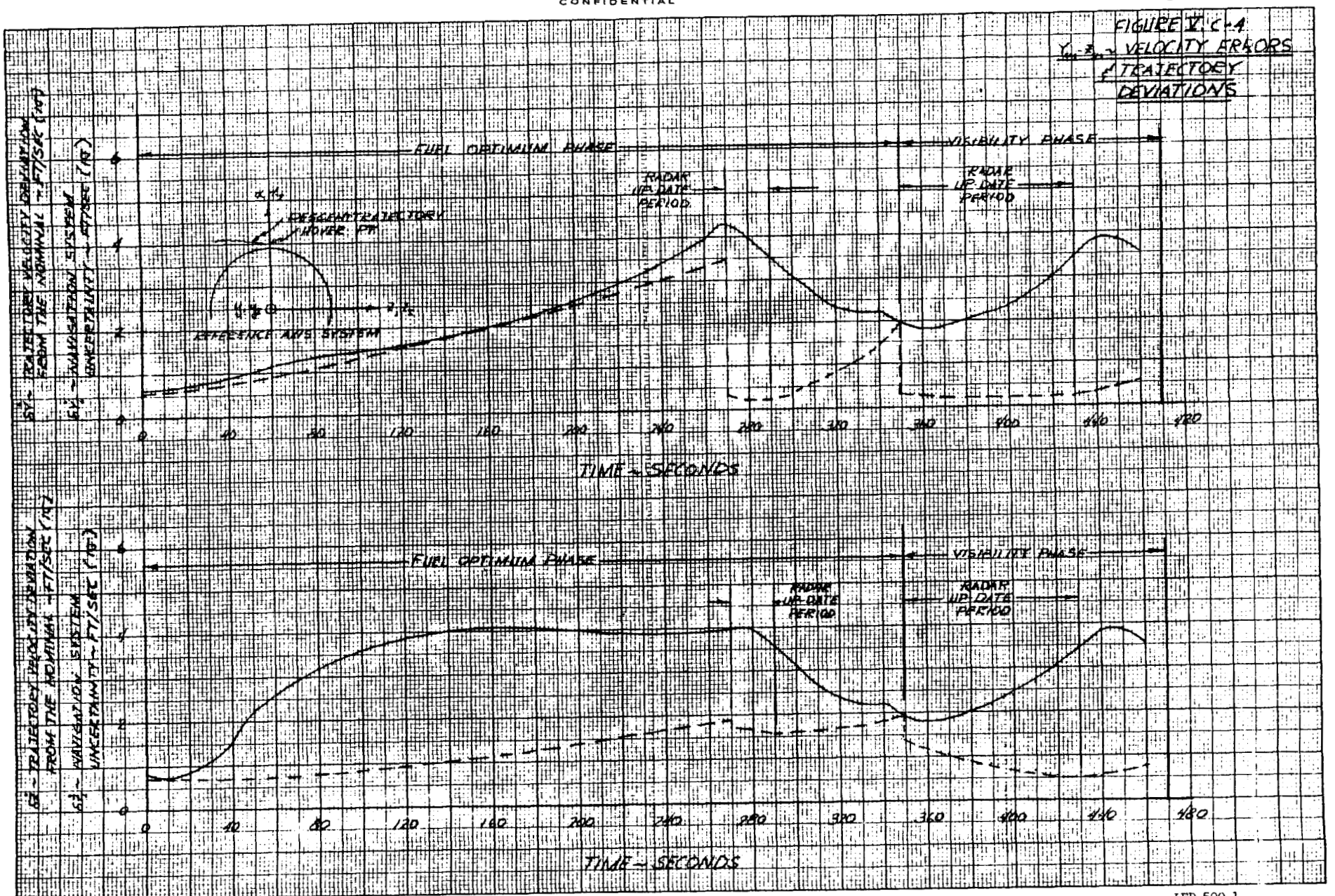
FIGURE V, C-4
VELOCITY ERRORS & TRAJECTORY DEVIATIONS
FUEL OPTIMUM PHASE
VISIBILITY PHASE
RADAR UP DATE PERIOD
RADAR UP DATE PERIOD
DESCENT TRAJECTORY HOVER PT
REFERENCE AMS SYSTEM
TIME - SECONDS
FUEL OPTIMUM PHASE
VISIBILITY PHASE
RADAR UP DATE PERIOD
RADAR UP DATE PERIOD
TIME - SECONDS

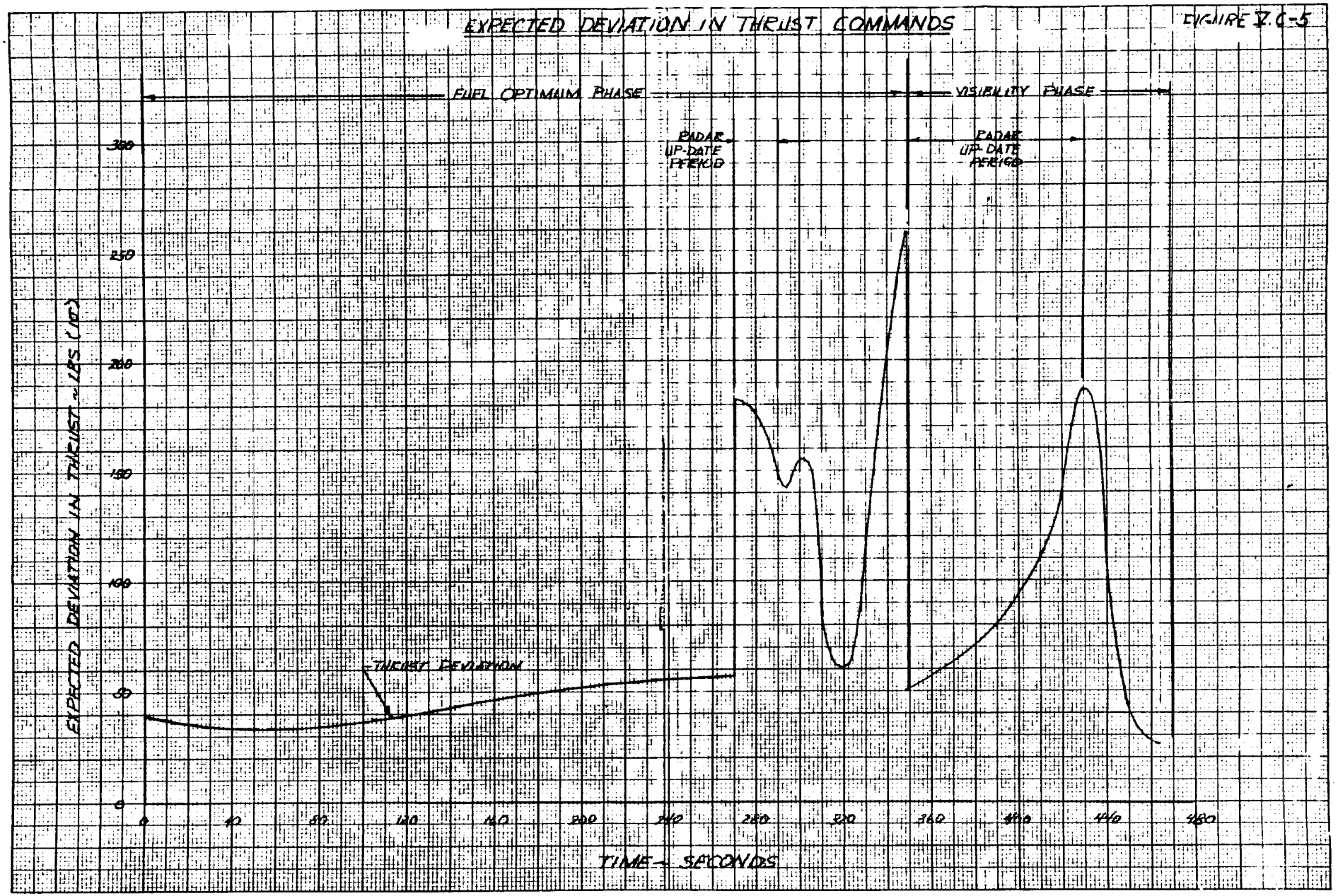
EXPECTED DEVIATION IN THRUST COMMANDS
FIGURE V.C-5
FUEL OPTIMUM PHASE
VISIBILITY PHASE
RADAR UP-DATE PERIOD
RADAR UP-DATE PERIOD
EXPECTED DEVIATION IN THRUST - LBS (1000)
300
250
200
150
100
50
0
THRUST DEVIATION
0
40
80
120
160
200
240
280
320
360
400
440
480
TIME - SECONDS

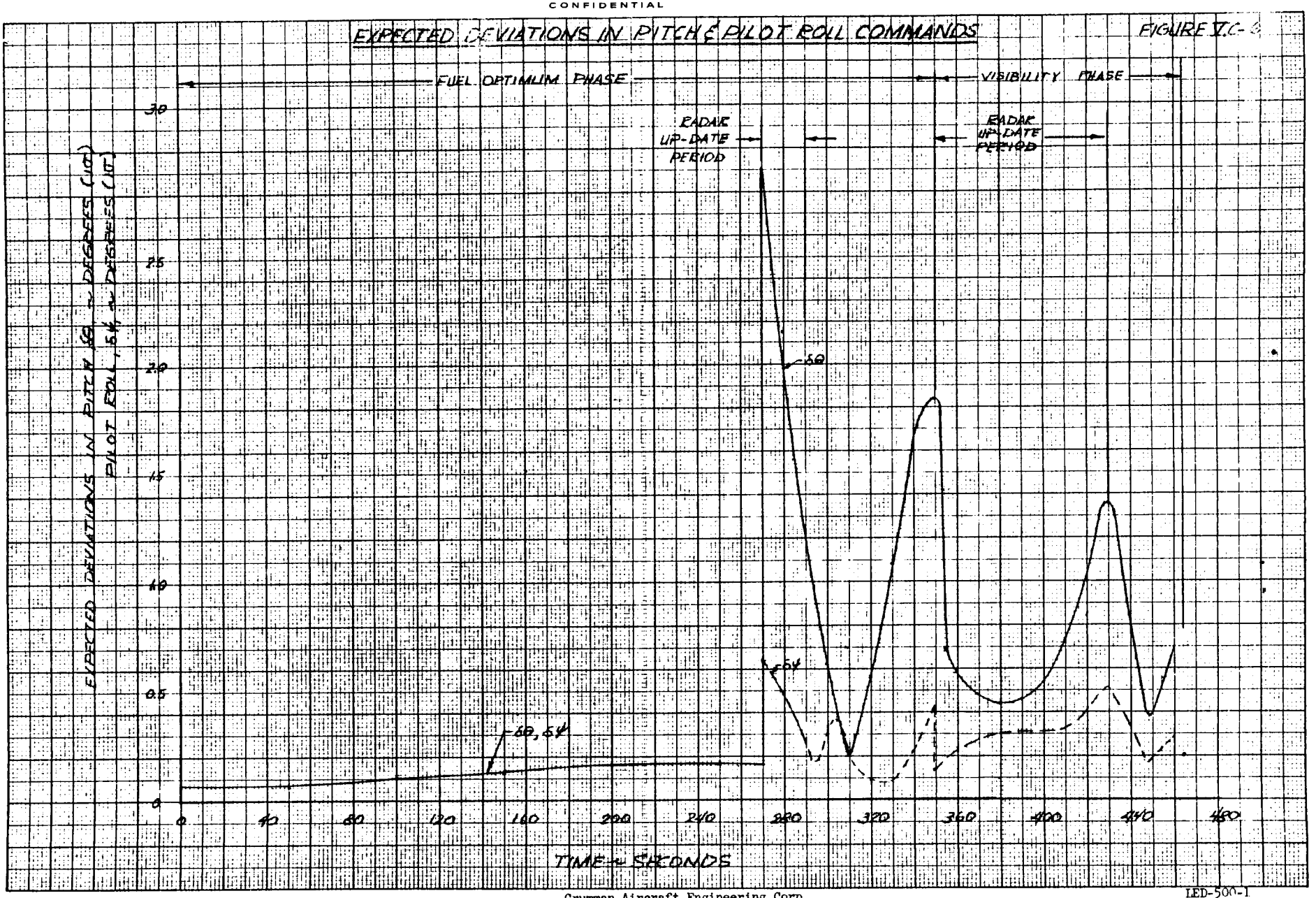
EXPECTED DEVIATIONS IN PITCH & PILOT ROLL COMMANDS
FIGURE V.C-4
FUEL OPTIMUM PHASE
VISIBILITY PHASE
RADAR UP-DATE PERIOD
RADAR UP-DATE PERIOD
EXPECTED DEVIATIONS IN PITCH (θ) - DEGREES (UP)
PILOT ROLL (φ) - DEGREES (UP)
3.0
2.5
2.0
1.5
1.0
0.5
0
θ
φ
θ, φ
0
40
80
120
160
200
240
280
320
360
400
440
480
TIME - SECONDS

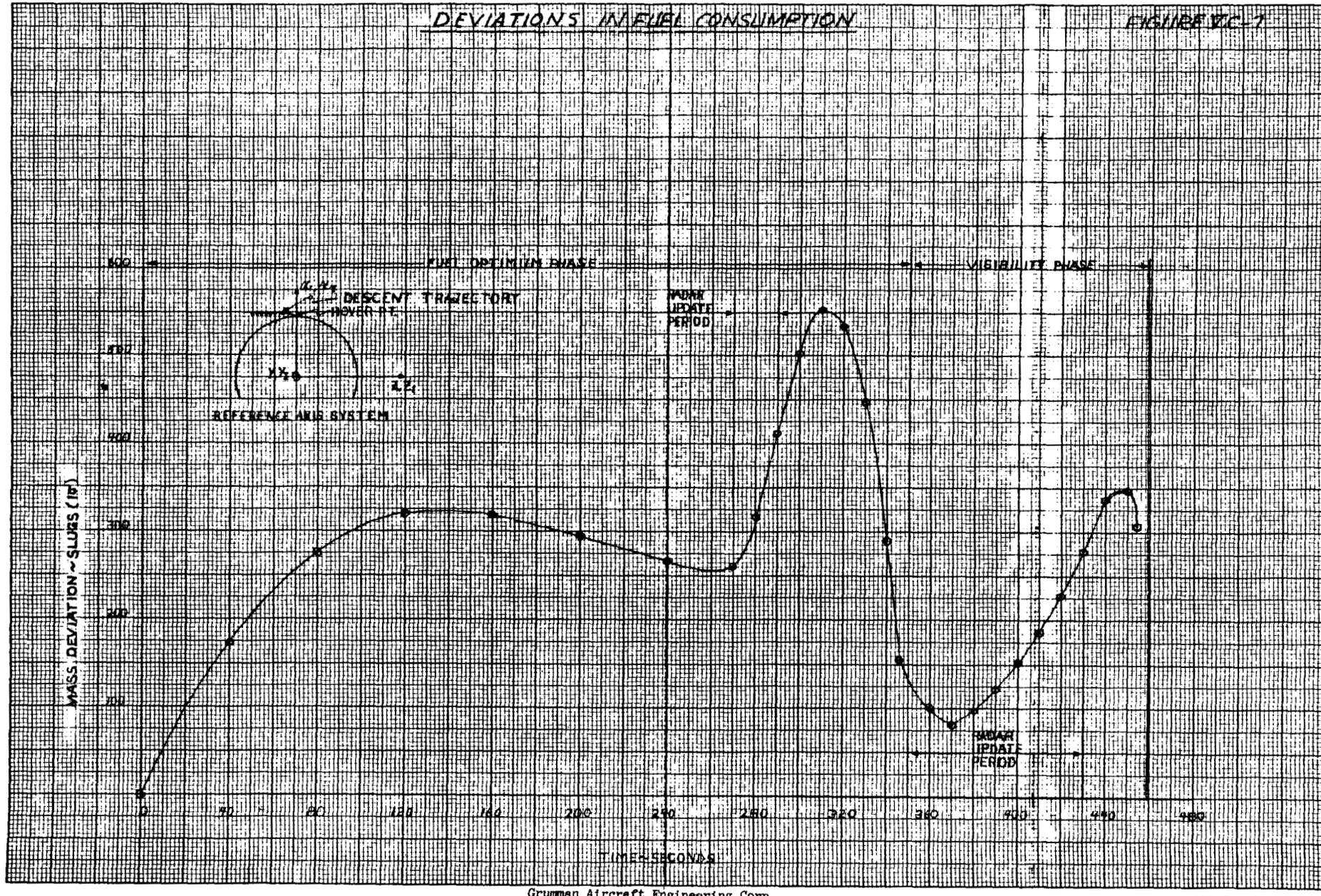
DEVIATIONS IN FUEL CONSUMPTION
FIGURE V.C-1
FUEL OPTIMUM PHASE
VISIBILITY PHASE
DESCENT TRAJECTORY
HOVER PT.
RADAR UPDATE PERIOD
REFERENCE AXIS SYSTEM
MASS DEVIATION ~ SLUGS (lb)
TIME-SECONDS
RADAR UPDATE PERIOD

~~CONFIDENTIAL~~

WEIGHTING FACTORS FOR ESTIMATING INERTIAL X

FIGURE IV C-8

$270 \leq t \leq 290$ SEC

$$x_E = x_I + W_{\Delta x}^{(x)}(r_{LR} - r_I) + W_{\Delta \dot{x}}^{(x)}(\dot{x}_{LR} - \dot{x}_I) + W_{\Delta y}^{(x)}(\dot{y}_{LR} - \dot{y}_I) + W_{\Delta \dot{y}}^{(x)}(\dot{z}_{LR} - \dot{z}_I)$$

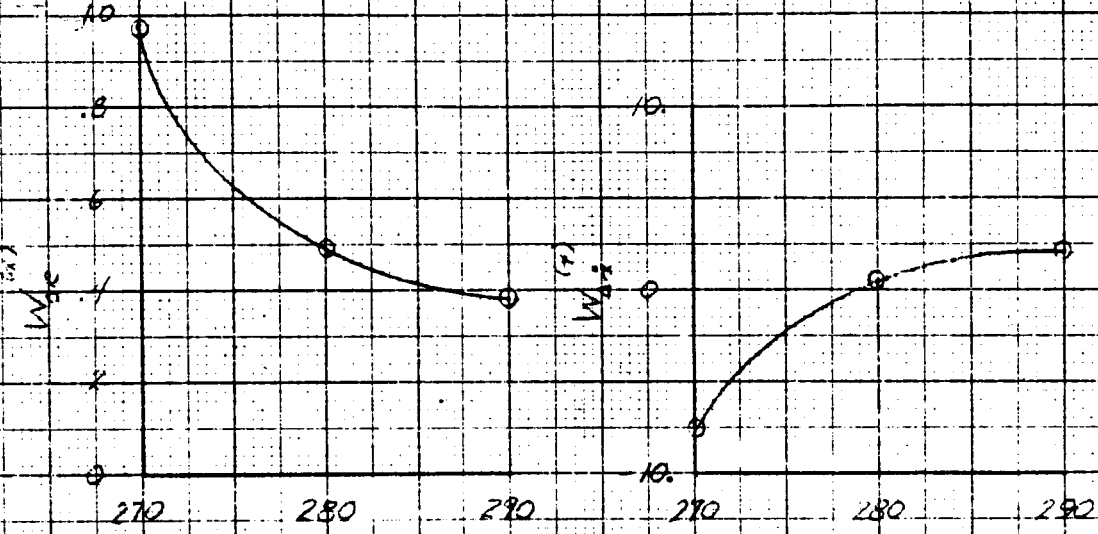

TIME (SEC)	$W_{\Delta r}^{(x)}$	$W_{\Delta \dot{x}}^{(x)}$	$W_{\Delta y}^{(x)}$	$W_{\Delta \dot{y}}^{(x)}$
270	.97744	-7.59007	.18279	.02926
280	.49781	0.67462	.02362	.00584
290	.38257	2.43513	-.00826	-.00456

$y_E = y_I$

$\dot{z}_E = \dot{z}_I$

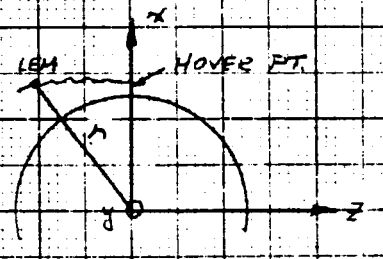

REFERENCE AXIS SYSTEM

~~CONFIDENTIAL~~

WEIGHTING FACTORS FOR ESTIMATING INERTIAL $\dot{x}$

FIGURE IV.C-9

$270 \leq t \leq 290$ SEC

$$\dot{x}_\Sigma = \dot{x}_I + W_{\dot{x}x}^{(\dot{x})}(x_{tk} - x_I) + W_{\dot{x}\dot{x}}^{(\dot{x})}(\dot{x}_{tk} - \dot{x}_I) + W_{\dot{x}y}^{(\dot{x})}(y_{tk} - y_I) + W_{\dot{x}\dot{y}}^{(\dot{x})}(\dot{y}_{tk} - \dot{y}_I) + W_{\dot{x}z}^{(\dot{x})}(z_{tk} - z_I) + W_{\dot{x}\dot{z}}^{(\dot{x})}(\dot{z}_{tk} - \dot{z}_I)$$

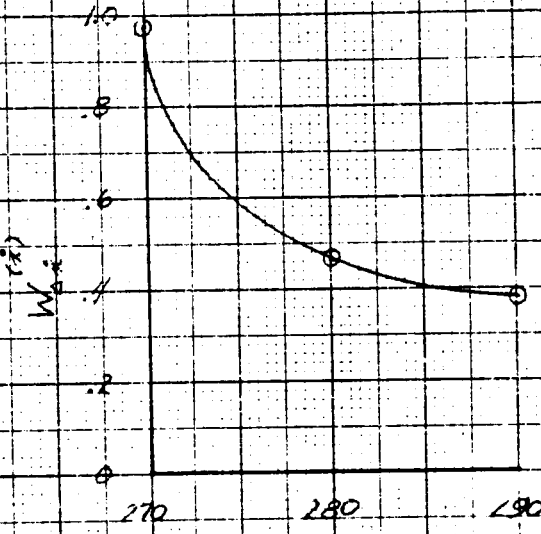

TIME (SEC)	$W_{\dot{x}x}^{(\dot{x})}$	$W_{\dot{x}\dot{x}}^{(\dot{x})}$	$W_{\dot{x}y}^{(\dot{x})}$	$W_{\dot{x}\dot{y}}^{(\dot{x})}$
270	-9.631×10^{-6}	.97915	4.1372×10^{-5}	6.12047×10^{-4}
280	-2.038×10^{-5}	.47523	8.8556×10^{-6}	4.0588×10^{-4}
290	1.965×10^{-5}	.38211	-1.4573×10^{-6}	4.742316×10^{-4}

WEIGHTING FACTORS FOR ESTIMATING INERTIAL $\dot{Y}$ FIGURE IV.C-10

$230 \leq t \leq 290$ SEC.

$$\dot{y}_c = \dot{y}_t + W_{\dot{x}c}^{(j)}(\dot{x}_{t+\Delta t} - \dot{x}_t) + W_{\dot{x}x}^{(j)}(\dot{x}_{t+\Delta t} - \dot{x}_t) + W_{\Delta\dot{y}}^{(j)}(\dot{y}_{t+\Delta t} - \dot{y}_t) + W_{\Delta\dot{z}}^{(j)}(\dot{z}_{t+\Delta t} - \dot{z}_t)$$

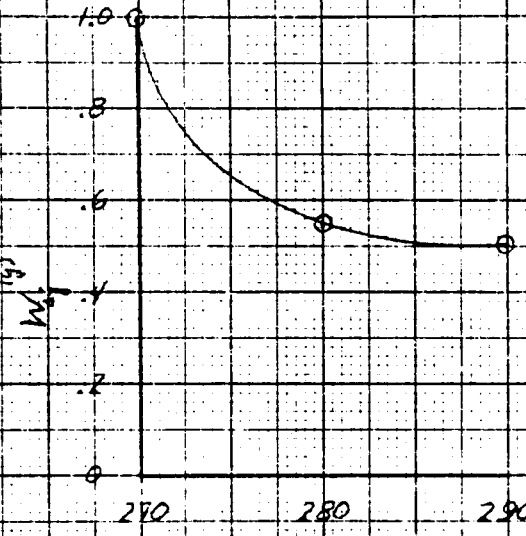

TIME (SEC)	$W_{\dot{x}c}^{(j)}$	$W_{\dot{x}x}^{(j)}$	$W_{\Delta\dot{y}}^{(j)}$	$W_{\Delta\dot{z}}^{(j)}$
270	-6.4437×10^{-7}	2.5317×10^{-5}	.99103	-1.2191×10^{-6}
280	-6.3010×10^{-7}	4.4655×10^{-6}	.54604	-6.0876×10^{-7}
290	3.4501×10^{-7}	-6.3647×10^{-7}	.50050	-1.9471×10^{-7}

~~CONFIDENTIAL~~

WEIGHTING FACTORS FOR ESTIMATING INERTIAL $\dot{z}$

FIGURE V.C-11

$270 \leq t \leq 290$ SEC.

$$\dot{z}_E = \dot{z}_I + W_{\Delta R}^{(\dot{z})}(r_{LR} - r_I) + W_{\Delta A}^{(\dot{z})}(\dot{x}_{LR} - \dot{x}_I) + W_{\Delta j}^{(\dot{z})}(\dot{y}_{LR} - \dot{y}_I) + W_{\Delta \dot{z}}^{(\dot{z})}(\dot{z}_{LR} - \dot{z}_I)$$

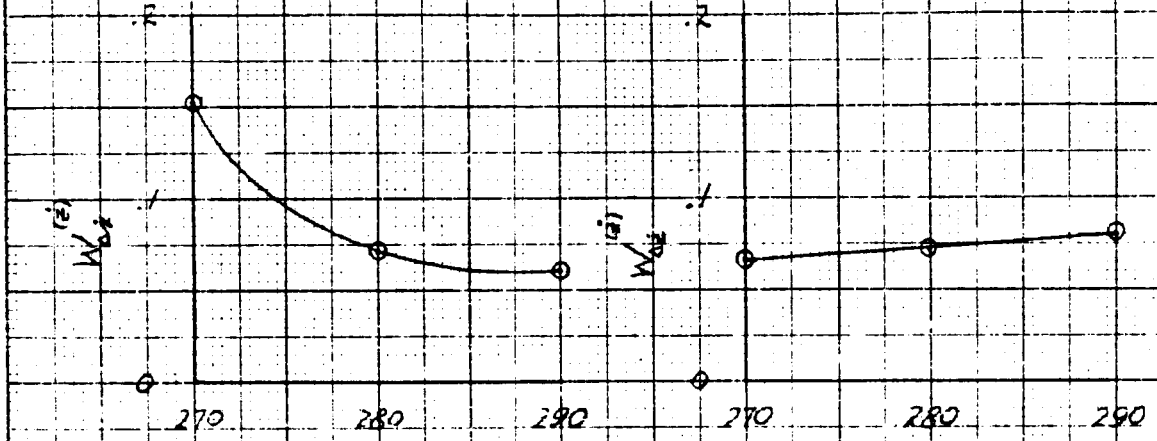

TIME (SEC)	$W_{\Delta R}^{(\dot{z})}$	$W_{\Delta \dot{r}}^{(\dot{z})}$	$W_{\Delta j}^{(\dot{z})}$	$W_{\Delta \dot{z}}^{(\dot{z})}$
270	-9.8383×10^{-4}	.15776	$+4.9731 \times 10^{-4}$	.06695
280	-1.1667×10^{-4}	.07112	-2.1152×10^{-4}	.07198
290	-8.9395×10^{-5}	.06030	-5.6694×10^{-5}	.08062

~~CONFIDENTIAL~~

~~CONFIDENTIAL~~

WEIGHTING FACTORS FOR ESTIMATING INERTIAL X

FIGURE V.C-12

$350 \leq t \leq 430$ SEC

$$x_t = x_I + W_{\Delta x}^{(x)}(T_{Le} - T_I) + W_{\Delta \dot{x}}^{(x)}(\dot{x}_{Le} - \dot{x}_I) + W_{\Delta y}^{(x)}(\dot{y}_{Le} - \dot{y}_I) + W_{\Delta \dot{z}}^{(x)}(\dot{z}_{Le} - \dot{z}_I)$$

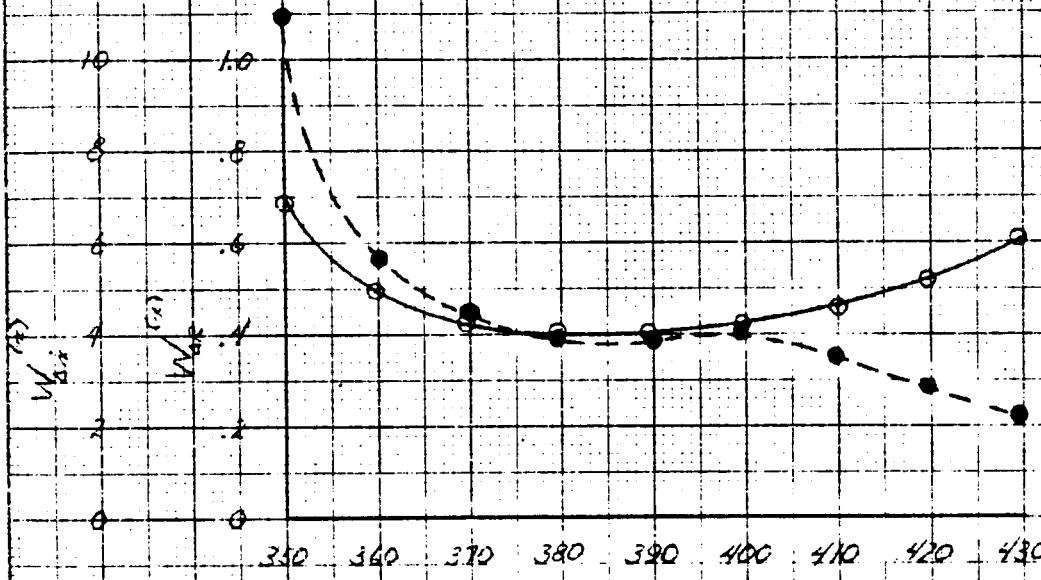

TIME (SEC)	$W_{\Delta x}^{(x)}$	$W_{\Delta \dot{x}}^{(x)}$	$W_{\Delta y}^{(x)}$	$W_{\Delta \dot{z}}^{(x)}$
350	.68795	10.9698	-3.6520×10^{-3}	-1.7242×10^{-2}
360	.49602	5.6635	-6.1678×10^{-3}	-6.1140×10^{-2}
370	.42630	4.4137	-6.2631×10^{-3}	-5.4513×10^{-2}
380	.40173	3.9863	-4.7531×10^{-3}	-5.2085×10^{-2}
390	.40219	3.9234	-3.0232×10^{-3}	-4.7509×10^{-2}
400	.42123	3.9932	-1.8713×10^{-3}	-4.2226×10^{-2}
410	.45954	3.9924	-1.2860×10^{-3}	-3.2841×10^{-2}
420	.52070	2.8828	$-.99105 \times 10^{-3}$	-2.0589×10^{-2}
430	.60912	2.2085	$-.77173 \times 10^{-3}$	-1.8972×10^{-2}

~~CONFIDENTIAL~~

WEIGHTING FACTORS FOR ESTIMATING INERTIAL $\dot{x}$

FIGURE IV.C-13

$350 \leq t \leq 430$ SEC

$$\dot{x}_E = \dot{x}_I + W_{\Delta\dot{x}}^{(\dot{x})}(\dot{x}_{LR} - \dot{x}_I) + W_{\Delta\dot{y}}^{(\dot{x})}(\dot{y}_{LR} - \dot{y}_I) + W_{\Delta\dot{z}}^{(\dot{x})}(\dot{z}_{LR} - \dot{z}_I) + W_{\Delta Y}^{(\dot{x})}(Y_{LR} - Y_I) + W_{\Delta Z}^{(\dot{x})}(Z_{LR} - Z_I)$$

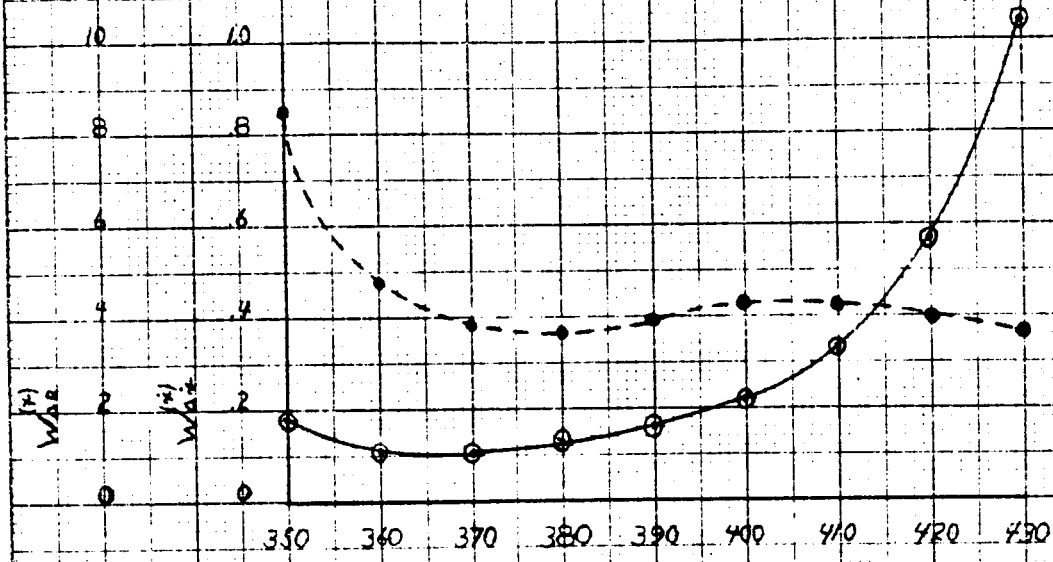

TIME (SEC)	$W_{\Delta\dot{x}}^{(\dot{x})}$	$W_{\Delta\dot{y}}^{(\dot{x})}$	$W_{\Delta Y}^{(\dot{x})}$	$W_{\Delta Z}^{(\dot{x})}$
350	1.8967×10^{-3}	.85088	-8.309×10^{-6}	6.1278×10^{-3}
360	1.1757×10^{-3}	.48716	-1.2410×10^{-5}	2.7414×10^{-3}
370	1.1397×10^{-3}	.38232	-1.2014×10^{-5}	2.1906×10^{-3}
380	1.3013×10^{-3}	.36663	-1.0603×10^{-5}	2.7856×10^{-3}
390	1.6543×10^{-3}	.39532	-1.0988×10^{-5}	3.9674×10^{-3}
400	2.2365×10^{-3}	.43829	-1.3109×10^{-5}	5.1554×10^{-3}
410	3.3856×10^{-3}	.42243	-1.6395×10^{-5}	6.6146×10^{-3}
420	5.7153×10^{-3}	.39550	-2.0158×10^{-5}	8.6213×10^{-3}
430	10.4098×10^{-3}	.36336	-2.3244×10^{-5}	$1.1309 7 \times 10^{-3}$

~~CONFIDENTIAL~~

WEIGHTING FACTORS FOR ESTIMATING INERTIAL $\dot{Y}$ — FIGURE VC-14

$350 \leq t \leq 430$ SEC

$$\dot{Y}_E = \dot{Y}_I + W_{a\dot{R}}^{(\dot{Y})}(\dot{R}_{LR} - \dot{R}_I) + W_{a\dot{x}}^{(\dot{Y})}(\dot{x}_{LR} - \dot{x}_I) + W_{a\dot{y}}^{(\dot{Y})}(\dot{y}_{LR} - \dot{y}_I) + W_{a\dot{z}}^{(\dot{Y})}(\dot{z}_{LR} - \dot{z}_I)$$

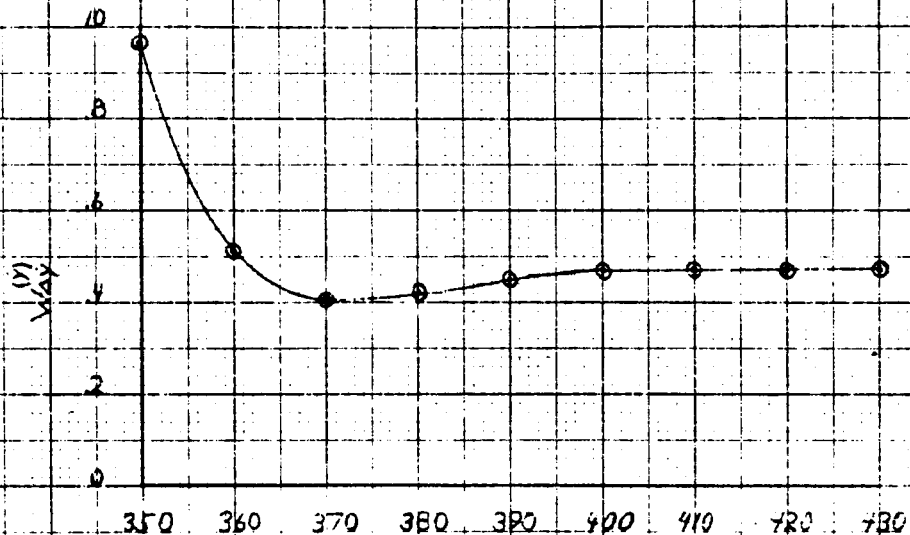

TIME (SEC)	$W_{a\dot{R}}^{(\dot{Y})}$	$W_{a\dot{x}}^{(\dot{Y})}$	$W_{a\dot{y}}^{(\dot{Y})}$	$W_{a\dot{z}}^{(\dot{Y})}$
350	8.3419×10^{-8}	-3.1417×10^{-6}	.96575	9.6540×10^{-9}
360	4.0077×10^{-7}	-5.3092×10^{-6}	.51397	6.3894×10^{-7}
370	5.5078×10^{-7}	-6.0658×10^{-6}	.41792	6.5021×10^{-7}
380	7.0632×10^{-7}	-6.3493×10^{-6}	.42604	6.5242×10^{-7}
390	1.0036×10^{-6}	-8.1290×10^{-6}	.45358	6.0205×10^{-7}
400	1.4351×10^{-6}	-1.2341×10^{-5}	.47007	5.6220×10^{-7}
410	1.9401×10^{-6}	-1.6395×10^{-5}	.47604	5.9182×10^{-7}
420	2.4505×10^{-6}	-2.0458×10^{-5}	.47780	7.3320×10^{-7}
430	2.8265×10^{-6}	-2.3844×10^{-5}	.47877	1.0638×10^{-6}

~~CONFIDENTIAL~~

WEIGHTING FACTORS FOR ESTIMATING INERTIAL $\dot{Z}$

FIGURE IV.C-15

$350 \leq t \leq 430$ SEC

$$\dot{Z}_E = \dot{Z}_I + W_{\dot{Z}R}^{(\dot{Z})}(\dot{X}_{LR} - \dot{X}_I) + W_{\dot{Z}\dot{X}}^{(\dot{Z})}(\dot{X}_{LR} - \dot{X}_I)$$

$$+ W_{\dot{Z}\dot{Y}}^{(\dot{Z})}(\dot{Y}_{LR} - \dot{Y}_I) + W_{\dot{Z}\dot{Z}}^{(\dot{Z})}(\dot{Z}_{LR} - \dot{Z}_I)$$

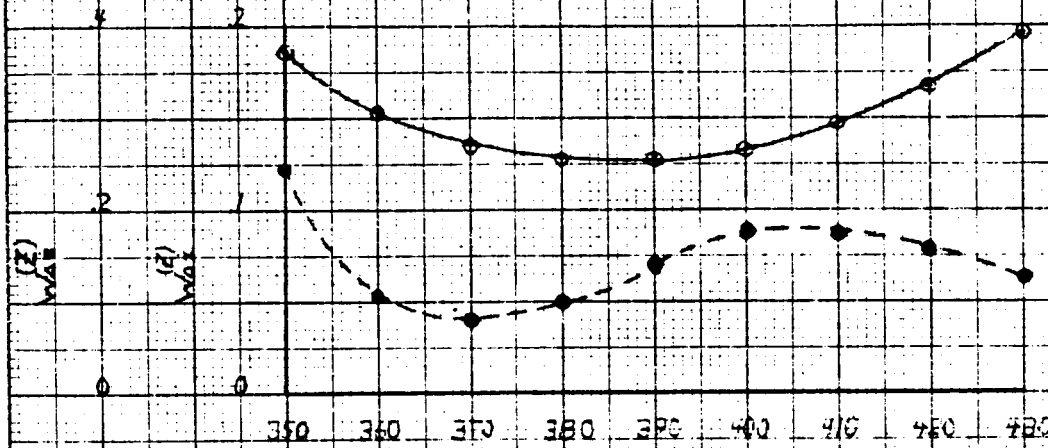

TIME (SEC)	$W_{\dot{Z}R}^{(\dot{Z})}$	$W_{\dot{Z}\dot{X}}^{(\dot{Z})}$	$W_{\dot{Z}\dot{Y}}^{(\dot{Z})}$	$W_{\dot{Z}\dot{Z}}^{(\dot{Z})}$
350	4.1146×10^{-4}	.12343	5.1931×10^{-5}	.37263
360	-4.8005×10^{-5}	.05333	2.8720×10^{-5}	.30693
370	1.4162×10^{-5}	.04120	2.4216×10^{-5}	.27280
380	5.7468×10^{-5}	.05072	1.9713×10^{-5}	.25761
390	1.1582×10^{-4}	.07001	1.4360×10^{-5}	.25655
400	2.0241×10^{-4}	.08828	1.0426×10^{-4}	.26856
410	5.6721×10^{-4}	.06763	7.8401×10^{-6}	.29834
420	6.7232×10^{-4}	.07603	6.6858×10^{-6}	.33369
430	1.6569×10^{-3}	.06358	6.0929×10^{-6}	.39286

~~CONFIDENTIAL~~

DISTRIBUTION LIST

Executive and Technical Review Board

Gavin, J. G. - Exec. - (1)
Hedrick, I. G. - Exec., Plant 5 - (1)
Hutton, R. - Exec., Plant 5 - (1)
Mullaney, R./ Canning, F. - (1)

Program Staff

Gardner, P. - (1)
Moorman, T. H. - (1)
Rathke, W. - (1)
Kelly, T. J. - (1)

Project Engineering

Barnes, T. - (1)
Carbee, R. - (1)
Whitaker, A. - (1)
Data Management File - (1)

Engineering Staff

Baird, E. - Plant 5 - (1)
Lewin, N. - Plant 5 - (1)

Subsystems Engineers

Dandridge, M. - (1)
Doennebrink, F. - (1)
Henderson, G. - (1)
LEM Project Eng'g File (1)
LoPresti, R. - (1)
Russell, J. A. - (1)
Thompson, R. - (1)
Williams, O. - (1)

Systems Engineers

Fleisig, R. - (1)
Katz, A. - (1)
Kress, R. - (1)
Salina, S. - (1)
Smith, G. - (1)
Stern, E. - (1)
Wiesinger, G. - (1)
Witte, R. - (1)

et. al.

Adornato, R. - (1)
Asbedian, V. - (1)
Biggers, J. - (1)
Chomak, S. - (1)
Cook, J. - (1)
Grossman, R. - (3)
Gustaitus, A. - (1)
Haggerty, T. - (1)
Hamilton, T. - (1)
Kelly, P. - (1)
Kuhn, A. - (1)
McNamara, J. - (1)
Munter, P. - (1)
Nathan, A. - (1)
Olstad, M. - (1)
Speiser, K. - (1)
Sperling, H. - (1)
Sprague, G. - (1)
Sullivan, G. - (1)
Tucker, L. - (1)
Yagi, F. - (1)

NASA DISTRIBUTION

LEM RASPO File - (1)
ASPO (30) Total - Including Copies To:
Battey, R. - ASPO-PA
Bryant, J. - MPAD/ASG
Bullard, J. L.
Chambers, T. V. - GCD
Cheatham, D. - GCD
Cohen, A. - ASPO
Coultas, G. - ASPO PE
Cox, K. - GCD
Duncan, C. - GCD
Funk, J. - GCD
Jenkins, N. V. - MPAD
Kurten, P. - ASPO
Lee, Wm. A. - ASPO
Lewis, R. - ASPO
Mayer, J. - MPAD
Maynard, O. - ASPO
Rector, W. - ASPO
Sevier, J. - ASPO
Shelton, D. H. - GCD
Ward, R. J. - ASPO-PA
Zito, F. - RASPO